MAX-PHASE SLURRY COATINGS FOR HIGH TEMPERATURE OXIDATION PROTECTION OF Ti BASED ALLOYS

BACHELOR THESIS IN AEROSPACE ENGINEERING

Department of Science and Materials Engineering and Chemical Engineering

Author:

María García Colón

Supervisors:

Sophia Alexandra Tsipas & Beatriz Velasco Núñez

Madrid, Spring 2014

UNIVERSIDAD CARLOS III DE MADRID

Acknowledgements

First of all, I want to thank my Dad for his support during all this time and for his patience listening as I went on about what could have happened during this project; also to everyone in my family who kept on asking how everything was going, specially my sister and mother for attempting to read it. I would like to dedicate this work to my grandpa, I'm sure he would have liked it.

Secondly, I want to thank my friends, we've been through a lot together and these last four years wouldn't have been the same without all of them. A special mention must be made to Nicolás, my lab-mate, who has been through the whole experimental process with me while doing both our projects and shared the same worries as me when anything went wrong.

Last of all, I would like to also thank both Sophia and Bea for their guidance through this project, they have been a great help and they have taught me a lot.

I know the final result seems to be quite long but to anyone who dares to read it I say: "Enjoy it!!"

ABSTRACT

It is a well-known fact that degradation of materials due to phenomena such as oxidation, corrosion or wear may result in early deterioration of a material. This deterioration can turn out to be very expensive in industries such as the Aerospace one, where the price of a piece can reach soaring figures and where the unexpected failure of a component can result catastrophic.

Titanium is a material widely used in the aerospace industry thanks to its good mechanical properties (high strength, low density and excellent corrosion resistance); however one of its drawbacks is its poor oxidation resistance at high temperatures. The purpose of this project is to be able to provide titanium with a coating capable of allowing it to improve its oxidation resistance.

MAX phases on the other hand are relatively new materials with a $M_{n+1}AX_n$ stochoimetry, where M is a metal, A is an A-group element and X is N or C. They are layered crystalline compounds with a hexagonal structure. These ternary phases are characterized by having extraordinary physical, chemical and mechanical properties related with their nanolayered structure. Among their properties their excellent high-temperature mechanical properties and their oxidation resistance makes them quite promising.

In this project, the slurry coating method has been used to develop the coatings, using as a donor material MAX-phases on Ti-6Al-4V alloy.

The reasons for choosing this alloy is that it is the most used titanium alloy in the Aerospace sector. The samples were to be coated using two different kinds of MAX-phase slurries: Ti_3SiC_2 and Ti_2AlC, respectively. The slurry diffusion treatment of the samples was carried out at different temperatures. Subsequently, samples were oxidized in static air at 600ºC for 300 hours. Characterization of the samples was performed by X-ray diffraction and Scanning electron Microscopy.

Key words: High temperature oxidation, Ti-6Al-4V alloy, MAX phases

CONTENTS

ABSTRACT 2
CONTENTS 3
CHAPTER 1: INTRODUCTION 6
1.1 Objectives 7
1.2 Phases of development 7
CHAPTER 2: TITANIUM AND ITS ALLOYS 9
2.1 Introduction 10
2.2 Titanium alloys: Classification 12
2.2.1 α Phase Alloys 13
2.2.2 β Phase Alloys 15
2.2.3 $\alpha + \beta$ Phase Alloys 15
2.2.4 Properties of Titanium alloys 16
2.3 Ti-6Al-4V 19
2.4 Extraction of Titanium and its alloys 21
2.5 Applications of Titanium and its alloys 22
2.5.1. Aerospace Sector 22
2.5.2. Biomedical Sector 24
2.5.3. Chemical Industry 25
2.5.4. Automotive Industry 25
2.5.5. Sports and Leisure 26
2.6 Future trends of titanium 27
CHAPTER 3: MAX-PHASES 28
3.1 Introduction to MAX-PHASES: Brief historical review and State of the Art 29
3.2 Synthesis of MAX phases 32
3.2.1. Synthesis of bulk MAX phases 32
3.2.2. Synthesis of MAX phase films 33
3.2.3. Synthesis of MAX phase powders 33
3.3 Background on Ti_3SiC_2 and Ti_2AlC 35
3.3.1. Ti_3SiC_2 35
3.3.2. Ti_2AlC 37
3.4 Crystal Structure 38
3.5 Properties of MAX phases 39

3.6 Potential Applications 42
3.7 Future Investigations 44
CHAPTER 4: COATINGS 45
4.1 Introduction 46
4.2 Fundamentals of the Oxidation phenomenon 47
4.3 Classification of coating techniques 51
4.4 Slurry Coatings 55
4.4.1 Introduction and description 55
4.4.2 Diffusion of the coating to the substrate 55
4.4.3 Advantages and Disadvantages of the Slurry Method 56
4.5 Composition of a slurry coating 58
4.5.1 Donor material powder 58
4.5.2 Liquid carriers 58
4.5.3 Binders 58
4.5.4 Additives 60
4.6 Previous Studies and State of the art of coatings 62
CHAPTER 5: EXPERIMENTAL PART 65
5.1 Introduction 66
5.2 Preparation of the substrates 66
5.3 Slurry composition 69
5.3.1 Introduction 69
5.3.2 Slurry composition and preliminary computations 69
5.4 Diffusion process 78
5.5 Oxidation Treatment 80
5.6 Metallographic preparation of the samples 83
5.7 Sample Characterization 86
5.7.1 Characterization by X-Ray Diffraction (XRD) 86
5.7.2 Characterization by Scanning Electron Microscopy (SEM) 88
CHAPTER 6: RESULTS & DISCUSSION 91
6.1 Introduction 92
6.2 Diffusion and Oxidation observations. Visual Inspection. 92
6.3 Characterization of Coatings 95
6.3.1. Characterization of the Ti-6Al-4V uncoated substrate 95
6.3.2. Characterization of the 211 Slurry Coating 98

6.3.3. Characterization of the 312 Slurry Coating 105
6.3.4. Summary of Results 112
6.4 Oxidation Curves 115
6.4.1. Comparison 211 Coating at 1100ºC and 1200ºC 116
6.4.2. Comparison 312 Coating at 1100ºC and 1200ºC 117
6.5 Discussion of Results 118
6.5.1 Phenomenon on 211 pieces during oxidation. What happened? 118
6.5.2 Influence of the kind of coating selected 121
6.5.3 Influence of the diffusion temperature 122
6.5.4 Influence of the oxidation temperature 124
CHAPTER 7: CONCLUSIONS 126
7.1. Conclusions 127
7.2. Future Studies 128
References 130
DEFINITIONS OF INTEREST 139
ABBREVIATIONS 140
Index of Figures 141
Index of Tables 144
Index of Equations 146
ANNEX I: TESTS DONE ON SLURRIES 147
A. Tests for Ti_2AlC 147
A.1 Test I 147
B. Tests for Ti_3SiC_2 150
B.1 Test I 150
B.2 Test II 152
ANNEX II: MEASUREMENTS OF THE SAMPLES AND AVERAGES 153
ANNEX III: CALCULATION OF THE FREE ENERGY FOR THE TiC REACTION 155

CHAPTER 1: INTRODUCTION

1.1 Objectives

Titanium and its alloys are widely used in the industry, in sectors as the aerospace, marine, and chemical due to their good specific properties. Their most outstanding properties are: high specific strength and excellent corrosion resistance. This high specific strength property is quite advantageous when working at high temperatures, the problem it has is that the operating temperature is limited by the oxidation of titanium. For this reason many attempts to try and improve its oxidation resistance have been and are still being carried out nowadays. (1)- (2)

The purpose of this project is to develop new novel slurry coatings based on Ti_2AlC and Ti_3SiC_2 MAX phases in order to improve the oxidation resistance of titanium at high temperatures so that the temperature limitations imposed on this material can be overcome.

Taking into consideration the good properties exhibited by MAX phases, in particular their good oxidation resistance; they will be employed as slurry coating to study the oxidation behavior of the coated Ti-6Al-4V substrate. Twenty samples will be center of the investigation. Eight of them will be coated with the two different MAX phase slurries, Ti_3SiC_2 and Ti_2AlC in each case. The remaining four will be used to study the normal oxidation behaviour of the substrate.

In addition, to the study of the two different slurries a new variable will be added, two different diffusion temperatures will be used for the slurry deposition process. Given their similarity to ceramic coatings the temperatures chosen for the slurry diffusion process will be 1100°C and 1200°C.

The final goal is to be able to establish a comparison between the oxidation behaviour of the bare substrate and the slurry-coated samples; with this it is expected that it will be possible to determine the effectiveness of these coatings to create a protective oxide scale protecting the substrate from further oxidation or slowing down the process. To do this two different characterization methods will be used to study the results obtained: SEM (Scanning Electron Microscopy) and XRD (X-Ray Diffraction).

1.2 Phases of development

Although the experimental process consists of many steps, the project can be summarized in the following:

1. Review of bibliography.
2. Preparation of the substrate.
3. Experiments with the slurries.
4. Diffusion of the slurries in vacuum.
5. Oxidation.
6. SEM and XRD observation of samples.
7. Analysis of results.

The whole experimental development was carried out at Universidad Carlos III in Madrid, in its Campus in Leganes. The process required especial equipment, such as a vacuum furnace, an oxidation furnace, cutting machines, grinding machines,… and also appropriate software for the analysis of the results. The specific programs used for the development and presentation of the result were the X-Pert High Score which is used to identify the phases obtained by the XRD characterization and Origin to display the oxidation curves and diffraction patterns. The use of each machine, at each step of the process will be described in detail in Chapter 5.

CHAPTER 2: TITANIUM AND ITS ALLOYS

2.1 Introduction

Titanium was discovered in 1791 by William Gregor; the British reverend, mineralogist and chemist. Examining the magnetic sand from the local river, Helford, in the Menachan Valley in Cornwall, England, he isolated "black sand", now known as "ilmenite". He removed the iron in the sand with a magnet and treated the sand with hydrochloric acid, producing the oxide of a new element, which he named mechanite after the location. Four years later a chemist from Berlin, Martin Heinrich Klaproth independently isolated titanium oxide from rutile. To name the element he associated the difficulty of extraction of the element with Greek mythology and the titans, held in captivity in the Earth's crust by their father. (3)

Since Titanium's discovery until it was able to be isolated more than 100 years went by. In 1910 Titanium was able to be isolated by heating titanium tetrachloride ($TiCl_4$) with sodium in a steel bomb ("Hunter process"). The first process that allowed obtaining good quantities of titanium and that is still the main process used nowadays is called the "Kroll process". The Kroll process was developed by Wilhelm Justin Kroll and it is based on using magnesium as a reducing agent to obtain titanium from $TiCl_4$.

Titanium is the fourth most abundant metal in the Earth's crust (0.6%). This fact brings up an interesting question; if it is so abundant why is it so expensive? The answer to this question is quite simple. The main problem regarding titanium, despite its abundance, is the difficulty of finding it in pure state and in high concentrations. Titanium occurs in nature only in chemical combination (usually with oxygen and iron). It is this difficulty and its processing what makes it expensive. (1)

The most common minerals in which titanium is generally found are: ilmenite ($FeTiO_3$) and rutile (TiO_2) (3)**.** Besides these there are other sources of titanium such as leucoxene. Ilmenite contains 44-70% titanium oxide and rutile 93-96%.

The main producers of titanium are Russia, the United States, Japan, United Kingdom and China.

Wide use of Titanium did not take place until the second part of the twentieth century. It now has a 70 year accumulated experience to guide through its use. Nowadays the primary use of Titanium's alloys is still mainly in aircraft and missiles as they have a low density and can withstand high temperatures; but its wonderful properties have not only attracted the aerospace sector, other industries and fields such as the chemical industry, medical engineering and even the leisure sector have taken interest in this material (2). Another potential activity it has is its use in desalination plants due to its excellent resistance to sea water.

Regarding its chemical properties it is worth classifying titanium as a metal, more precisely as a transition metal belonging to group IV of the periodic table; as such it is a non-ferrous light metal. Most of its properties are determined by its metallic bonding. Its strength is as high as steel's but with a much lower density. Despite being lower than steel's and with a value of 4.51 g/cm^3 it is the highest density of the light metals. Its low density is one of the things that make

it be one of the most important alloying agents with many metals (aluminum, molybdenum and iron).

Advantages	Disadvantages
High specific strength (also at high temperatures).	Low hardness.
High resistance to fracture.	Low load bearing capacity.
Good corrosion resistance.	Poor resistance to sliding wear.

Table 1 Summary of properties of Ti and Ti alloys

As already mentioned titanium and its alloys exhibit excellent mechanical properties, which along with its low density make them a very attractive structural material for aerospace applications. The specific strength of titanium alloys is only exceeded by that of fiber reinforced plastics at low temperatures below 300 K (see Figure 1), therefore it is reasonable that it is at high temperatures above 750 K where its specific strength has a higher potential use and its use is more attractive. (3)

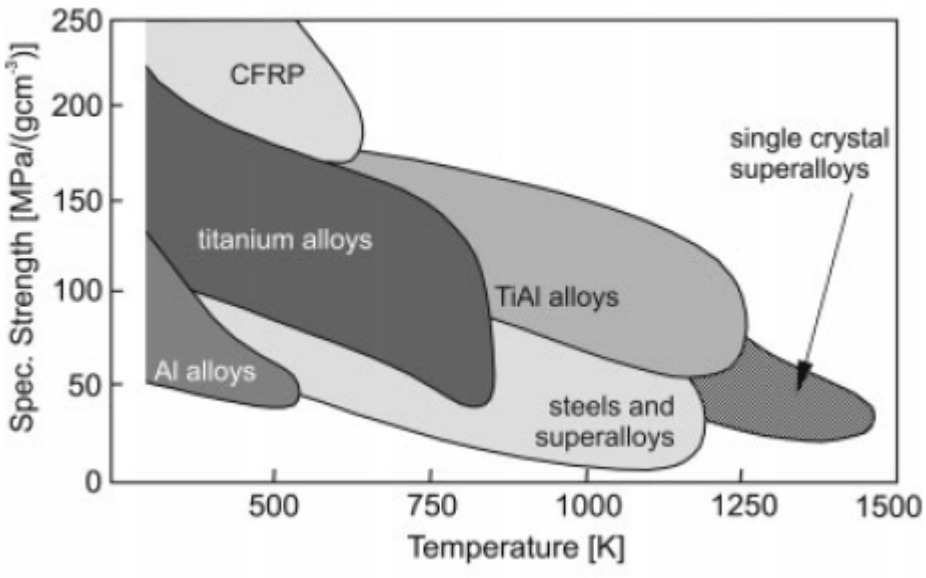

Figure 1 Comparison Specific strength of different materials with respect to temperature (3)

Despite its good characteristics one of its main problems is its temperature range limitation due to its oxidation behaviour; this limitation lies in the 540-800℃ range. Above this temperature the diffusion of oxygen through the oxide layer is too fast leading to a quick growth of the oxide layer and embrittlement of the adjacent oxide layer. (4)

Titanium is therefore highly reactive with oxygen; this high reactivity leads to the formation of a stable oxide layer when exposed to air, which although it gives it a poor oxidation resistance, protects the material from corrosion in environments such as aqueous acidic ones,

reason why despite having a poor oxidation resistance it has an outstanding resistance to corrosion.

Another property that can be highlighted is its high melting temperature which surpasses that of Aluminum, its main competitor in light weight structural applications, giving it a clear advantage at temperatures above 150℃.

2.2 Titanium alloys: Classification

Titanium's alloys have a good combination of properties. Titanium has the ability to crystallize into different crystal structures. Each structure is only stable within a certain temperature range.

Unalloyed titanium has two allotropic forms, the low temperature form, α, and the high temperature form, β, with HCP (hexagonal closed-packed) structure and BCC (body centered cubic) structures respectively.

Pure titanium exhibits an allotropic phase transformation at 882.5℃, this temperature is what is called the *transus temperature* where its structure changes from the BCC to the HCP crystal structure. The *transus temperature* is influenced by interstitial and substitutional elements, depending on the purity of the metal. (3)

Stabilizing element	Properties
Aluminum (Al)	α stabilizer. Reduces alloy density and increases: moduli and tensile and creep strengths.
Tin (Sn)	α stabilizer. Often used along with Al to increase strength avoiding embrittlement.
Zirconium (Zr)	Weak β stabilizer. At low or intermediate temperatures increases strength.
Oxygen (O_2)	Strengthens Ti until around 300℃. Its content should be kept low.
Molybdenum (Mo)	β stabilizer. Promotes high strength and hardness in quenched alloys.
Niobium (Nb)	β stabilizer. Added to improve long term high temperature exposure.
Silicon (Si)	Increases strength at all temperatures and has beneficial effects on creep.

Table 2 Summary of some of the most important Titanium alloying elements and their effects (5)

The alloying behavior of elements with titanium is defined by their effects on α and β. Titanium alloying elements can by divided into two types. Elements that when dissolved in Titanium cause little change in the transformation temperature or increase it are what are called α *stabilizers*. α Stabilizing elements (Al, O, N, C) take the α phase to high temperatures. They are simple metals, such as aluminum or oxygen. Aluminum is considered the most important alloying element of the α stabilizers.

Alternatively, elements that when dissolved decrease the *transus temperature* stabilizing the β phase are known as β *stabilizers* (Mo, V, Ta, Nb, Fe, Mn, Cr, Co, Ni, Cu, Si, H); β stabilizing elements tend to take the β phase to lower temperatures. In this last case, they are transition elements and noble metals.

Besides these elements there are also important impurity elements, oxygen, hydrogen, nitrogen and carbon. Oxygen and hydrogen are the two most important impurities. Oxygen is an α-stabilizer and hydrogen a β-stabilizer. These four impurity elements are referred to as interstitial elements because their atomic sizes are much smaller than those of the metallic alloying elements and they fit in the spaces (interstices) between the crystallographic positions of the metal atoms in the α and β phases. (6)

The stabilizing elements determine the different phase diagrams of Titanium alloys as can be seen in Figure 2.

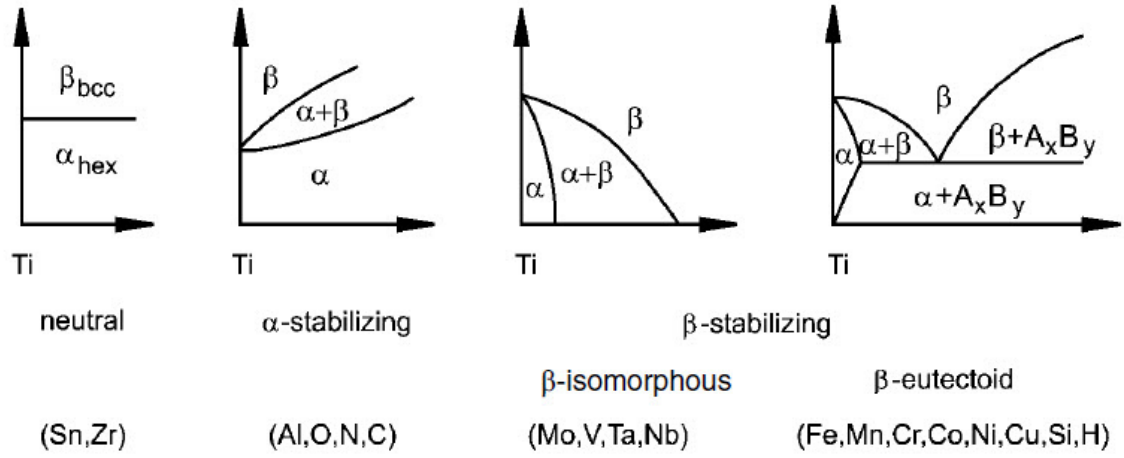

Figure 2 Influence of alloying elements on the phase diagram of Titanium alloys. (3)

Titanium alloys are generally classified by their structure in three groups: α, β and $\alpha + \beta$ phase alloys. A further subdivision can be made into near-α and metastable β alloys.

2.2.1 α Phase Alloys

Pure Titanium and most titanium alloys exclusively alloyed with α stabilizing or neutral elements belong to this group. The crystallization of this kind of alloys takes place at low temperatures and results in an HCP structure. α Titanium alloys are also characterized by being anisotropic.

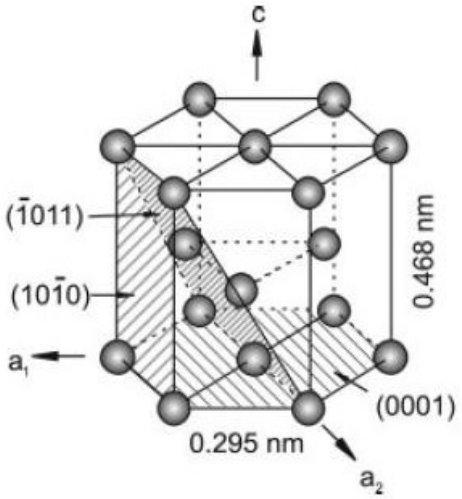

Figure 3 Crystal structure of the α phase in Titanium alloys. (3)

Single-phase and near-single phase alpha titanium alloys posses a good weldability. They usually have a high aluminum content which provides good strength characteristics and oxidation resistance at high temperatures. They have a major drawback which is the fact that they cannot be heat treated to develop higher mechanical properties due to the fact they are single-phase alloys.

They have a low easiness to be plastically deformed. The reason for it is that the HCP crystal structure is the structure with the lowest ease to deformation. This is related to two main factors:

- The number of slip systems.
- The energy needed for the plastic deformation.

To start off, the number of slip systems is the product of the number of slip planes times the number of slip directions. Slip planes and directions of highly dense packed atoms are energetically more favorable to plastic deformation, in other words, the higher the amount of atoms in the slip plane the easier it will be for the dislocations to guide and then deform. Comparing Figures 3 and 4 it can be easily seen how the HCP structure is more packed than the BCC, therefore it should be easier for this structure to deform; which contradicts what was stated previously.

Considering the second determining factor it is known that the energy needed for plastic deformation is directly proportional to the length of the minimal slip path, which in this case is higher for an HCP structure than for a BCC. If the energy needed for plastic deformation to take place is higher than for a BCC structure it then makes sense to state that its plastic deformation will be harder to take place. (3)

When small fractions of β stabilizing elements are added to α alloys then near-α alloys are formed. Near-α alloys are heat treatable and stronger than α alloys. Some early examples of near-α alloys are Ti-6Al-2Sn and Ti-8Al-1Mo-1V. Nowadays there exist more complex alloys that have been developed to achieve a higher creep resistance.

2.2.2 β Phase Alloys

Contrary to α phase alloys, crystallization takes place at high temperatures into a BCC structure. They have a high percentage of β stabilizing elements. β Alloys are metastable, this means they tend to transform to an equilibrium. These kind of alloys have excellent formability and very good response to heat treatment.

Examples of β-alloys are Ti-15Mo-3Nb-3Al-0.2Si and Ti-10V-2Fe-3Al. (7)

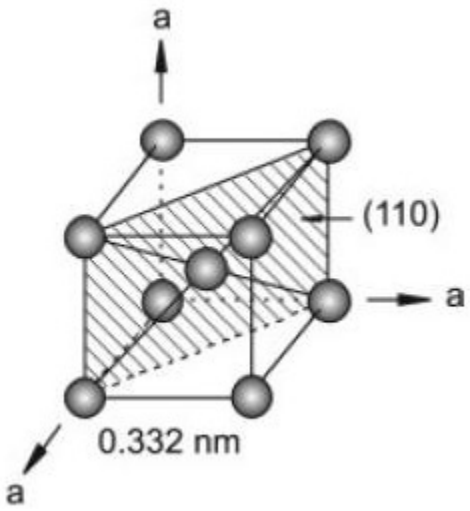

Figure 4 Crystal structure of the β phase in Titanium alloys. (3)

2.2.3 $\alpha + \beta$ Phase Alloys

This group of alloys is the most used. They are characterized by having a β volume fraction at room temperature which ranges from 5-40%. Addition of controlled amounts of beta-stabilizing alloying elements causes the beta phase to maintain itself longer below the *transus* temperature until reaching room temperature, resulting in a two-phase system. These two-phase alloys can be strengthened by heat treatment just like β-phase alloys. Heat treated α-β alloys are stronger than alpha alloys but their ductility is also proportionally lower.

If the amount of β stabilizers is increased to a level where β is no longer capable of transforming to martensite when quenched, the alloys still belong to the two-phase field and are termed metastable β alloys.

There are elements which are capable of reducing the α/β transition and stabilizing the β phase, they can be divided into two subgroups: the β-isomorphous (Mo, V, Ta and Nb) and β-eutectic (Fe, Mn, Cr, Co, Ni, Cu, Si, H). (8)

2.2.4 Properties of Titanium alloys

The mechanical properties of titanium alloys depend on the relative amounts and distribution of the α and β phases; on their volume fraction and their arrangement in the structure. Nevertheless, their strength is in any case higher than both α and β alloys.

As β titanium alloys and α titanium alloys are characterized by having BCC and HCP crystalline structures respectively, it is easy to note that the packing of the atoms will be denser for α alloys.

In the following a brief mention to some of the most important general properties of titanium alloys will be made, in some cases Ti-6Al-4V will be highlighted due to its importance in this project.

WEAR RESISTANCE

The wear resistance of titanium alloys is quite poor due to their high affinity to oxygen. Adhesive wear can occur by the transfer of oxygen towards non-metallic materials. Additionally, the HCP structure of the alloys provides them with a high wear coefficient and bad tribological properties. A possible way to avoid wear is to use lubrication.

STRENGTH

Different strength levels correspond to different types of titanium alloys. Single-phase α alloys have a moderate strength. On the contrary, α+β alloys and metastable β alloys can be hardened to achieve high strength levels.

High strength levels unfortunately result in low ductility in metastable β alloys, so unless they are age-hardened they will have a ductility similar to that of α and α+β alloys. The ductility is closely related to the microstructure. Equiaxed microstructures usually exhibit high ductility and fatigue strength. (3)

FRACTURE TOUGHNESS

This property is strongly dependent on both the microstructure and the aging condition; therefore there is no relation with the alloy kind. Coarse and lamellar microstructures show high fracture toughness in comparison to fine and equiaxed microstructures. This high fracture toughness is caused due to the ability of the structure to deflect propagating cracks along the different orientation lamella packets. (7)

MACHINABILITY

Machinability of titanium alloys is considered very poor due to several inherent properties. To start off, titanium is highly reactive, making the cutting tool weld when machined, leading to early tool failure. Not only this, but when machining titanium alloys tool life has been observed

to be very sensitive to the feed and also that when combining a small contact area with a low thermal conductivity when machining, high pressures and temperatures are developed, creating the need of using low cutting speeds. Additionally, its high strength, which is maintained at high temperatures, and its low modulus of elasticity also affect its machinability. (9)

To overcome some of the machinability problems titanium alloys have solutions such as the development of suitable cutting tools (straight tungsten carbide, cubic boron and polycrystalline diamond; the last two mentioned limited due to their high cost) or the use of cutting fluids. (9)- (10)

OXIDATION RESISTANCE

The application temperature of titanium alloys is limited by oxidation. Titanium dioxide has five possible forms in which it may appear in nature; the three most common are rutile (tetragonal), anatase (tetragonal) and brookite (orthorthombic). Rutile is the thermodynamically stable form of titanium dioxide. Besides the already mentioned it is worth pointing out that there are two additional pressure forms (monoclinic baddeleyite and an orthorthombic one). (11)

Chlorides and hydroxides deposited on its surface can accelerate oxidation. (7)

From all the titanium alloys the ones that have the best combination of properties and a higher resistance to oxidation belong to the α+β and to the near-α alloys, although for high temperature applications the best ones are TiAl alloys.

Ti-6Al-4V exhibits a poor oxidation resistance at temperatures above 650℃, creating a thin layer of oxide (TiO_2) at room temperature. Above 650℃ Ti-6Al-4V becomes hard and brittle due to the dissolution of oxygen and nitrogen. The thickness of the oxide layer usually ranges from 2 to 7 nm; however the composition and thickness of the oxide scale will depend on the environmental conditions. (12)

The oxidation behavior of Ti-6Al-4V varies in accordance with the temperature (5)**:**

- From 650-700℃ it follows a parabolic rate law.
- Above 700℃ it becomes linear.
- At 850 ℃ it becomes parabolic once more.

To improve the oxidation resistance alloying, pre-oxidation and coating techniques have been developed, they will be seen in more detail in Chapter 4.

CORROSION RESISTANCE

Despite being chemically reactive titanium alloys exhibit an excellent behavior to corrosion due to the affinity they have to oxygen, even at room temperature, developing a thin protective layer of oxide on top (mainly TiO_2).The corrosion resistance of titanium is closely related to its ability to create stable oxides (TiO_2, TiO, Ti_2O_3, Ti_3O_5 and TiO_2). Usually after

extended oxidation in air or high-pressure O_2 atmospheres at high temperatures the predominating and detected oxide formed is TiO_2.

This is the case of most oxidizing environments (salt solutions, sulfites and sulfates, nitric acid solutions, etc.); in reducing environments however, titanium's resistance to corrosion is not good because the protective nature of the oxide film breaks down. The stability and integrity of the protective oxide film can be improved in reducing environments by adding inhibitors (oxidizing agents). (1)

Titanium alloys are generally less resistant to corrosion than commercially pure titanium (3). Out of the three types of titanium alloys, the ones which tend to oxidize the least are α alloys. Ti-6Al-4V, for example, has an excellent resistance to corrosion when in an aqueous environment. (12)

HEAT TREATMENTS

Commercially Ti-6Al-4V alloy is heat treated quite often through a variety of treatments. In order to soften the alloy and make it easier to machine mill annealing is used. Other heat treatments of certain relevance are duplex annealing and aging treatments. (7)

In Figure 5 a brief summary of the properties of Titanium alloys (α, β and $\alpha + \beta$) that have been mentioned above is made.

	α	α+β	β
Density	+	+	−
Strength	−	+	++
Ductility	−/+	+	+/−
Fracture toughness	+	−/+	+/−
Creep strength	+	+/−	−
Corrosion behavior	++	+	+/−
Oxidation behavior	++	+/−	−
Weldability	+	+/−	−
Cold formability	− −	−	−/+

Figure 5 Summary of the properties of the different Titanium alloys. (3)

From the previous it can be concluded that in comparison to β alloys α are characterized by (3):

- A higher resistance to plastic deformation.
- Reduced ductility.
- Anisotropic mechanical and physical properties.
- A lower diffusion rate (about two orders of magnitude).
- Higher creep resistance.

As the main α stabilizing element is aluminum, and its density is only half of titanium's specific weight, α alloys have a lower density than β alloys. Additionally, usually β alloys are alloyed with heavy elements such as Mo and V, which accentuate this difference even more.

2.3 Ti-6Al-4V

Ti-6Al-4V was initially developed in the 50s and mainly used in compressor blades and gas turbines. Its development took place in the Technological Institute of Illinois, in the United States. Nowadays this kind of Titanium alloy accounts for more than 50% of all the Titanium tonnage in the world.

Up to the present day there are more than a hundred different titanium alloys but there seems to be no other alloy that threatens its primary position. Its use is especially widespread in the aerospace industry representing its use more than an 80% of the total use. The next field where its application is significant is in the medical sector, especially in the use of prostheses, being this 3% of the market. There are other sectors which use it as well, but in lower amounts, they are the marine, chemical and automotive. (4)

Ti-6Al-4V is unique in the fact that it combines attractive properties with inherent workability, allowing it to be used for both small and large-sized products, good shop fabricability, production experience and commercial availability. This is what makes it be the reference of comparison with other alloys. One of its outstanding properties with respect to other titanium alloys is the fact that it is heat treatable. (7)

Studies on this alloy and modifications of its composition have been made, making it be one of the most studied titanium alloys, especially in the aerospace sector.

Regarding its structure, Ti-6Al-4V is an alpha-beta alloy with a chemical composition of 6% aluminum, 4% vanadium in weight and a maximum amount of iron and oxygen, 0.25% and 0.2% respectively. Ti-6Al-4V is characterized by being significantly stronger than commercially pure titanium, but is has a lower thermal conductivity. (13)

Ti-6Al-4V can exhibit different microstructures depending on the thermomechanical treatment applied. Microstructures will be different if heat treatments are performed above or below the β transus temperature (see Figure 6 with the β transus temperature and the indications of the different phase fields). When annealing above the βtransus a fully lamellar microstructure is created. The equiaxed or bi-modal microstructure on the other hand, results from a recrystallization annealing below the β transus temperature processes. Additionally, the microstructures can be fine or coarse (3), (14)- (15)

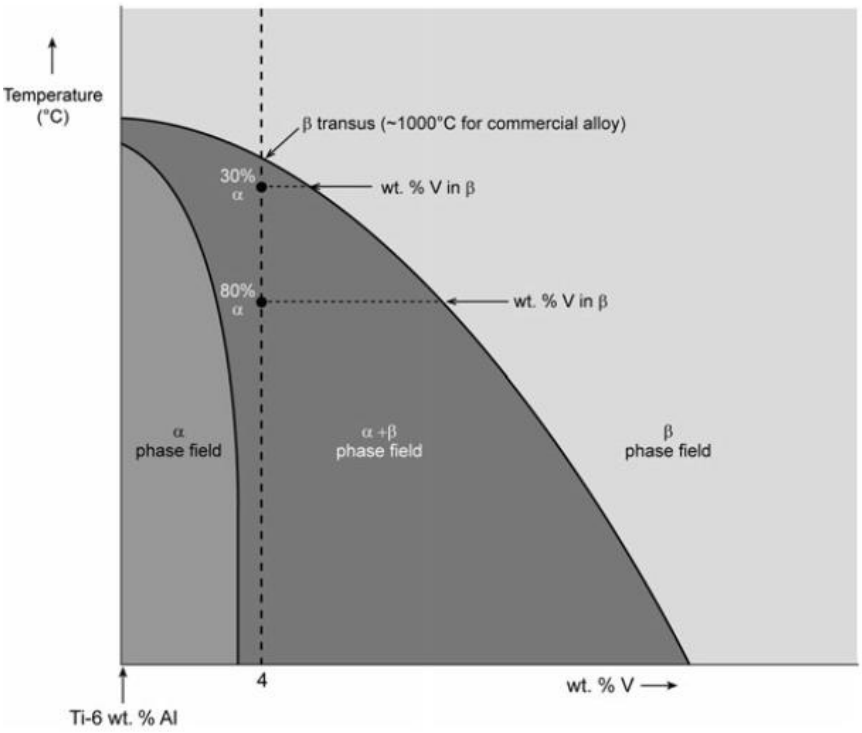

Figure 6 Pseudo-binary equilibrium phase diagram for Ti-6Al-4V. (7)

Typical uses of Ti-6Al-4V in the aerospace sector include pressure vessels, aircraft compressors and turbine blades and disks.Ti-6Al-4V is generally used in temperature conditions up to 400℃. A brief summary of some of its most important properties can be seen in Table 3.

Properties of Ti-6Al-4V	
β transus Temperature (℃)	995
Density (kg/m^3)	4420
Young's Modulus (GPa)	110-140
Tensile Strength (MPa)	900-1200
Yield Strength (MPa)	800-1100
Hardness (HV)	300-400
%EI	13-16
K_{IC} (MPa m$^{1/2}$)	33-110

Table 3 Elementary properties of Ti-6Al-4V (2), (13)

The substrate used for the analysis of oxidation is this one. Ti-6Al-4V in its wrought form was provided as a sheet.

2.4 Extraction of Titanium and its alloys

Extraction of pure titanium is a difficult task, for this reason its use wasn't as extended until an effective production method was found in the twentieth century. The difficulty in the extraction of pure titanium lay in the high reactivity this metal has with oxygen, nitrogen and carbon at elevated temperatures. (1)

There are several different processes for extracting titanium from the mineral as the Kroll Process, the Hunter Process, Electro-deoxidation Process, the Van Arkel-de Boer method, the Armstrong process …; however from all the extraction processes used the only that has survived for economic reasons, despite its high economic cost, is the Kroll process. In some countries like the UK other processes as the Hunter process are still in use. (8)

- KROLL PROCESS:

The process takes place in large sealed steels vessels in an inert argon atmosphere to avoid contamination by air or moisture of the final product. In the Kroll process rutile (TiO_2) is converted into titanium sponge through a series of steps (3)- (4).The first step is chlorination of the ore to produce titanium tetrachloride ($TiCl_4$).

$$TiO_2 + 2Cl_2 + C \rightarrow TiCl_4 + CO_2$$

Equation 1 Chlorination reaction: Kroll process

Liquid $TiCl_4$ is then purified by fractional distillation and reacted with Mg to obtain titanium sponge. A sponge made of titanium is formed in the wall of the vessel. The final product is obtained by compaction of the sponge. (16)- (17)

$$2Mg\ (l) + TiCl_4(l) \rightarrow 2MgCl_2(l) + Ti\ (s)$$

Equation 2 Reaction to obtain Titanium

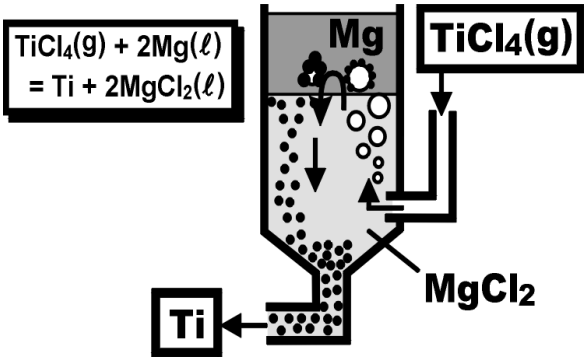

Figure 7 Schematic diagram of the Kroll process. (18)

❖ HUNTER PROCESS:

The Hunter process was used before the Kroll process. The operating procedure is similar to the one followed in the Kroll process but instead of using magnesium (Mg) as reducing agent sodium (Na) is used. The resulting sponge would be granular so its compaction would be easier.

❖ ELECTRO-DEOXIDATION PROCESS:

An example of a more up to date extraction process is this one. This method of extraction is an electrolytic method for the direct extraction of metals from the original cathode by separating oxygen from the titanium ions by using a molten bath of $CaCl_2$ and a graphite anode. Two different mechanisms were used to describe the electrochemical process: the FFC Cambridge and the OS. (19)

On the contrary of the Kroll process the FCC process is continuous and it starts off directly from titanium oxide, which allows obtaining titanium at a lower cost. For these reasons it is being extensively studied.

2.5 Applications of Titanium and its alloys

The wonderful properties of titanium and its alloys make it be one of the metals with a wider range of applications and in a large variety of sectors, some of which will be briefly mentioned below. It is a very versatile metal which can be used in a variety of different things, from buildings (as the Guggenheim) to golf clubs. Despite this large variety of fields of application it is worth pointing out that it is the Aerospace sector, with 50% of the worldwide titanium consumption the one in which titanium alloys gain most importance.

The incorporation of titanium in all of the most important sectors worldwide is due to two of its most outstanding properties: low weight and corrosion resistance.

2.5.1. Aerospace Sector

Attempting to decrease expenses and energy consumption the Aerospace is one of the sectors with the most up-to-date technology and involved in the development of new materials. For this reason it is the sector in which Titanium and its alloys play the most dominant role. Weight saving in this field is very attractive; 1 kg saved can be more than 1000 euro in the case of large aircraft and even up to 10000 euro in the space sector. (20)

The relevance of decreasing weight has led to studies on the materials which would be more suitable for weight-saving. The properties needed have been analyzed reaching the conclusion that the best option would be to use materials with a lower density. The decrease in density causes a proportional decrease in weight of the same amount. This fact highlights the importance of the use of light materials in the Aerospace Industry.

Comparing titanium with steel and aluminum alloys, it is clearly a younger structural material. The first alloys that were developed were in the 40s; among them was Ti-6Al-4V.

Some of the drivers for the use of titanium alloys is the Aerospace Industry are: weight reduction, temperature application and corrosion resistance (substituting steels and aluminum alloys).

Although in the past decades the use of titanium in different aircraft components has increased, in large commercial aircraft the main component in which titanium still remains mostly used is the engine, especially in gas turbine engines. Approximately one third of a modern turbine engine is made of titanium. Nowadays in other components, such as the fuselage, it can comprise 9% of the airframe (Boeing 777). In other parts of the aircraft using titanium alloys allows increasing the component's life cycle, this occurs for example in the landing gear. Typical proportions in which titanium is used in the airframe and the engine of aircraft can be seen in Figure 8.

Examples of how it has replaced steel are for example in hydraulic tubing. This change has allowed a 40% weight reduction.

Despite being of great importance, the use of titanium alloys in commercial aircraft is not as important as its use in military aircraft. In the former its proportion can exceed 50%, as in the "Blackbird", which had 95%. Reasons for using them in this field may be kinetic heating from the surface skin that reaches temperatures which aluminum alloys can no longer stand.

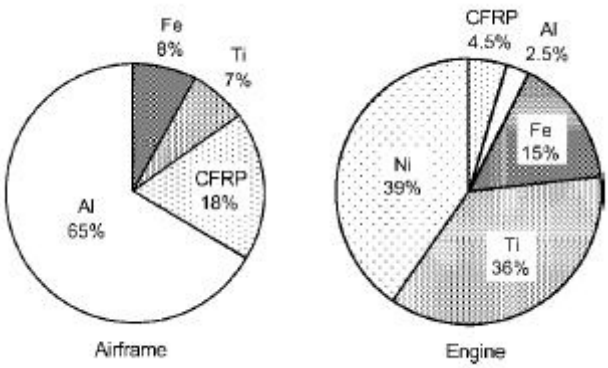

Figure 8 Percentage of materials in large modern aircraft. (20)

As the trend to increase the amount of titanium used has increased, the kind of alloy used has also varied. At first α+β alloys were the most used kind of alloys, but now they have been replaced by elevated temperature near α alloys.

The first engine components made of titanium alloys were compressor blades, nowadays even front blades of modern jet engines are made of titanium alloys. It is true, though; that some companies as General Electric have started using fiber reinforced polymer composites with the purpose of reducing weight, however, titanium is still used in the leading edges of the blades to avoid erosion.

Regarding Ti-6Al-4V, its temperature limit is around 315℃ therefore it is used for fan blades and disks as they are used at low temperatures. Ti-6Al-4V can also and is still used in the low-pressure compressor where the temperatures reached are not too elevated; as the temperature increases in the high-pressure compressor other kind of titanium alloys, more suitable, are used, near-α alloys. The temperature limit imposed for near-α alloys is 540℃, this limitation is due to the moderate oxidation resistance. For this reason the compressor parts subjected to the highest temperatures, blades and disks at the last stages of the compressor, have to be made from Ni-based superalloys at twice titanium alloys weight to be able to stand these extreme temperatures. (20)

Moving on to helicopters, titanium alloys are also of use, especially in the most highly stressed components, as the rotor head. Eurocopter BO 105 and BK 117 helicopters use forged Ti-6Al-4V in their rotor heads.

Titanium alloys are also of great importance in the space sector, where even in the time of the Apollo and Mercury programs they were already widely used.

The last 40 years have allowed huge developments on the maximum temperature for titanium alloys. This has allowed rising the limiting temperature of titanium alloys from 300 to 600℃. In engine locations at even higher temperatures TiAl alloys are used due to their excellent creep resistance, another important aspect of these kind of alloys is that they minimize the risk of titanium fire. TiAl alloys are being extensively studied due to their lower density than conventional titanium alloys, higher melting temperatures and moduli, some of their current limitations are the tendency of oxide scales formed at temperatures above 871℃ to spall when cooled down. (7)

2.5.2. Biomedical Sector

Just as in the Aerospace sector, titanium alloys are very attractive in the biomedical sector. Ti-6Al-4V is one of the alloys most extensively used, unfortunately awareness on the fact that the released vanadium and aluminum may result toxic to the health has taken place and new alloys have started being used instead, for example Ti-6Al-7Nb.

The reason why titanium alloys are favored in this sector as well is their excellent corrosion resistance. However, this one is not the primary one but biocompatibility, which in this field is of even more importance. Titanium is from all the biomaterials the newest.

The biocompatibility of titanium is related with its oxides. The properties resulting in biocompatibility are (21)**:**

- Low level of electronic conductivity.
- High corrosion resistance.
- Low ion-formation tendency in aqueous environments.
- An optimum iso-electric point of the oxide of 5-6.
- Thermodynamic state at physiological pH values.

In the case of Ti-6Al-4V its biocompatibility is especially good when in direct contact with bone or tissue. Although it does comply with the two most important requirements it has a disadvantage related with its poor shear strength. Sadly, this makes it less appropriate for bones screws and plates.

Making the most out of its non-reactive properties (inertness) some of the most common uses of titanium alloys in this field are implants to replace failed tissue, and dentistry, in crowns, bridges, etc.

2.5.3. Chemical Industry

Titanium is a material that has a high affinity with oxygen and any moisture present in air, this makes it be a highly reactive material and posses an excellent corrosion resistance due to the formation of a thin oxide film on its surface, this thin film is always there and when damaged immediately regenerates keeping it protected. This high resistance to corrosion makes it be an ideal material for use in aggressive environments. (3)

At first titanium's use in this field was basically restricted to oxidizing chloride environments, whereas nowadays titanium is used in areas with acetic, nitric acids, wet bromine, and acetone. Titanium is ideal in those areas where stainless steels can no longer provide an adequate corrosion resistance.

Being used in chloride environments does not make titanium totally unaffected by these operating conditions. Ti-6Al-4V, for example, is susceptible to chloride, but despite this it still remains as one of the most resistant alloys to it.

Some of its main applications in the field of chemical engineering are for containers, pumps, heat exchangers, pipes…

2.5.4. Automotive Industry

The use of lightweight materials in this field, such as titanium, has an important issue in hand, the cost. However, using lighter materials would allow a decrease in the fuel consumption.

The first time titanium was used in the automotive industry was in the mid-fifties, this car was not sold but the construction of its entire outer skin out of this material made the titanium industry set as goal the objective to enter the automotive industry. At first its use was limited to racing cars and sports cars from which excellent performances were expected. In the late 90's Toyota introduced titanium engine valves in its cars for the first time, soon after titanium started moving on to other components such as titanium spring coils. (22)

Despite its cost titanium has nonetheless been extensively used in race cars where cost is not as important. Titanium has a great potential in many car components, some of which can be seen in Figure 9, besides those seen there they can also be used for many engine and chassis components.

Ti-Al compositions would seem appropriate for components which are subject to high temperatures as exhaust valve, whereas Ti-6Al-4V would be adequate for components at lower temperatures that require certain mechanical properties. Use of the previous mentioned titanium alloys has already been carried out with successful results in both cases. In 1998 the Toyota Altezza was the first car to use titanium valves, using Ti-6Al-4V for the intake valve and TiB/Ti-Al-Zr-Sn-Nb-Mo-Si for the exhaust one. Ti-6Al-4V is also used quite frequently for fasteners. Regarding γ-TiAl, its use in valves would specially lead to a pronounced reduction in mass, allowing a 10% increase in the engine speed and also have the advantage of reducing valve chatter at high speeds.

Figure 9 Potential automotive applications of titanium. (22)

Among the most promising applications of titanium in this field is the use of its alloys for cars' exhaust pipes and their suspension springs.

2.5.5. Sports and Leisure

The fact that titanium is considered a supreme metal makes it be used as candidate when trying to develop instruments, tools or anything where a high-performance is required. Some examples of their use in the field of sports and leisure are in the head of golf clubs, in bicycles, in scuba diving equipment. (3)

In golf, a titanium head, given its low weight allows making larger heads and still maintain the lightness expected from it allowing the player to obtain larger distance while applying the same force in his swing. The typical preferred titanium alloy that is used for golf club heads is Ti-6Al-4V.

All of the applications mentioned for titanium are just a brief overview of the many uses titanium has in our everyday lives which we may be unaware of, but besides them other simpler uses of Titanium are also known such as in jewelry, architecture or even in toothpaste.

2.6 Future trends of titanium

Titanium represents a small amount of the worldwide metal market. From the total amount of titanium produced, 45% is used in the Aerospace sector, mainly in engine-components, another 45% for industries that require a high corrosion resistance, and the remaining 10% is used for the new needs created by emerging markets. (23)- (24)

The expense of titanium and the presence of highly qualified competitors make the increase in the use of titanium uncertain. According to the industry in which it is being used, different competitors, not always cheaper than titanium, are encountered. In the Aerospace Industry, for instance, the main competitors of titanium at high temperatures are superalloys and at low temperatures fiber carbon composites. In Aircraft like the A350, the material distribution is 14% titanium, 53% composite, 6% steel, 19% aluminum alloys and the remaining 8% of other materials. Other aircraft like the Boeing 787 Dreamliner exhibit similar proportions. To exemplify numbers in terms of weight and get an idea of the figures we are dealing with we can mention that the A380 uses 67 tonnes of titanium in its body and 10 tonnes in its engines.

Before the Global Financial Crisis (GFC), 2007-2008, the titanium demand was expected to grow rapidly until 2020. These predictions were affected by the GFC and the titanium demand decreased. Recent reports made have predicted a recovery and subsequent growth in its use. (24)

Titanium is expected to be the material of use for aerospace fasteners until 2018. The global demand of titanium fasteners for both commercial and airframe applications is projected to double in the near term mainly due to its favourable strength-to-weight ratio advantageous over ferrous, aluminum and nickel alloys. Not only this, but the new aircraft B787, A350 and A380 contain larger amounts of titanium than the older aircraft; and as the world fleet of airplanes is expected to double by 2029 the tendency expected would lead to an increase in the demand of titanium. (25)

In the automotive industry the main competitors are steel alloys, and although titanium's properties may be superior the cost still leaves the former behind, making its widespread use in this sector quite improbable. However, an attractive way to increase the use of titanium would be to enhance the use of Ti in the automotive industry would be to use Ti composites. Ti composites allow overcoming wear limitations of Ti and obtaining good moduli of elasticity.

Although titanium sponge is also expensive, although less than titanium pieces, the titanium sponge production also expects a 27% increase until 2015.

The sectors mentioned previously are quite sensitive to the economy and to cost, therefore it makes sense to expect the highest growth in areas were cost is not as important as the leisure sector, the biomedical industry or in sport articles. (26)

CHAPTER 3: MAX-PHASES

3.1 Introduction to MAX-PHASES: Brief historical review and State of the Art

Few materials are capable of combining characteristics typical of ceramics, such as high temperature and oxidation resistance and stiffness with those of metals, such as machinability, damage tolerance and good thermal and electrical conductivity. It turns out that a material with such combination of properties was discovered in the 60's by Nowotny and his coworkers (27).The materials found were a number of nitrides and carbides with a behavior like no other known before. These materials proved to be stiff, lightweight, machinable, relatively inexpensive and most important of all; they allowed reaching temperatures beyond 1300°C.The discovery took place when Nowotny and his coworkers were synthesizing a large number of carbides and nitrides due to their good mechanical properties.

In their accomplishment more than 100 new carbides and nitrides were discovered. Out of all of them more than thirty were classified as H- or Hägg phases (28). These Hägg phases have a M_2AX chemistry with M_2X layers interleaved with layers of pure A.

The next important discovery took place in 1967, when Ti_3SiC_2 and Ti_3GeC_2 were discovered (29)- (30). The structure of these new materials is closely related to the M_2X structure, having in this case M_3X_2 layers separating the A layers. It wasn't until Ti_4AlN_3 was discovered that it became obvious that these phases shared a common structure which gave them similar properties. It was at this time when the complete group of materials was definitely termed MAX phases (in the year 2000). (31)

MAX phases ($M_{n+1}AX_n$) belong to the family of layered ternary compounds given their layered nature and their three elements composition. Their three elements are M, an early transition metal, A, a group A element (belonging to group III, IV or V from the periodic table) and X is either carbon or nitrogen (see Figure 10). When the discovery took place it was believed that the values of n ranged from 1-3, since then reports of phases with n=4 and n=5 have occasionally been reported.

In the 90's Ti_3AlC_2 was added to the group by Pietzka and Schuster (32)- (33). After that, not many updates on new MAX phases were made. However, quite recently this changed with the discovery of new nine phases (34).

Not so long ago these phases were considered an uncharted category of solids due to uncertain nature, but as time went on and studies on their properties were made, they started drawing attention due to their unusual properties.

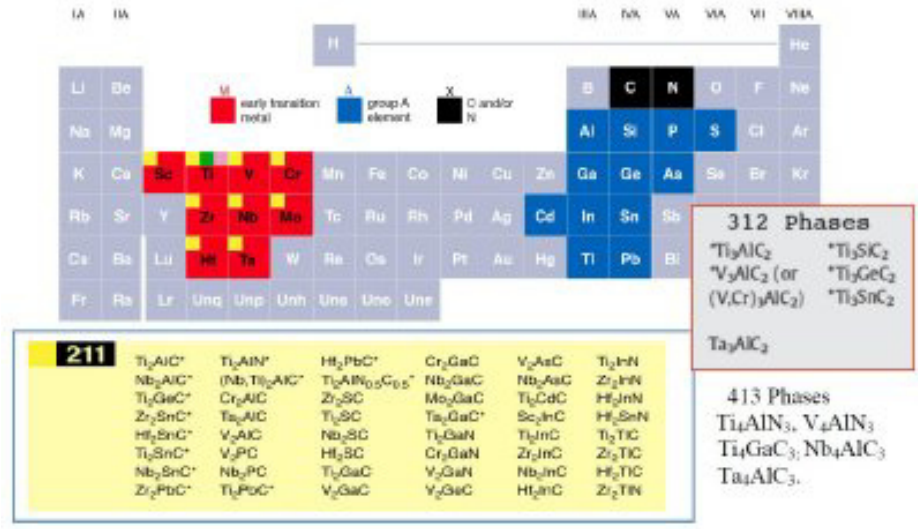

Figure 10 Elements in the periodic table that react to form MAX phases. **(35)**

<u>Note:</u> The red squares represent M-elements, the blue A elements and the black or X is C or N. The currently known phases are 211, 312 and 413. The first two discovered in the 60's by Nowotny and his coworkers.

Until 2004, more than 50 M_2AX phase compounds had been identified, only three M_3AX_2 compounds (Ti_3SiC_2, Ti_3GeC_2 and Ti_3AlC_2) and one M_4AX_3 compound (Ti_4AlN_3). In the last ten years up to nine MAX phases have been reported. Further investigations since then have found other possible probable stable phases Ti_4AlC_3, V_4SiC_3, etc. which have been identified although there still remains need of confirmation by experimental work of them being stable phases. (36)

MAX phases are a somewhat uncertain kind of material with both metallic and ceramic properties; their classification is still unclear. These carbides and nitrides posses unusual and even unique physical, chemical, mechanical and electrical properties. They are electrically and thermally conductive, machinable, not susceptible to thermal shock, plastic at high temperatures and exceptionally damage tolerant. A brief summary of the combined properties of both sorts of materials can be seen in Table 4.

Metal properties	Ceramic properties
Machinable	Refractory
Thermally and electrically conductive	Oxidation resistant
Resistant to thermal shock	Stiff
Plastic at high temperatures	Light
	Relatively low thermal expansion

Table 4 Ceramic and metallic properties of MAX phases

Besides the properties mentioned above some MAX phases like Ti_3SiC_2 and Ti_2AlC are elastically rigid, lightweight, creep, fatigue, oxidation and corrosion resistant and maintain their strengths at high temperatures. It is worth mentioning, given the fact that they will be used to coat a titanium alloy in this project, that most of the MAX phases are better electric and thermal conductors than Ti.

From all the properties MAX phases have, there's one of utter importance due to the implications it comes along with, its machinability. The ease of machinability allows first of all fabricating cheap prototypes, which results in saving money; secondly in cases where very tight tolerances are required they manage to prevent the post-machining step that usually needs to take place; and last of all it facilitates joining.

Three of their properties characterize the unique way they deform in comparison to other solids, especially to layered solids. They are:

- The metallic-like nature of the bonding.
- Basal dislocation slip.
- The unique combination of kink and shear band formation joined with the delaminations of individual grains.

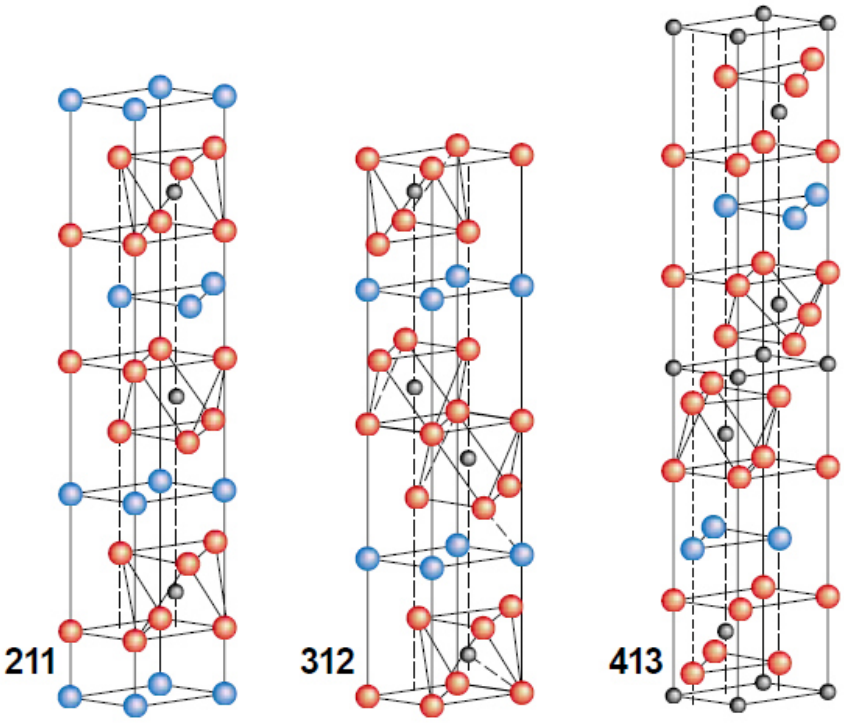

Figure 11 Crystal Structures of MAX phases. **(37)**

<u>Note:</u> The blue atoms correspond to the A-group element (for the phases we are working with either Si or Al), the red ones represent Ti and the black ones are the carbide.

It is not any particular property of MAX phases what is expected to make them revolutionary, but rather, the combination of all of them. Unfortunately, their synthesis process both in bulk and powder form is quite complex and the cost of these powders is between $500 per kg. (38)

Bulk synthesis of these carbides has been done by a large variety of processing techniques, some of which include: Hot isostatic pressing (HIP), Spark Plasma Sintering (SPS), Combustion Synthesis (SHS), Slip Casting (SC) or Pressureless Sintering (PS). In addition to pure MAX phases the number of solid solutions is greater, being this a promising way to discover new MAX phases.

When their discovery was made the field where their impact was expected to have the greatest potential was the transportation one, given the need to improve the efficiency of planes and cars beyond the current performances.

Some of the potential MAX phase applications considered are their use in heating elements, gas burner nozzles in corrosive environments, high-temperature bearings and diamond/Ti_3SiC_2 composites for dry drilling of concrete. (35)

The most studied phases up to the present date are Ti_3SiC_2, Ti_2AlC and Ti_4AlN_3.Though the investigations carried out have lightened the way the path ahead in the study of MAX phases is still very long and many mysteries still await to be solved.

3.2 Synthesis of MAX phases

MAX phases have many ways in which they can be processed, as bulk materials, powders, porous foams, coatings and thin films. The three main possible forms in which MAX phases can be synthesized will be described in what follows. (39)

3.2.1. Synthesis of bulk MAX phases

At the beginning the procedures used to synthesize MAX phases were based on either the reaction of gaseous reactants at temperatures of the order of 2273 K or involved Chemical Vapor Deposition (CVD) (29), (40)- (41) These processes where not practical for the production of bulk MAX phases. Later techniques used were Hot Isostatic Pressing (HIP) or the latter combined with combustion synthesis. These processes had the drawback that unwanted phases as TiC also formed, but the quickness of the reaction developing from the combustion synthesis was so attractive that although the trade-off made was quality vs. speed these techniques spread soon enough for the synthesis of other MAX phases as Ti_2AlC and Ti_3GeC_2.

Bulk MAX phase synthesis was also attempted by Pulsed Discharge Sintering (PDS). This process is similar to HIP by holds several advantages over the previous. By PDS synthesis it only took a few minutes to obtain single phase, fully dense compounds, starting off from different molar ratios of reactants Ti/SiC/C (42)- (43)- (44)- (45),Ti/Si/TiC (42), (46), Ti/Si/TiC (40)- (41)-

(42)- (43), Ti/SiC/TiC (47)and Ti/$TiSi_2$/TiC (48). HIP and PDS hold the drawback that they cannot be easily applied to mass production. (31)

A more economical method is pressureless sintering. When developed at first, mechanical alloying was used; this caused the creation of a high amount of unwanted phases. Sun et al. eventually discovered an effective method of achieving a high purity by this method. It was later discovered that an effective way to improve density and formation of the target phase was achieved by adding small amounts of Al. (49)

3.2.2. Synthesis of MAX phase films

The first deposition method used for MAX phase films was CVD. This method was not very effective resulting in the formation of single phase samples with strange properties and later failed to create single phase films. Physical Vapor Deposition (PVD) methods however, were successful. By magnetron sputtering Ti_3SiC_2 and the Ti-Al-C, Ti-Al-N and Ti-Ge-C systems were able to be synthesized (50)- (51)- (52)- (53)- (54). Besides the already mentioned, pulsed cathodic arc, plasma sprayed coatings and high velocity oxy fuel spraying techniques have also been used.

Formation of thin phase films usually takes place at high synthesis temperatures limiting their potential industrial use. Lower temperatures, in the 300 ℃ range create nanocomposite films which are very promising for coating electrical friction contacts due to their good electrical conductivity and resistance to wear and corrosion. MAX phase films are not yet applicable for deposition on large areas but there is the perspective that not far from now this limitation will be overcome. (55)

3.2.3. Synthesis of MAX phase powders

Synthesis of MAX phase powders is an excellent alternative to bulk synthesis and allows an increase in the applications related with the synthesis of MAX phase composites. MAX phase powder can be obtained from porous samples or made directly in this form. The first Ti_3SiC_2 powders that were synthesized were done by the combustion reaction process. To obtain good MAX phase content in the powders variations were done to the previous. By a fluctuation synthesis method or a solid-liquid reaction process with NaF (sodium fluoride) addition powder of less than 85 wt.% can be obtained. Higher purity powders can be achieved by isothermal heating of Ti-Si-TiC powder mixtures. The typical size of the particles obtained by this method ranges from 2-4 µm. (56)

Both Ti_3SiC_2 and Ti_2AlC powders, which have been used in our experiment, are patented and registered as Maxthal 312 and Maxthal 211 respectively. The properties of these powders are given by the Swedish Ceramics Institute in Gothenburg, Sweden and can be seen in Table 5.The powders are obtained by isothermal heating. According to what is stated in the patent the process in order to obtain the 312 powders three main components are required for the initial powder mixture:

1. A transition species (M): In this case Ti.
2. A co-metal (A): Si
3. A non-metal (X): C

Usually the starting point of the powders is also a powder mixture. The particle sizes will vary according to the component we are dealing with. The transition metal species will have an average particle size ranging from 1 to 100μm, the co-metal from to 0.1 to 80μm and the non-metal from 0.1 to 100 μm. To obtain a single pure phase 312 the phase content of the phase obtained ought to be about 95 vol.% or more.

The powders are then mixed for about two hours thoroughly with a machine to obtain an homogeneous mixture. They are then heated in a controlled way to a temperature around 1300-1550°C, the heating rate should be lower than 25°C/min otherwise ignition of the powder mixture could occur. The sealed zone in which the mixture is heated should contain a minimum amount of O_2, maximum 1×10^{-8}. The sealed atmosphere usually contains a noble gas such as Argon. By following this process the powders will be formed after the heating process and if wanted they could be sintered to form bulk phases. The stoichiometry obtained in the final powders is 3:1:2**.** (56)

The process followed to obtain Maxthal 211 is similar; the only variation will be the starting point powder mixture.

	Maxthal 312	**Maxthal 211**
Flexural strength at RT, MPa	350	250
Hardness, GPa	4.2	4.0
Fracture toughness, K_1C ($MPam^{½}$)	8	7
Thermal shock, ΔT(°C)	1400	1400
Max. service temperature, °C (°F)	1000 (1830)	1450 (2640)
Density, g/cm^3	4.5	4.2
Thermal expansion, K^{-1}	$9x10^{-6}$	$8x10^{-6}$
Thermal conductivity, W/mK	32–37	40
Composition	Ti, Si, C	Ti, Al, C

Table 5 Properties of Maxthal 211 and 312 powders. Source: Swedish Ceramics Institute. Gothenburg, Sweden.

Figure 12 Maxthal 211 and Maxthal 312 Powders fabricated by Sanvik heating technology, Sweden (38)

3.3 Background on Ti_3SiC_2 and Ti_2AlC

3.3.1. Ti_3SiC_2

On the contrary to most MAX phases Ti_3SiC_2 has an elaborate history. The discovery of Ti_3SiC_2 took place when fabricating hard borides and carbides. In an attempt to improve the poor oxidation resistance exhibited by the later Bo was substituted for Si, this change seemed to solve the problem and led to the study of Ti-C-Si systems, eventually leading to the discovery of Ti_3SiC_2 in 1967. (37)

Already when discovered Nickl et al. (57) noticed it was clear that it was not like other carbides for the fact that it was too soft. Additionally, it was discovered that its hardness was an anisotropic property of the material, opposite to that of other carbides. Twenty years later the results obtained initially were corroborated by Goto and Hirai (41).

BULK SYNTHESIS

Ti_3SiC_2 was synthesized for the first time in 1967 by Wolfgang Jeitschko and Hans Nowotny at Vienna University; its structure was also studied. It was not until 1972 when a polish group guided by Roman Pampuch in Poland got close to obtaining a single-phase bulk sample; they were able to achieve 85% volume purity. (37)

As Ti_3SiC_2 is a material that doesn't melt, what it does is it decomposes in non-stochiometric TiC and Si, which evaporates. It is stable up to 1600℃ either in vacuum or in an Ar atmosphere, but its stability decreases when placed in a N_2, O_2, CO and CO_2 atmosphere. When exposed to the atmosphere it is stable to oxidation up to 1100℃. Synthesis of Ti_3SiC_2 has been developed by processing of different starting products. A recent work on the topic has been done by Jóse M. Córdoba et al describing different synthesis procedures. (58)

Usually, the starting materials used for its synthesis are: 3Ti/Si/2C, 3Ti/SiC/C, Ti/Si/2TiC, 4Ti/2SiC/TiC and 2Ti/2Si/3TiC.

Standardization of the synthesis process is not possible because in every process used to synthesize Ti_3SiC_2 different proportions of other phases are formed as well (TiC, SiC, $TiSi_2$ and Ti_5Si_3)

The methods used to process it are those mentioned in the introduction. Although the synthesis of this phase has been one of the main topics of research results obtained by different people are easily misinterpreted and in many cases they can turn out to be contradictory. Different authors, for example propose different global reactions for its synthesis. Below we can see the two mentioned by José M. Córdoba and Wu et al. (see the table below).

DIFFERENT SINTHESIS MECHANISMS PROPOSED
Wu et al.→ From it we can Ti_3SiC_2 seems to be able to nucleate on top of TiC or Ti_5Si_3C crystals. (59)
$$9Ti + 3SiC + 3C \rightarrow 4TiC + Ti_5Si_3C + C \rightarrow 3Ti_3SiC_2$$
José M. Córdoba→ Ti_3SiC_2 only grows on $Ti_5Si_3C_y$ by diffusion of C and Ti atoms. (58)
$$Ti_5Si_3C_y + TiC_{1-x} + (3 + x - y)C \rightarrow 2Ti_3SiC_2 + Si \uparrow$$

Table 6 Proposed synthesis mechanisms for Ti_3SiC_2 (60)

Despite the different mechanisms proposed, something they both agree on is the fact that $Ti_5Si_3C_y$, with variable carbon content, is of major importance in the formation of Ti_3SiC_2; being found as a subproduct in nearly all MAX phases.

PROPERTIES

Experiments with these samples showed that Ti_3SiC_2 is quite stiff, being almost 3 times as stiff as Titanium with the same density (done with the samples from Pampuch's bulk synthesis).

Other outstanding properties of MAX phases (of this MAX phase in particular) are (37)**:**

- Regarding their oxidation resistance (up to 1400°C): after leaving a sample over the weekend at 1000°C showed it had gained less than 1% weight, proving it was able to resist oxidation.

- Resistance to thermal shock: Heating the material to high temperature and then quenching it in water (the higher the heating temperature the more probable it is the material will shatter) they showed that even at 1400 °C the material was able to survive, but also, that its strength increased after quenching.

- High Young's modulus (~ 325 GPa).

- Relatively low hardness (4-5 GPa).

- Machinability: It is as machinable as graphite (once you break through the hard crust of TiC).

This is just an overview of the properties which will be seen in a more detail in section 3.4.

Titanium silicon carbide has an odd nature even when compared to other phases. On the one hand the metallic properties it possesses are being machinable, thermally and electrically conductive, resistant to thermal shock and plastic at elevated temperatures, whereas on the other hand, being refractory, oxidation resistant, quite stiff and relatively light are properties that correspond to ceramics. Another property that makes it closely related to ceramics is its coefficient of thermal expansion, which is low, being more similar to that of ceramics than of metals (see Table 4).

Similar compounds, which behave like Ti_3SiC_2, known as 312 compounds, have been identified. They are Ti_3GeC_2 and Ti_3AlC_2. In the 80's Ti_3SiC_2 started to be extensively studied, revealing some of their mechanical properties.

The importance of MAX phases and the ignition of their worldwide research was detonated by the amazing properties discovered in Ti_3SiC_2. But not all is advantageous, Ti_3SiC_2 already has several disadvantages. To start off it is quite brittle at room temperature, something that could be solved by orienting the grains. It is quite clear that study of these phases will be focused on their microstructure and how it affects its material properties, on their effect in solid solutions and on their behavior as reinforcement phases, to be able to improve the properties which are of major interest in each case.

3.3.2. Ti_2AlC

Ti_2AlC belongs to the 211 MAX phase group, also called H phases at the beginning. The structure of the H phases is made up of layered and hexagonal M_2X layers combined with layers of the pure A group element. The history of this group of phases of quite brief and is mainly reduced to the synthesis of Ti_2AlC and Ti_2AlN by Russians in the 70's and the description of Ti_2AlC and Cr_2AlC in two Russian reports, besides that not much information has been reported.

From the MAX phases Ti_2AlC along with Ti_3AlC_2 are the most light-weight and oxidation resistant layered ternary carbides, making them be promising in many applications related with high temperature applications. They display superior properties such as fracture toughness, electrical and thermal conductivities, and oxidation resistance over their binary counterpart. (61)

3.4 Crystal Structure

MAX phases are layered hexagonal crystal structures with two formula units per unit cell. Their general formula is $M_{n+1}AX_n$ (where n=1, 2 or 3 for sure up to the current date). The general way in which these materials are referred to is as 211 (n=1), 312 (n=2) and so on. In the nomenclature used M is the transition metal, A the group element and X nitrogen or carbon. According to the X element that the MAX phase holds they can be called either MAN, if the X element is nitrogen or MAC if it is carbon.

Transition metals known to form MAX phases are: Sc, Ti, V, Cr, Zr, Nb, Mo, Hf and Ta. The A group element denomination owes its notation to the old CAS notation used (old American nomenclature for the periodic table), this element is one of those seen in columns 13 to 16 in the periodic table (Al, Si, Ge…).

Ti_2AlC and Ti_3SiC_2 are structurally related to ternary carbides, they crystallize in the $P6_3/mmc$ (Wyckoff Positions of group 194) space group. A summary of its crystallographic information can be seen in Table 7.

Their crystal structure can be seen as an alternative stacking of edge-shared M_6X octahedra (Ti_6C in our particular case) and two-dimensional close-packed Al plane. The only changing parameter in both structures is the number of stacked Ti layers in every Al-/Si- plane. For n, the A-layers are separated by n+1 M-layers. Therefore for Ti_2AlC n=1 the number of Ti in each Al plane is two and for $Ti_3SiC_2$the number of Ti layers in each Si plane it is three (see Figure 11).

Compound	Lattice parameters	Atoms	Wyckoff positions	Internal coordinates		
Ti_2AlC	**a=0.304 nm c=1.360 nm**	**Ti Al C**	**4f 2d 2a**	**1/3 1/3 0**	**2/3 2/3 0**	**0.086 3/4 0**
Ti_3SiC_2	**a=0.3075 nm c=1.858 nm**	**Ti(1) Ti(2) Al C**	**2a 4f 2b 4f**	**0 1/3 0 1/3**	**0 2/3 0 2/3**	**0 0.128 0.25 0.564**

Table 7 Crystallographic information of Ti_2AlC and Ti_3SiC_2. (61)

Up to the current date the phases that have been confirmed have shown a M_3AX_2, M_2AX and M_4AX_3 structure. However, phases awaiting confirmation with $n \geq 4$ are known to exist. At least, Ta_6AlC_5 (n=5) for sure, others like $Ti_7Si_2C_5$ are still uncertain. It is believed that even more phases can be discovered by assuming stochiometric compositions and making them by high temperature sintering. (36)

All the previous can be mentioned regarding the crystal structure. For the microstructure on the other hand it is known that it plays a major role affecting the physical, mechanical and chemical properties of the materials. Microstructure studies are mainly done by investigating XRD and the grain boundaries, which are known to determine the high temperature properties of MAX phases.

3.5 Properties of MAX phases

MAX phases have shown to have unique mechanical, chemical, thermal and physical properties. The most extraordinary properties have been revealed mostly in their mechanical performance. This performance has been attributed to their nanolaminate structure.

The most studied MAX phase so far is Ti_3SiC_2, for this reason its properties are the ones that are best determined. In this section an overview of some of the general properties of MAX phases will be done focusing specially on the two MAX phases involved in our study ($Ti_3SiC_2$and Ti_2AlC). When mentioning their oxidation resistance a more detailed description will be provided due to its importance in this project.

POLYMORPHISM: MAX phases have polymorphic phase transformations. Polymorphism is different for each MAX phase's structure, in 211 and 312 phases it is related with the different positions the atoms in the unit cell can take, whereas in 431 phases however, it is not clear what determines polymorphism as these phases seem to exhibit different stacking sequences depending if it is an α orβ structure. (37)

ELECTRICAL CONDUCTIVITY: MAX phases are in general excellent conductors, as the temperature increases so does the conductivity. Ti_3SiC_2 and Ti_3AlC_2 are better electric conductors than titanium. (31)

Some phenomena, like the Hall Effect and the Seebeck-Peltier Effect influence the electrical properties of materials. Some MAX phases ($Ti_4AlN_{2.9}$ and $Ti_3Al_{1.1}C_{1.8}$) have a positive R_H (Hall coefficient) and are consequently electron hole carriers; Ti_3SiC_2 on the other hand may have either a positive or negative R_H, appearing to be a compensated conductor. Yoo et al. (62) showed that Ti_3SiC_2 has a negligible Seebeck coefficient, being a mixed conductor in terms of the temperature and confirming what Barsoum had already mentioned in 2000 (28).

SPECIFIC HEAT: The specific heats of MAX phases in comparison with titanium are greater because of their large specific stiffness. (31)

THERMAL CONDUCTIVITY: MAX phases are good thermal conductors due to their good electrical conductivity. In Figure 13 the thermal conductivity of several MAX phases is displayed showing that Ti_2AlC's thermal conductivity is greater than both TiC, TiAl, Ti_3SiC_2 and pure Ti. (28), (31)

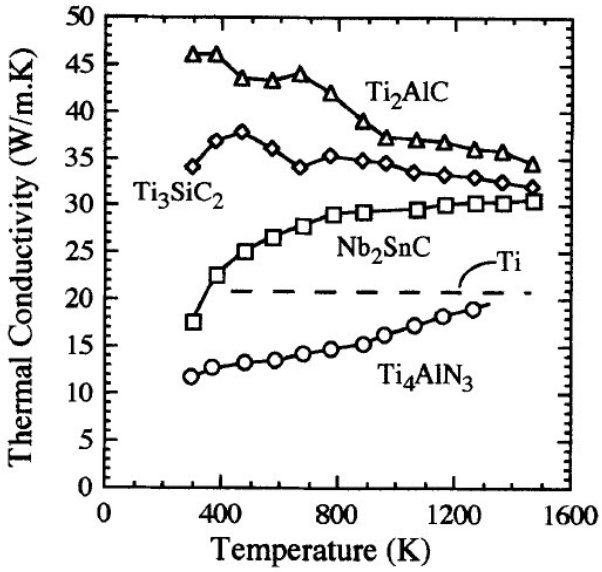

Figure 13 Thermal conductivity of some representative MAX phases (28)

THERMAL EXPANSION: MAX phases tend to have little anisotropy to thermal expansion. Quite recently MAX phases with high thermal conductivity have been discovered, so far the one with highest thermal conductivity known is Cr_2GeC, making it an excellent candidate for coating large areas on steels. (31)

ELASTIC PROPERTIES AND DEFORMATION: MAX phases are in general elastically stiff; being the most stiff the 413 and 312 phases. Stiffness is related to the number of M-X bonds, for this reason as 211 phases possess a lower number of M-X bonds than the 413 and 312 compounds it makes sense that the latter are the less stiff compounds. (63)

According to Barsoum (28) the deformation properties of MAX phase materials are determined by a single slip system located in the layers of the A atoms. In particular Ti_2AlC has a high elastic constant. (31)

Ti_3SiC_2, Ti_2AlC and Ti_3AlC_2 on the other hand have a non-linear elastic deformation when subjected to cyclic loading they Kink. Kinking is a form of plastic buckling; it is a quite common phenomenon which happens in materials with high anisotropy in their slipping tension.

These MAX phases deform forming *'Kink Bands'*. '*Kink Bands'* usually result in a decrease in the mechanical integrity of materials; once damage starts the point damage becomes weaker leading to further damage and point failure. In MAX phases even after damage initiation the ternary phases can still carry

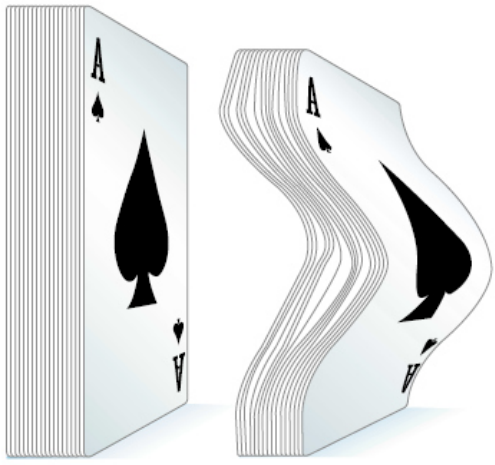

Figure 14 Kink Bands analogy. Explanation of the behaviour of MAX phases by card-deck analogy. (37)

substantial loads, this phenomena is called *damage tolerance*. In most materials this does not happen, usually once damage starts, the point where damage is occurring starts giving in getting weaker and leading to eventual failure. (63)

The behaviour of Kink Bands can be explained using a deck of cards (see Figure 14). When a deck of cards is subjected to a pressure from the top each card bends as each one bends progressively, however as the load is removed it returns to its original position. (28)

Additionally, Kink boundaries have the ability of stopping crack propagation, once the damage starts instead of weakening the area as in other metals Kink Boundaries tend to harden it and therefore the damage moves to another area. (37), (39)

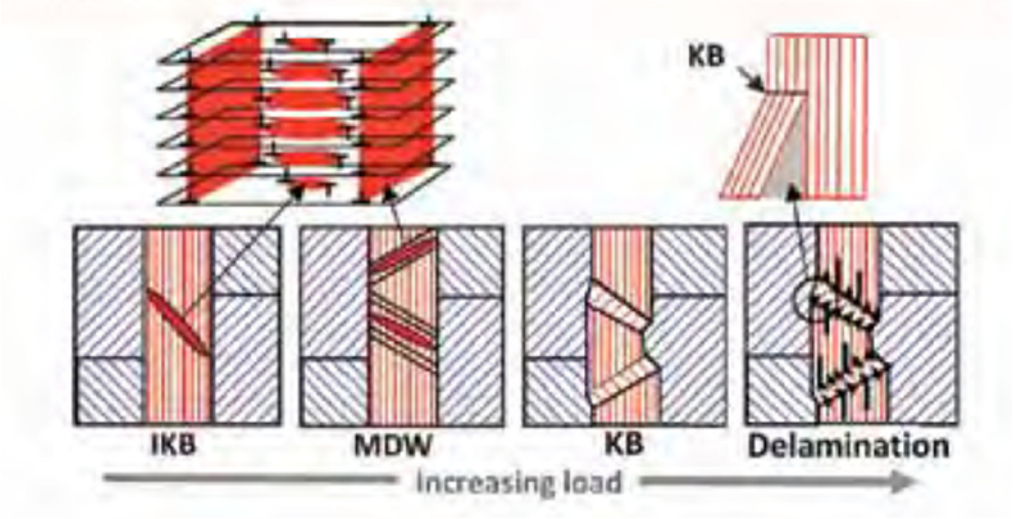

Figure 15 Schematic formation of an incipient Kink band, mobile dislocation Kink Bands and delaminations. (38)

Note: Red grains are hard grains, while blue grains are soft grains with the basal planes favourably oriented for easy slip.

HARDNESS AND MACHINABILITY: MAX phases have a low hardness (1.4-8 GPa). It is their low hardness combined with their layered nature is what makes them so easily machinable.

OXIDATION RESISTANCE: MAX phases oxidation resistance is related with the composition and properties of the protective scale formed under oxidation. Ti_3AlC_2 and Ti_2AlC are exceptionally oxidation resistant because they form a stable and adherent protective Al_2O_3 scale. The formation of this highly protective alumina scale has led to comparison of their oxidation resistance with that shown for Ti-Al alloys, which up to date are the most used kind of titanium alloys used for high temperature applications in components such as turbines. (61)

Studies carried out by Meier et al. (64) and Rahmel and Spencer (65) done in Ti-Al alloys showed that they do not create a protective alumina scale but rather a scale composed of TiO_2 and Al_2O_3. Comparing the minimum Al content needed to form a continuous layer of Al_2O_3 in

Ti-Al alloys with the amount of Al needed for Ti_2AlC, the former is much lower. Bonds between the elements were also studied by other scientists, Zhou and Sun (66), to see how bonding could determine the protective scale formed. The conclusion they reached was that as the bonding created between Ti-C is strongly covalent and the one for Ti-Al is weak. The strength of the covalent bond would decrease the activity of Ti, therefore increasing the activity of Al, which is high enough then to be preferentially oxidized. These two factors mentioned; the low Al content to form a protective scale and the bonding, make the formation of a continuous Al_2O_3 layer on Ti_2AlC favorable. These exceptional characteristics are what made Brady and al. (67)- (68) propose them as oxidation resistant coatings for materials in the Ti-Al system.

Ti_3SiC_2 on the other hand forms a SiO_2 layer. SiO_2 has the advantage that it is almost impermeable to oxygen. Of all MAX compound the only one that contains Si is Ti_3SiC_2, but its concentration is not enough to form a pure layer of SiO_2 so a duplex layer of SiO_2 and TiO_2 forms instead. This layer is as protective as Cr oxide but increasing the temperature the oxidation rate becomes troubling. To avoid this, the surface is reacted with silicon to form $TiSi_2$ and SiC; this is able to improve the oxidation resistance 5 orders of magnitude. (28)

Although the protective character of the scales formed for MAX phases is mentioned among the relevant characteristics of these materials, it is of importance to mention that there exist discrepancies on the studies that have been carried out. Not all the scales formed in experiments have proven to be protective. Investigations have shown that the purity of the samples is determinant. The presence of TiC largely influences the final protection achieved by the scale. TiC/TiC_x's presence is known to be detrimental to the oxidation resistance given studies done by Wang and Zhou. (69)

CORRODION RESISTANCE: MAX phases are also corrosion resistant; however corrosion resistance of all MAX phases has not yet been established. The key to the corrosion resistance of MAX phases is the formation of a passivating layer. In some cases phases such as Ti_3SiC_2have shown to be even more oxidation resistant that pure Ti; the reason for such a behavior is the formation of the thin passivating layer of SiO_2 formed. Other MAX phases also exhibit good corrosion resistance; such is the case of $Ti_3GeC_2$and Ti_2AlN. (31)

3.6 Potential Applications

Due to their excellent electrical, thermal and high-temperature mechanical properties, MAX phases are being considered for use in structural and nonstructural high temperature applications. Barsoum listed in 2000 (28) the potential applications of MAX phases exploiting their excellent properties. Some of the uses he mentioned were their use in heat exchangers, given their high temperature resistance, in rotating parts, due to the low friction and others related with their use as oxidation and corrosion protective materials. The list of potential applications is quite large so only a few will be mentioned: (31), (35), (38), (61)

- Heating elements and electrodes.
- Directly heated catalyst support for automobiles.

- Oxidation and corrosion resistant films or coatings.
- Aeronautical industry: It is expected that light phases such as Ti_2AlC and Ti_3AlC_2 might find a use in this field.
- Free-cutting elements.
- Microelectronics.
- Biomaterials.
- Defense applications.
- Nuclear applications: cladding materials.
- Toughening brittle ceramics.

So far, MAX phases have been successfully used in:

- Gas burner nozzles: Ti_2AlC has shown to behave much better than steel when in corrosive environments. When exposed to a sulphur gas corrosive environment a protective α-Al_2O_3 layer is formed allowing an increase of 200K in the process temperature. The former and the excellent machinability have led to a substitution of steel nozzles for Ti_2AlC ones**.** (31), (70)

- Foil bearings: Given the low friction and wear, combined with the high temperature of MAX phases they have been used for foil bearings at temperatures between 25-823 K. (31)

- Pantographs: In China MAX phases are currently being implemented in pantographs in the high speed railway train as they have shown to perform better than carbon based ones. (31)

- Oxidation resistant coatings: Application on large steel areas by the PVD process have already been carried out with successful results. They have also been proposed, by Brady et al. (67)- (68), as candidates to coat intermetallic phases (Ti-Al) as Ti_3Al to increase the oxidation resistance, especially Ti_2AlC and Ti_3AlC_2. (61)

- Light-weight armor materials: Early investigations already showed their suitability in add-on ceramic armors. (61)

- Composites: Both MAX and MAX-based metal composites have been studied. Experiments with the addition of Ti_3SiC_2 in Cu matrix composite have been done showing superior mechanical properties than single Cu-graphite composites. To solve the problems encountered when adding large volume fractions of Ti_3SiC_2, the composite was reinforced with Cu coated Ti_3SiC_2 achieving this way a higher density and a more homogeneous distribution. To Cu matrix composites other MAX phases have also been added, as $Ti_3AlC_2$and Ti_2SnC. In the case of Ti_3AlC_2 without reaching positive results as the electrical conductivity was reduced two orders of magnitude with respect to the original matrix composite. On the contrary, Ti_2SnC (which has the highest electrical conductivity of all MAX phases known) has shown to be the best possible MAX phase reinforcement for Cu as far as mechanical and electrical

properties are concerned. Ti_3SiC_2has also been added to hydroxyapatite at 50 vol.%, decreasing the hardness and increasing fracture toughness and strengths as the Ti_3SiC_2content increased, favouring bio-mechanical applications. (31)

3.7 Future Investigations

Ever since the discovery of MAX phases, more than 40 years ago, more than 1000 papers have been published. Out of all the publications around half of them are focused on Ti_3SiC_2, therefore studies of other phases still remain. As use of MAX phases in the market and industry has not yet widespread it is expected that as their use increases further research will be carried out leading to new discoveries on the field. (38)

So far research has been quite limited, there are still many mysteries hidden in these compounds which yet await to be solved. In order to be able to progress in the study of these compounds it is of major importance to be able to know which phases are mechanically and thermodynamically stable. The main priorities on the study of MAX phases so far are the understanding of their properties, which still remains unclear and the discovery of new phases. As new synthesis methods have been developed in the past years this last priority would seem to have been eased. (31)

MAX phases could be a possible solution to the brittleness encountered in ceramics. For some time the possibility of increasing turbine efficiencies has been considered to be closely related with an increase in the operating temperatures. This increase has been thought to be possible by using ceramic materials. Up to now the limitation has been the brittleness of ceramics, but as MAX phases overcome this limitation they might be just what has been yearned for so long. Superalloys have been used in this sector as an alternative but it has been shown that their trade-off between performance and cost is not as positive as expected. Superalloy components need large amounts of cooling air, decreasing the efficiency of the engine.

Increasing the operating temperature to around 1300℃ would provide an efficiency increase of 20% in the fuel consumption, doubling the power obtained for the same engine size. As MAX phases are in general light materials, resistant to high temperatures and oxidation and corrosion resistant a possible sector in which they could be used in the gas turbine one. (37)

The resistance of MAX phases to high temperatures has led to a large study on MAX phases for this purpose, being one of most up to date applications being explored nowadays the use of the Ti_2AlC MAX phase not just as a heating element, but also as a gas-heated surface emitting heat radiation element. (71)

CHAPTER 4: COATINGS

4.1 Introduction

Coatings are surface treatments done in order to be able to improve certain properties of the material they are covering. A coating as such is any protective film applied to the surface of an object. For thousands of years coatings have been used with decorative purposes. It was after World War II when their industrial importance was noticed. All forms of transport (trains, ships, aeroplanes…) and metallic structures require the use of coatings, for this reason this industry has one of the largest productions. (72)

Just as it has been mentioned previously, poor corrosion and oxidation resistance of materials at high temperatures increases the interest set into finding possible solutions to overcome their effects. There are three possible ways of improving oxidation resistance: by addition of alloying elements, by pre-oxidation and by coatings. Corrosion and oxidation protection by the use of coatings is one of the most common methods used. (3)

Some of the solutions that have been subject to experiments are adding an alloying element or carrying out a surface treatment. However, using alloying elements to modify the microstructure of a material can lead to negative results in the mechanical properties. This happens for example when alloying silicon with titanium as silicon tends to modify the properties of titanium. The former reason is one of which leads to the preferred use of surface treatments rather than bulk alloying to improve the oxidation resistance of materials. (1)

Oxidation attack is mainly limited to the outer part of the component and as the mechanical properties are determined for the whole cross-section, surface modifying technologies, specially coating techniques seem to be a very promising method to achieve both oxidation protection and the desired mechanical properties. It is in this field where high temperature coatings gain importance.

High temperature coatings must satisfy a series of requirements to fulfill different purposes; these requirements are listed in Table 8.

Property	Requirement
Oxidation Resistance	During oxidation the coating material must form a protective oxide scale on the basis of Al_2O_3, Cr_2O_3 or SiO_2.
Compactness and gas tightness	The coating must be free from cracks, pores or other defects, which can be paths for fast diffusion of aggressive components from the atmosphere.
Adhesion	Good adhesion between substrate and coating prevents spallation of the coating.
Chemical Compatibility	The chemical composition of the coating must be similar to that of the substrate material to decrease the concentration gradients of the elements, thus limiting interdiffusion in the system.
Physical Compatibility	Phases in coating and bulk material must have similar physical properties to reduce mechanical and thermally induced stresses.

Table 8 Property Requirements for high temperature coatings (73)

Additionally, to achieve proper oxidation resistance there are several key factors that have to be taken into consideration. First of all, the coatings must be thermodynamically stable, creating a protective surface scale of uniform thickness. Secondly, they must have a slow growth of the protective surface scale. Good substrate adhesion properties, determined greatly by the coating method used. And last of all, they should not cause degradation of the substrates' mechanical properties. (74)

Coatings can be applied by a large variety of methods according to desired properties, cost, etc. Methods such as powder siliconizing or pack cementation are very efficient and inexpensive coating techniques used to modify the surface of titanium base alloys. Despite there being so many coating methods, the application of coatings by the slurry method (technique used in our experiment) has drawn much attention and has gained large acceptance in the industry because the application process is easy, low cost and flexible. Application of the coating can take place by several means, by using a brush, by immersion of the substrate in the slurry or by spray coating. (75)

Trends in coating processes to improve oxidation and corrosion resistance of substrates have varied as time has gone by. The life of coatings has increased also to up to 20 times thanks to the development of new processes and to an increase in their use in the industry to increase the life of their components.

Life of coatings is determined by composition, thickness and the homogeneity of deposition. Most of the new coatings applied nowadays are done by the Plasma Spray technique to ensure proper and controlled deposition.

4.2 Fundamentals of the Oxidation phenomenon

In order to achieve a better understanding of the phenomenon under study several questions should be answered. They are: What exactly is oxidation? Where does it take place? And, how does the oxide scale form?

To start off, oxidation is the phenomenon that takes place when a metal is exposed to an oxidizing environment. When this happens metal consumption takes place forming an oxide scale that separates the metal surface from the oxidizing environment. Oxidation, just like hot corrosion reactions, mainly occur at a material's surface.

The oxide layer formed is what protects the sample from further oxidation by slowing down the rate of consumption of the metal. Oxidation protection is therefore achieved by the formation of an oxide scale. The key to an oxidation resistant material is for this reason the ability of a material to form a long-term protective scale.

In order to achieve oxidation protection, not only does the coating need to satisfy several requirements but also oxide scales formed must fulfill the next (3)**:**

- Have a high thermodynamic stability: high negative Gibbs energies of formation.
- Low interdiffusion between the oxide scale forming elements.

- Low vapor pressure of the oxide: This way the oxide will form as a solid and won't evaporate.
- Crack healing ability.
- Good adhesion with the metal.
- Thermomechanical compatibility with the metal.

The working temperature is also a determining factor. There are a few elements that are able to provide resistance above 1000°C; some of them are Si, Al and Cr. The oxides which have shown to best meet these requirements are: (3)

- **Cr_2O_3:** Limited to service temperature below $1000°C$ due to the formation of volatile CrO_3.
- **SiO_2:** At low partial pressure of O_2 SiO_2 dissociates to volatile SiO.
- **Al_2O_3:** Out of these three oxides it is the most thermodynamically stable of the oxides and provides the best protection in reducing and oxygen deficient atmospheres. (71)

However for the highest temperature applications only Co or Ni based superalloys can be used to stand such extreme conditions.

Oxidation is the result of a chemical reaction in which a change of state takes place. Chemical and thermodynamic reactions use Gibbs Free Energy to quantify whether a reaction is spontaneous or not; therefore to determine whether oxidation will spontaneously take place Gibbs free energy can be used. If Gibbs Free Energy is negative then the reaction will be spontaneous.

The two mechanisms that determine the overall behaviour of the oxidation reactions are thermodynamics and kinetics.

Thermodynamics allows predicting the oxidation products that will be formed but gives no information on the reaction rates. The formation of an oxide decreases the entropy of the system, resulting in a reduction of the oxide stability with increasing temperature. Besides this, the other known aspect is that the enthalpy of formation of the oxide is dependent on the temperature and is related with the partial pressure of O_2 (below this pressure the oxide decomposes into metal and O_2). Other oxidation conditioning aspects are surface preparation of the metal and pre-treatments.

Oxidation kinetics on the other hand explains how the growth of the oxide scale takes place, setting the following steps when dealing with a pure metal surface.

1) O_2 adsorption at the surface.
2) Oxide nucleation.
3) Lateral growth of the nuclei. The thin film separates the metal surface form the environment.
4) Formation of a compact oxide scale.

Once the oxide film is formed its growth is controlled by mass transport.

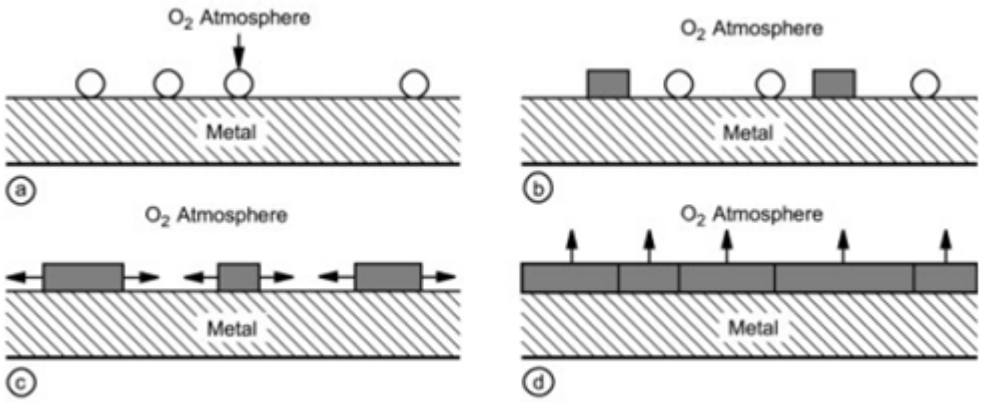

Figure 16 Mass transport of the oxide scale during oxidation of a metal substrate (3)

Note: The steps a), b), c) and d) correspond to the steps 1), 2), 3) and 4) mentioned above.

Oxidation kinetics of different elements and under different conditions may display alternative behaviors. To explain the different oxide growth mechanisms several models have been developed. The three main models with which almost all oxide growth mechanisms can be described are: (76)- (77)

- **Parabolic:** The diffusion of ions through the oxide determines the rate of growth. The rate of growth is inversely proportional to the weight of the oxide formed and therefore its thickness. Most metals and engineering alloys follow this model at high temperatures.

- **Logarithmic:** Characteristic of low temperature regimes in which oxide growth decreases with time. It can be both direct and inverse logarithmic depending on whether it is ion (inverse) or electron (direct) metal transport.

- **Linear:** The rate of oxidation remains constant with time independently of the amount of metal consumed.

In Figure 17 the behaviour of the three growth mechanisms mentioned can be seen, along with a fourth behaviour, the cubic one, less often encountered.

For example, Ti_3SiC_2 oxidized at 1300℃ exhibits a parabolic behavior, whereas increasing the temperature in 100 ℃ it changes to parabolic-linear. (78)

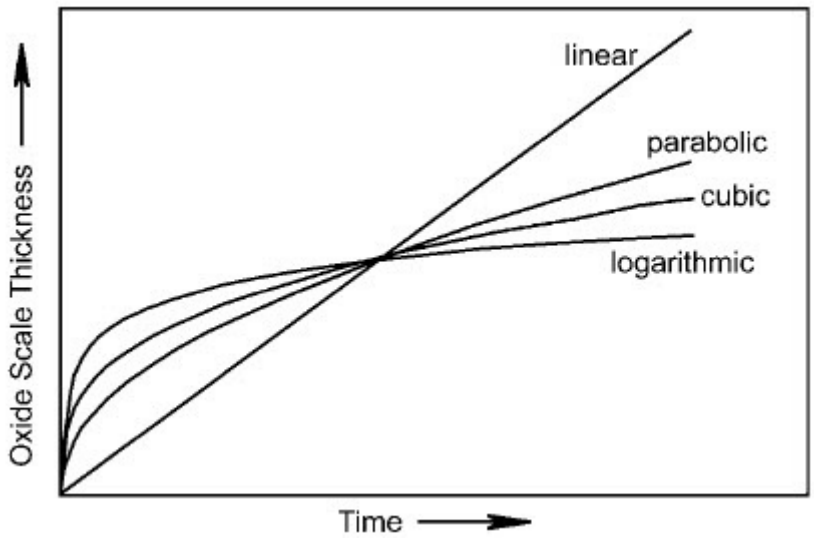

Figure 17 Schematic representation of the rate laws for the oxide scale formation (3)

The oxide scale growth is directly influenced by both the thermodynamic and kinetic mechanisms. Different base substrates will have a higher or lower ability to create protective oxide scales. In Figure 18 a schematic representation on the comparison of the formation of protective oxide scales for different substrates can be seen. (3)

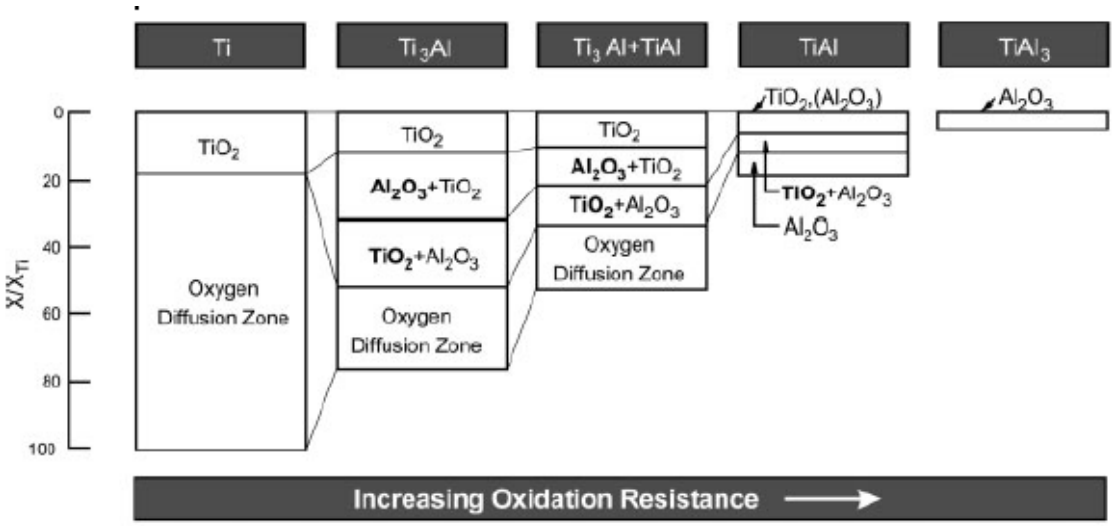

Figure 18 Schematic representation of oxide scales and oxygen diffusion zones of titanium-based alloys. (3)

The effect of temperature on the oxidation rate is determined by Arrhenius's Law. In our case the oxidizing environment to which the samples will be exposed is a high temperature oxygen one. Titanium (our Ti-6Al-4V substrate) has a high solubility of oxygen; more than 50% oxygen is incorporated into the metal, forming a diffusion zone. A smaller amount is used for forming the external rutile (TiO_2) oxide layer. (3)

4.3 Classification of coating techniques

There is a large variety of existing coating techniques which provide surface protection, each of which has its own properties and limitations. In order to achieve the desired properties of a coating a careful study of the appropriate coating method to achieve the latter must be made. The coating method will determine the thickness, uniformity, adhesion of the coating to the substrate, etc.

The large variety of coating methods shows that a successful solution that provides an oxidation-resistant coating has not yet been achieved. The most important and currently available coating techniques used to coat substrates nowadays are: pack-cementation, slurry, hot-dipping and chemical vapor deposition. In Figure 19 the most common coating processes can be seen and how the thicknesses vary according to the method.

In many occasions a coating can be applied by more than one technique. It must be remarked though that not all methods are capable of providing coatings with the same thickness. In what follows a brief overview of some of the coating methods will be made. The coating technique selected for our study, the slurry method, will be described in further detail in the next section.

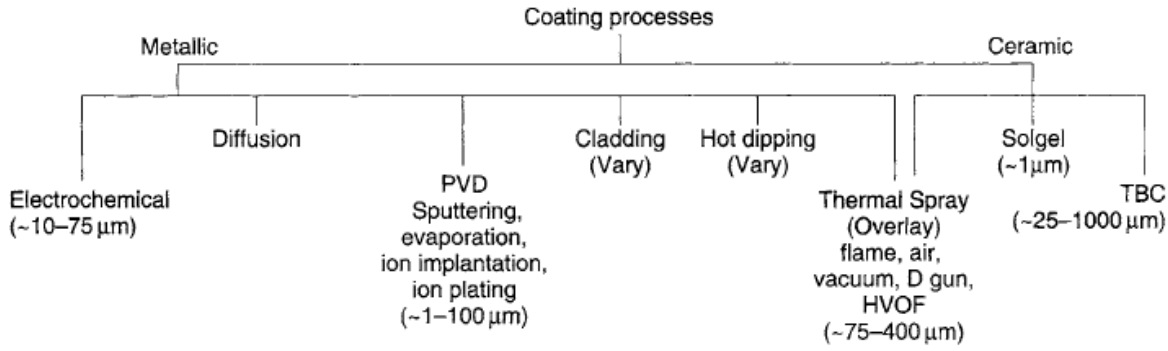

Figure 19 Most common coating processes (74)

According to the mechanism of the coating process high-temperature coatings can be classified into: Diffusion coatings and Overlay coatings. (77)

DIFFUSION COATINGS

Diffussion coatings are coatings in which a substrate is enriched with the oxide scale formers Al, Cr, Si or a combination of them to a depth of 10-100μm. They are basically a kind of surface enrichment in which vapours are deposited. The combination of these elements with the primary constituents of the substrate alloy form intermetallics with significant levels of oxide scale formers. Coatings that aim to achieve oxidation protection are usually created by

diffusion aluminides. The reason for this choice is the fact that the aluminides create a protective oxide scale upon exposure to high temperatures.

The basis of the deposition of diffusion coatings is made up of the following steps (79):

1) Creation of the Al-, Cr- or Si- containing vapors.
2) Transport of the vapor to the component surface.
3) Reaction of the vapors with the substrate alloy and later diffusion within the alloy.
4) Additional heat treatments to obtain the final coating composition and substrate properties.

Final coating thickness will be determined by the substrate alloy and other parameters like the later heat treatment and the temperature at which it is carried out.

Among the different diffusion processes the most characteristic examples of interdiffusion between aluminum and other metal elements to produce new aluminide phases are Chemical Vapour Deposition (CVD) and pack cementation.

- ✓ *Chemical Vapour Deposition (CVD)*

Process in which a solid material is deposited from vapor formed by a chemical reaction, or when heating the surface of a substrate resulting in the formation of a thin film, powder or a single crystal. The coating is obtained by thermal decomposition. Some of the variables that determine the final result of the process are: substrate material, temperature, reaction gas composition, etc. (80) This process has the ability to create uniform thickness coatings. (81)

- ✓ *Pack-cementation*

Pack-cementation processes are widely used to form coatings due to their ability to form coatings with uniform thickness. (81) The main disadvantage of the pack-cementation process is the need for long heat-up and cool-down times.

The basis of the method is to pack the object that is to be coated in a powder mixture composed of: the coating metal, a halide activator and an inert filler to prevent sintering of the powders. The substrate and coating powders are placed in a reaction chamber with an inert atmosphere (to prevent oxidation of the substrate and coating powders) and the sealed pack system is then heated to high temperatures causing the decomposition of the halide compound into a halide gas. This halide gas then reacts with the metal forming a metal-halide gas. (82)

During the coating process the deposited metals diffuse into the substrate, this diffusion process requires holding a high temperature for some time. The final composition of the coatings created by this process is that of metallic and/or intermetallic compounds formed from alloys of both the coating metal and the substrate to be coated.

Variations of the pack-cementation process would be 'halogen streaming' and the 'slip-pack technique'. The differences of 'halogen streaming' and the 'slip-pack technique' with respect to pack-cementation are that 'halogen streaming' the halogen gas is introduced into the reaction chamber from an external source instead of using a halide compound added to the powder mix as in pack-cementation, whereas in the 'slip-pack', used for coating large objects, a slurry composed of the coating metal powder suspended in a vehicle (water or laquer) is used without requiring the use of a halide activator. The slurry is applied to the substrate (by dipping, spraying or using a brush) and then allowed to dry. If no halide compound is used the coating is placed in the reaction chamber and supported by an inert refractory oxide powder, otherwise the component is heated for the coating process to occur**.** (83)

The main difference between the first and second method is the fact that in CVD $AlCl_3$ vapours are introduced in a chamber along with H_2 which react with the substrate forming Al; whereas in pack-cementation the metal surface is packed with a powder containing aluminum or an Al alloy as well as a halide activator and during the heating process the aluminum halides form and are transported from the pack to the substrate. (84)

OVERLAY COATINGS

Overlay coatings minimize the dependence diffusion coatings have on the substrate alloy, where the behaviour of the coating is strongly dependent on the substrate alloy because it takes part in the formation of the coating. Unlike in diffusion coatings here the material is deposited on the surface of the substrate. The typical composition of overlay coatings is MCrAlX; being M Ni, Co and sometimes Fe, and X an an oxygen-reactive element (Zr, Hf, Si and Y). (74)

The most common deposition methods for overlay coatings are either spray or arc processes. To set examples of overlay coatings two coating methods will be described: Thermal Spray, the coating process with the greatest range of coating materials, thicknesses and characteristics (see Figure 20), and Physical Vapour Deposition.

- ✓ *Thermal Spray coatings*

In thermal spray coatings thermal energy is used to deposit the coating on the substrate. It is a common process used for coating mechanical components. The resulting coating provides wear resistance and acts as an insulator for components exposed to highly energetic systems.

The process is based on a source of thermal energy that melts the coating particles and then an accelerating mechanism that sprays the molten coating particles on the component to be coated. Once the particles are deposited on the substrate they adhere to the surface and solidify forming the coating.

According to the sources of thermal energy used, four kinds of thermal spraying can be identified (74): Detonation Gun process, Flame Spray process, High-Velocity Oxygen Fuel (HVOF), and Plasma Spray process.

Out of the four it is of interest to mention a curiosity of HVOF and Plasma spray. HVOF developed from the Detonation Gun process and it has been used to spray coatings of Ti_2AlC powders on stainless steel substrates (61)**.** Whereas, the Plasma spray process on the other hand, has the advantage main advantage of having the ability to spray all materials considered sprayable (metals, refractory ceramics…). Jet engines are commonly coated by this method. (85)

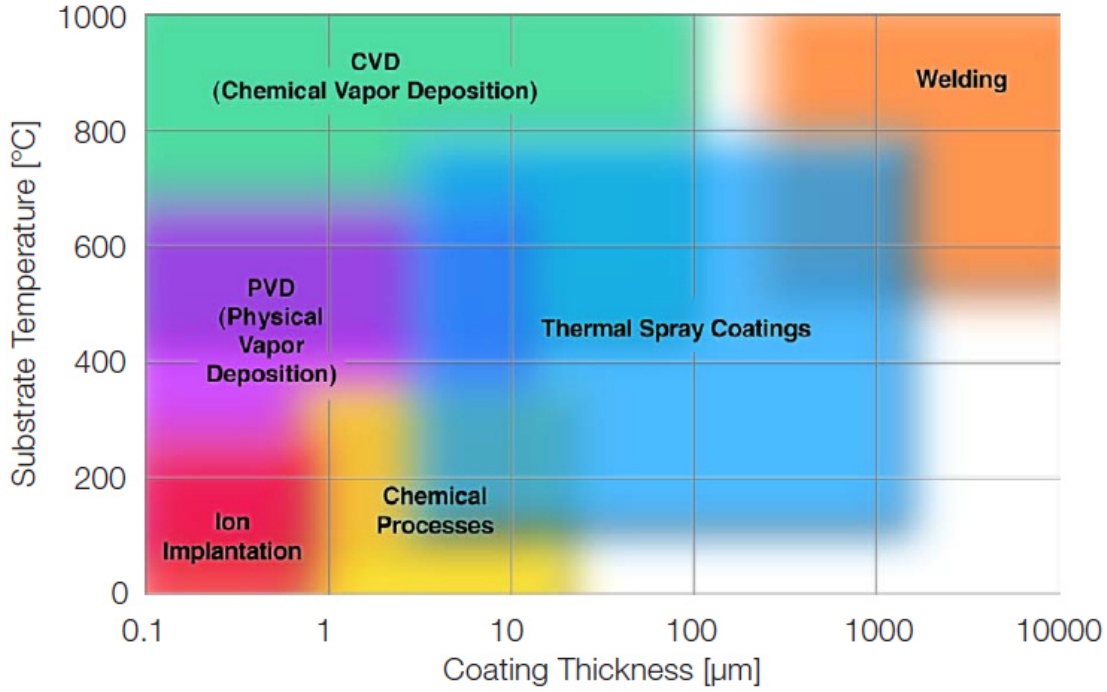

Figure 20 Range of operating thicknesses for the different Coating Methods **(86)**

- ✓ *Physical Vapour Deposition (PVD) process*

The material used for the coatings (liquid or solid) is vaporized by physical procedures into atoms, molecules or ions. The species formed are transported by a gaseous environment and then deposited on the substrate, creating upon condensation the coating. The entire process takes place under vacuum or at a very low pressure. All PVD processes have a method to minimize contamination and suitable holders for the coating and substrate that is to be coated. There are many different PVD processes usually differentiated by the way in which vaporization is carried out (87). Representatives of this technique are ion plating and sputtering. In the first vaporization is achieved by heating electrons over a crucible containing the metal, whereas in the second it is due to bombardment of ions of an inert gas (Ar) over either a metal or a ceramic material. (88)**-** (89)

4.4 Slurry Coatings

4.4.1 Introduction and description

The slurry coating method is one of the oldest coating techniques used for the deposition of aluminide coatings on nickel superalloys, titanium alloys and steel. It is characterized by its simplicity and by being relatively inexpensive. Additionally, it allows a simple modification of the coating chemical composition by addition of powders of different types, mainly silicon. (90)

The slurry coating method belongs to the group of diffusion coatings. It is an advantageous coating technique when dealing with large and complex shapes. The slurry is made of the saturating element powders with a particle size less than 40µm and an organic binder. The coating element in powder form is mixed with a liquid carrier and with the binder. The final composition is then spread on the surface of the substrate either by spraying, immersion or using a brush and left to dry. After drying the suspension is given a diffusion anneal at a high temperature to burn of the binder and deposit the metal or ceramic, in this case the MAX phases, on the substrate. (74), (81), (91)

This technique has been used for several decades for the protection of turbine blades and has allowed obtaining diffusion coatings on cast steel or intermetallic γ-TiAl alloys. (90)

This is the method used in this project to deposit the MAX phase coatings on the titanium substrate. Application of this method to MAX phases is something new in the field; so far films have usually been deposited by techniques as magnetron sputtering, pulsed cathodic arc and high velocity oxy-fuel spraying, for these reason the background for the composition of the slurries, deposition method, etc. has been taken from slurry aluminide coatings.

4.4.2 Diffusion of the coating to the substrate

Diffusion is the term used for the mechanism in which a solid chemical compound is formed as a continuous layer between two initial substances. Diffusion will take place between the coating that will be deposited on the substrate and the latter in our experimental process when the diffusion treatment is carried out in the vacuum furnace.

There are three mechanisms for diffusion in solids: volume diffusion (atoms diffuse through vacancies), diffusion through defects and movement of interstitial atomic sites. The formation of this layer takes place through two steps: (92)

1) Diffusion of the reacting substances across its bulk in opposite directions.
2) Chemical transformation at the interface between the two components with the presence of the diffusing surface atoms from one component to the other.

What drives diffusion is the tendency to decrease the free energy, in other words, diffusion will be driven by the existence of a concentration gradient. The diffusion mechanism of coatings is common to all coating techniques and can be summarized in three steps:

1. Formation of active atoms from the coating material that will diffuse in the substrate. The atoms will form according to the composition of the diffusion phase.

2. Adsorption of the active atoms by the substrate. The mutual inter-reactions between the components in phase of diffusion and the substrate will determine the adsorption.

3. Diffusion of the metal or alloy atoms takes place. It can be of an element or several elements. It is controlled by the relationship between the atomic radii of the coating material that diffuses and the substrate, the activation energy, etc. In crystalline structures with vacancies, dislocations and other defects diffusion of active atoms can be easier.

It is convenient either for the solubility of the diffusing material with the substrate to be limited or to form metallic compounds and/or chemical bonds. If the diffusing material does not have this property then diffusing elements may create independent structures. (8)

The diffusion process is based on the principle that whenever there exists a concentration gradient the coating atoms will move from the highest concentration region to the lowest to balance it, therefore decreasing the free energy. The quantity that diffuses is the difference between the elements of the diffusion layer that diffuse to the substrate and the opposite direction (the elements of the substrate that diffuse in the opposite direction to the layer).

4.4.3 Advantages and Disadvantages of the Slurry Method

Just as mentioned previously the slurry coating technique is very attractive due to its low cost in comparison with other coating techniques. Deposition methods for coatings such as electroplating, physical vapor deposition and chemical vapor deposition can be used for producing coatings, the problem lies in that they are very expensive and have certain limitations. Improvements however, still have to be carried out to make this coating technique competitive in order to increase its use in the industry. A summary of its advantages and disadvantages is made below. (83)

Disadvantages:

- ✘ A major problem regarding slurry coatings is thickness control.

- ✘ Lack of homogeneity and uniformity of the coating. This affects its reliability. If the surface where the coating is deposited has a bad surface finish then there will be regions where the coating is thicker than needed, affecting the final quality of the coating.

- ✘ The lack of significant requirements for coated refractory metals excludes this method from its use despite its manufacturing capabilities.

- ✘ Hard to coat inside walls of long small diameter holes with this method. (83)

- ✘ It is non-automatic.

- ✘ Storage conditions should allow long-term storage without deterioration of its properties. For example in the experimental process it is mentioned that the slurries had to be made from one day to the next to avoid deposition of the slurry particles and the slurry losing its properties.

- ✘ Regarding the composition: The resulting viscosity should ensure proper handling of the deposition of the coating on the substrate and diffusion annealing must ensure total volatilization of organic components without deterioration of the alloy and this cannot be ensured.

Advantages:

- ✓ Shorter thermal cycle of coating application than other techniques due to quick heating and cooling of the treated part.

- ✓ Allows the possibility of local aluminizing. (91)

- ✓ Allows coating large-size and complex parts. (83)

- ✓ The liquid phase is the most favourable for reactions of the saturating elements with the substrate surface allowing a higher quality coating.

- ✓ As the liquid carrier most often used is water this method is among the most environmentally friendly technique.

- ✓ Regarding slurry aluminizing it has the important advantage that the slurry is easily saturated.

- ✓ The application of coatings via the slurry method is easy, cheap and flexible and it can be done using a brush or simply by immersion or spray coating. (93)

- ✓ Uses simple equipment.

- ✓ Unlike other coating techniques the slurry method has the potential of automatization. Automatization of the coating process would make it be more competitive. (91)

4.5 Composition of a slurry coating

The composition of slurry coatings is quite similar to the composition of paints, which in a way are also coatings and posses several characteristics in common. Slurry coatings may be formed by different components, their use is usually determined by the method of application, the desired properties, the substrate that is to be coated and even ecological and economical constrains. (94)

Slurry coatings will usually contain the following constituents: liquid carriers, donor material powder (metallic or ceramic), binders and additives (dispersants and wetting agents).In some cases activators are also used.

4.5.1 Donor material powder

It is the main constituent of slurries. In most cases they account for up to values between 35 and 65.wt% to obtain dense powder structures and therefore facilitate the post heat treatment. Particle properties (grain size, shape, density) greatly determine the final behaviour of the slurry. If the particle size is too large the increase in viscosity will be relatively small leading to possible trouble in coating the substrate effectively.

4.5.2 Liquid carriers

Liquid carriers have the purpose of holding the donor powder particles and binders in suspension. They are usually substances with a low molecular weight that can easily evaporate, for example ethanol or water. The main two kinds of liquid carriers are water and organic solvents.

Solvents are mainly volatile organic compounds, for this reason they evaporate; they may contribute to the creation of ozone in the lower atmosphere and may also be toxic to human health, being the component of coatings that arise a higher concern.

Although organic liquid carriers have been successfully used (acetone, collodionbutyl acetate and nitrocellulose lacquers) (83), water is the most commonly used liquid carrier because it is environmentally friendly, non-toxic, non-flammable, easily available and cheap (95). De-ionised or distilled water are the liquid carriers most commonly used (as in the case of our slurry, see Chapter 5).

4.5.3 Binders

A binder is a mixture of ingredients that form the film that covers the surface of an object. Its main purpose in the film is to hold the coating's components in suspension while the slurry is applied and dried. It acts as an adhesive, binding the coating to the substrate. Binders are removed from the slurry just as the liquid carrier to avoid their diffusion to the substrate. (96)

The development of an appropriate binder with good water compatibility and that provides the desired properties of the intermediate and final products is of vital importance in the slurry process because it is this factor the one that determines the final stability, viscosity and strength of the dried products.

Binders can be either organic or inorganic; the preferred ones in coatings are the organic. The classification of binders is done according to their chemical reactions. They are classified as: oxygen reactive binders (epoxy esters), lacquers (PVC polymers), heat conversion binders (plastisols), co-reactive binders (epoxies and polyurethanes), condensation binders (phenolic resins), coalescent binders and inorganic binders. (95)

The most common water-based binders are:

- ***Polyvinyl alcohol (PVA)****:* It is a water-soluble synthetic polymer. It is white, translucent, odourless and colourless powder. It is soluble in water and highly soluble in ethanol, but insoluble in other organic solvents. It is used in treating textiles and paper. Unlike other polymers, which are created by polymerization reactions, PVA is created from the dissolution of polyvinyl acetate (PVAc, another polymer) in an alcohol and treating it with an alkaline catalyst (hydrocide). The hydrolysis that takes place removes the acetate groups without altering the long-chain structure of the acetate. (97)- (98)

- ***Thermoplastic Starch****:* It is an environmentally friendly, biodegradable, and readily available biopolymer. It has been used as a binder for gel-casting processes due its gelling properties and also as binder in porous ceramics. Starch is insoluble in water. (98)

- ***Latexes***: Latexes are colloidal dispersions of polymeric sub-micron particles in water. During evaporation of the solvent the latex particles coalesce and form a polymeric network, providing strength to the dried product. The polymer particles are usually spherical with a particle size between 30-500 nm. (98)**-** (99)

- ***Methylcellulose:*** It is a hydrophilic, odourless white powder. It is non-toxic, non-allergenic and non-digestible. It is used as thickener and emulsifier in cosmetic and food sectors to avoid separation of mixed liquids. It may also appear in tooth-paste, soap and ice-cream.

- ***Polyethylene glycol (PEG):*** It is a polyether compound with many applications for industrial medicine. Its chemical structure is:

$$H-(O-CH_2-CH_2)_n-OH$$

Equation 3 Chemical composition of PEG

There are several kinds of PEG according to their molecular weight. For the experimental procedure the PEG we used was PEG 20000. PEG 20000 is a high-molecular-weight grade of polyethylene glycol. It is a clear, colourless, viscous liquid

with a low toxicity. This polymer has a high affinity for water (hydrophilic), but it is also soluble in acetone, alcohols, benzene, glycols…

- ***Cellulose and derivatives:*** As cellulose is an insoluble polymer in water. Modifications of cellulose are carried out in order to increase its solubility by substituting the hydroxyl groups by methyl carboxymethyl or hydroxyethyl groups and be used as binders. Common cellulose binder derivatives are:

    - ***Carboxy methyl cellulose (CMC):*** It is a cellulose derivative formed by its reaction with alkali and chloroacetic acid. Its use in the food industry is known as a thickener and emulsifier in products such as ice-cream.

    - ***Hydroxypropylcelullose:*** It is a non-ionic water soluble cellulose. This polymer possesses a combination of organic solvent solubility and thermoplasticity, yielding flexible, clear films. It is used as a thickening, suspending or anti-clumping agent, and as a binder and film coating in pharmaceutical tablets. It is non-toxic, physiologically inert and has been approved for use as an additive. (96)

From all the previous mentioned the most common binders used are PVA, PEG and CMC. Studies carried out by Busch et al. (100) showed that PEG and PVA are the binders that produce slurries with the lowest viscosity whereas CMC produced harder grains. The binder used must provide quick drying of the slurry and an even layer to ensure it stands the following operations to which the slurry will be subjected. (101)

4.5.4 Additives

Additives are low molecular weight chemical substances added to slurries to provide certain properties and functions to the coating. The most common additives are dispersants and wetting agents. In addition activators will also be included as additives.

- ***Dispersants***: are substances that can be added to the suspension to improve the separation of particles and to prevent settling or clampling. They are usually organic compounds (especially polymers) with one or more water soluble groups on the main chain or ring. The dispersing action is believed to be caused due to the protection of the dispersed material by the adsorption of the dispersing agent on the surface of the particle. (102)

    They are added to make the film stable. Dispersions may become stable through two mechanisms, charge stabilization (due to electric or repulsion forces) and steric or entropic stabilization (repulsive forces maintain the particles separated from one another). (103)

    Dispersants are made up of two different components: a solvent and a surfactant.

    Surfactants are usually amphiphilic organic compounds, meaning that they have a water-soluble group (the head) attached to a non-polar water insoluble hydrocarbon chain

(the tail). Surfactants lower the surface tension of a liquid, increasing contact between the liquid and the hydrocarbon, in other words they interact with the surface of the liquid to change its properties.

Most dispersing agents contain an appropriate solvent or combination of solvents that distribute the surfactant in the hydrocarbon. Surfactants generally work with oil, water and other liquids. A well-known example of a surfactant is soap.

The dispersants that were used in the experimental part are:

- PAA (poly acrylic acid): It is a high molecular weight polymer of acrylic acid. PAA is soluble in water and is generally used as a scale inhibitor and dispersant. PAA is obtained from polymerization of acrylic acid. It belongs to the class of commercial polymers produced on a large scale which are used in industries, medicine and agriculture. PAA, its salts and PAA-based polymeric materials are used as emulsifiers and thickening agents for aqueous solutions and dispersions of both natural and synthetic latexes, floccuants… (104)

$$(CH_2 = CH - COOH)_n$$

Equation 4 Chemical Composition of PAA-monomer of acrylic acid

- PEI (polyethyleneimine): It is a polymer with repeating units composed of the amine group and two aliphatic carbon spacers (CH_2CH_2). Its structure may be either linear or branched. The PEI used for the slurries is the branched one, it is characterized by being liquid. It is used in products like adhesives, cosmetics or detergents.

$$H(NHCH_2CH_2)_nNH_2$$

Equation 5 Chemical Composition of PEI. Molecular formula

Another common dispersant is carboxylic acid.

- ***Wetting agents**:* They are a stable mixture of the slurry components. Their purpose is to reduce the surface tension between the binder solution and the powder particles to improve the stability of the coating. What they do is they spread the liquid on a surface putting the solid substrate in contact with the liquid. An effective wetting agent can be a surfactant. An example of a wetting agent would be COLA®CARB BEA. This wetting agent is used in metal cleaning, bottle washing…

- ***Activators:*** In some coating methods as pack cementation and Chemical Vapor Deposition (CVD) halide activators are used. Activators are halide salts, generally chlorides and fluorides that react with the metallic component of the pack to form metallic halides with high vapor pressures. Their use is based on the fact that when heated at high temperatures the activator generates volatile metal halides which

diffuse through the gas phase and deposit on the substrate. Slurry coatings don't usually contain this extra component because they rely on melting and subsequent diffusion of the deposited coating to the substrate. Another drawback they have is the fact that they lead to contamination of the surface of the substrate. (74), (81), (105)

4.6 Previous Studies and State of the art of coatings

Components in turbo engines and other energy producing systems are subjected by a series of attacks such as sulphidation, oxidation, chlorination, etc. There have been many attempts to improve the high-temperature oxidation resistance of titanium. For 60 years coatings that are able to answer this problem have been perfected**.** Overcoming this limitation has been attempted by several methods; some of the most common are by the addition of ternary elements (Nb, Si or W) and by surface treatments with the addition of alloying elements (82). Unfortunately the addition of ternary elements by modification of the microstructure has shown to have a negative effect on the mechanical properties of the material.

Another approach followed in the field was the development of advanced coating techniques. In many cases the use of these techniques has led to an excessive variability and unpredictability in the operating conditions required discarding their use. An example of such is the use of thermal barrier coatings. Thermal barrier coatings are currently used in several engines (GE's CF6-80C2, CFM56-5a and Pratt & Whitney's PW2000 and PW 4000 series) to improve their performance. What thermal barrier coatings (TBC) rely on is the capability of thermal insulation in order to be able to improve the life of the coated component. Despite their use, they have not been yet widely accepted for temperatures that will result in a rapid degradation of the substrate and will not be until they can be produced with predictable and reliable properties. (106)

Some of the latest studies carried out will be mentioned due to their importance or due to their relation with our project (as in the case of MAX phase films):

❖ ADDITION OF ALLOYING ELEMENTS

Regarding the addition of alloying elements different approaches have been followed.

Alloying with silicon: Silicon does not only reduce the oxidation rate of titanium, it also improves its wear and creep resistance. The reason for surface alloying is that silicon modifies the mechanical properties of titanium; therefore bulk alloying would not be as effective. (37)

Ti-Si alloys when Si is scaled are thought to play several functions:

- Reduces the oxygen atoms diffusion rate through the scales.
- Modifies stress-relaxation processes in the oxide layer promoting the formation of a layer characterized by a lower porosity.

***Alloying with Nb and Cr to pack aluminizing*:** As aluminide coatings have shown to provide good oxidation resistance properties aluminide coating have been a focus of research. Experiments have been done for TiAl substrate, which has been noticed to be a good candidate for high temperatures due to its high specific strength at elevated temperatures, and carried out by the pack cementation method. These experiments have shown that the addition of small amounts of Nb or Cr helps improve aluminizing kinetics increasing the diffusion of aluminum and creating a stable Ti_3Al layer which protects the substrate from oxidation. This layer that is formed has a different crystal structure which instead of being brittle is ductile. (82)

***Alloying with alumina forming materials*:** Other lines of investigation have been based on favouring the formation of highly protective alumina scales by using alumina forming materials, such as Ag and Cr. Positive results have been obtained with γ-TiAl+Cr (10-20% Cr content) and γ-TiAl+Ag (1-5% Ag content) but the poor mechanical properties achieved make them unsuitable for construction. (73)

Slurry-aluminizing: This is one of the most common procedures to create high-temperature coatings. It is a simple a simple, effective way to form which are similar in microstructure to chemical vapour deposits. One of the limitations encountered with slurry coatings is determining the optimum amount of slurry to the substrate to ensure that the thickness is consistent. This seems to be the main reason why this coating method hasn't spread in the industry. If the slurry is too thin the slurry won't contain enough amount of aluminium to provide the adequate protection to the substrate, whereas if it is too thick, the coating is very likely to crack due to the formation of brittle aluminides, leading to a mismatch between the expansion coefficient of the substrate and the coating. (96)

❖ MAX PHASE FILMS

Nanolaminate ternary ceramics have attracted attention for some time due to their excellent combination of ceramic and metallic materials (see Table 4). It is for this reason that they have been considered excellent candidates for high temperature coatings. Besides their applications in bulk form these last ones are also technically attractive, it is true though, that despite their outstanding properties due to the complexity of ternary ceramic surface states most studies carried out so far have been focused on binary compounds which posses simpler particle states.

MAX phase slurry coatings are something quite new to the field of oxidation resistant coatings; therefore the background obtained for this project was taken from slurry aluminide coatings.

Nonetheless, studies with films and coatings have been carried out leading to discoveries in the field of MAX phases. Some of the methods used are (61):

- ***Magnetron sputtering*:** The deposition of ternary compounds in the Ti-Al-C system (Ti, Al and C) in ultra-high vacuum was made by depositing almost pure phase films of Ti_3AlC_2 and Ti_2AlC on a Al_2O_3substrate with a TiC seed layer. By doing this it was discovered that:

- Formation of MAX phases is temperature dependent, needing temperature superior to 800°C. (107)

- Pressure does not influence the composition of the MAX phase coating, but temperature does, increasing the temperature leads to further reduction of the Ti content in the composition (108)

- ***Pulsed cathodic arc*****:** TiC_x thin films were deposited also on a Al_2O_3 substrate at 900°C. These experiments proved that Al_2O_3 is not an ideal substrate material for the growth of transition metal carbides and MAX phase thin films.

- ***High velocity oxy-fuel spraying (HVOF)*****:** In this case the experiments were done on stainless steels substrates, by doing this it was discovered that the powder size increased as the amount of powder sprayed decreased. Using larger powder-sized particles retained a higher volume fraction of MAX phase in the coatings, however, increasing the porosity. (109)

❖ DEVELOPMENT OF NEW COATING TECHNIQUES

As time goes on deposition technologies improve and become more advanced. Some of the latest emerged are (110)

- Vacuum polymer deposition (VPD)
- Atomic layer deposition (ALD)
- High-power pulsed magnetron sputtering (HPPMS)
- Filtered cathodic arc deposition.
- Glancing angle deposition (GLAD)

VPD and ALD have recently emerged as processes that can achieve molecular doping, polymer thin films and nanocomposites. GLAD can achieve unique microstructures impossible to obtain with conventional substrate-source configurations and deposition processes. HPPMS films have a high density and excellent adhesion to the substrate, making them excellent candidates for corrosion-resistant coatings, barrier coatings and electronic applications.

Other approaches under investigation are the attempt to improve the reliability of thermal barrier coatings and the study of coating processes that allow obtaining even coatings. Work on TBC is now on its way to achieve a careful process control that allows a more thermal fatigue resistant coating for their use in both stationary and rotating gas path components. For the second matter of study the technique which seems to be most promising in the area of overlay coatings is the high-velocity plasma technique due to the impact of the powder onto the workpiece which results in a much stronger bond between coating and workpiece than that achieved for example by conventional subsonic plasma spray deposition. (110)

CHAPTER 5:
EXPERIMENTAL PART

5.1 Introduction

To study the improvement of the oxidation resistance on Ti-6Al-4V 20 pieces were prepared. Five different conditions were studied. The first one were the normal oxidation of the Ti-6Al-4V substrate, for the four other groups, two different slurries were used, a Ti_3SiC_2 (312) and Ti_2AlC (211) MAX-phase slurry coating were used with two different deposition methods. To clarify this explanation the following schema shows in more detail the purpose of each piece.

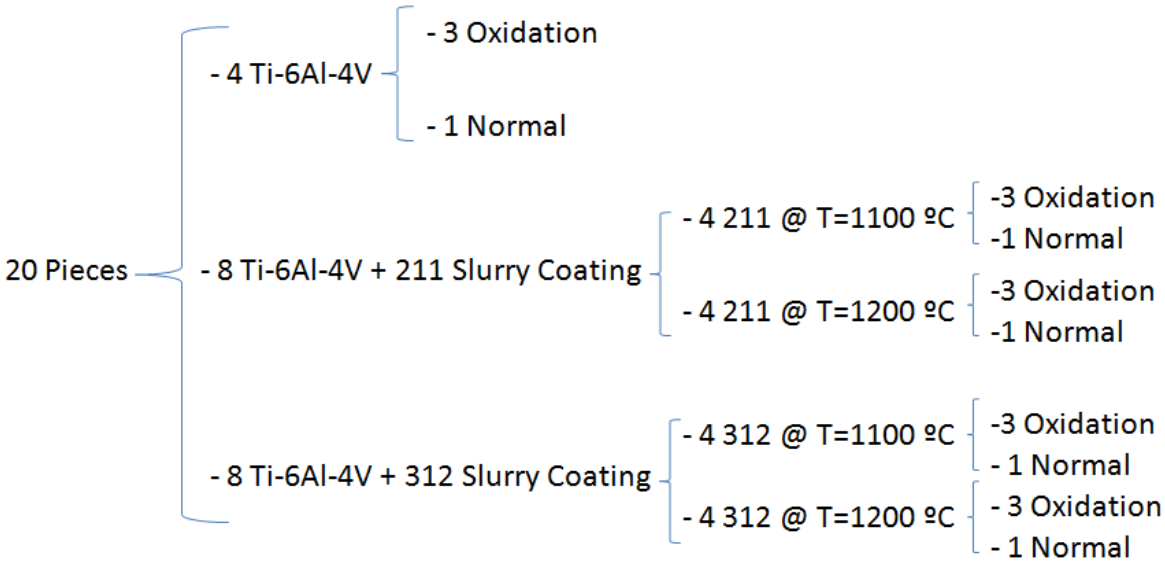

Figure 21 Schematic diagram of distribution and treatments carried out to each of the samples

The experimental procedure can be divided into several steps:

I. Preparation of the substrates.
II. Slurries composition.
III. Diffusion of the slurries.
IV. Oxidation treatment.
V. Metallographic preparation of the samples.
VI. Characterization of the samples: XRD and SEM.

5.2 Preparation of the substrates

In this project a single substrate was used. The starting point of the whole experimental process began with a sheet of wrought Ti-6Al-4V. Even before cutting the material it could clearly be noticed how the raw material had scratches. This fact is will influence later processes.

As the substrate used is wrought Ti-6Al-4V, there was no need to manufacture the pieces. To obtain the desired sample size the samples were cut with the appropriate measurements. Eventually the approximate size of the pieces was 10 mm×15 mm× 1.5 mm (see Figure 22).

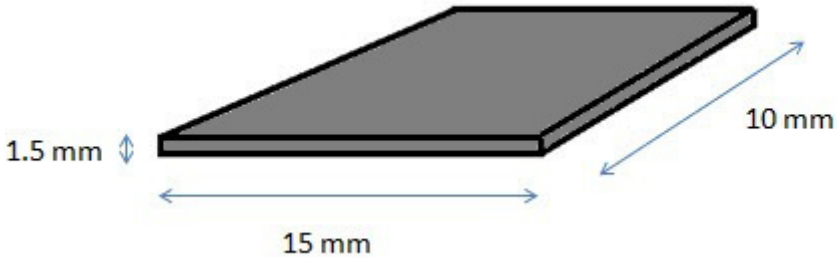

Figure 22 Approximate Substrate geometry of the samples treated

The machine used can be seen below (Figure 23). The disk used had a diamond contour which was the one responsible of cutting the piece. It is known that despite the expense of diamond tools they are one of the few materials that have a good cutting performance and reduce the wear rate. (9) The cutting speed used was 1000 rpm, due to the fact that using higher speeds resulted in sparks. To help heat dissipation a cutting fluid was used.

Figure 23 Cutting machine used to cut the wrought Ti-6Al-4V sheet into the different samples to be treated

Once all the pieces had been cut both top and bottom surfaces had to be ground on both sides in order to ensure that the surface finish of all the samples was homogeneous. Grinding removed the external natural oxide layer on the samples. Removing this layer allowed the coating to be in direct contact with the substrate. The main reason for grinding both sides of the samples is to allow a better adhesion of the coating and also to provide an homogeneous surface finish.

In this step the grit paper used was P180, P360 and P400, the grit that provides the finest grain out of the three is P400. The grain composition of the grit paper was silicon carbide. Eventually the surfaces were grinded to a 400-grit finish.

Figure 24 Grinding machine to grind samples

The last action in this step was to clean the pieces ultrasonically (the machine used can be seen in Figure 25) using ethanol. The cleaning was done for five minutes; with this all the possible contaminants were removed. After the cleaning process the pieces were dried and after manipulating them with tweezers, to avoid contamination by foreign particles, placed in sealed bags so the pieces wouldn't oxidize.

Figure 25 Ultrasounds bath machine used for cleaning the samples

5.3 Slurry composition

5.3.1 Introduction

Determining an optimum slurry composition is of mayor importance; the weight content of solids, the use of a dispersant, the kind and amount of binder used and pH are some of the factors that determine the behavior of the slurry (75). Before making the final slurries several tests were made to determine if the viscosity was the appropriate one, if the solid concentration desired could be achieved, etc.(see Annex I)

Feedback on the slurry composition of Ti_3SiC_2 was able to be provided from previous studies; therefore the slurry used had already been optimized for pH and dispersant quantities. For the experiment these parameters were used increasing the solid content to see the actual outcome of the predictions and whether they could be used for our purpose.

Regarding the Ti_2AlC it is worth mentioning that there has been no previous experience; then the final composition for this suspension will be based on the results from the Ti_3SiC_2.

From the usual components a slurry coating has (see Chapter 4) only the dispersant, solvent and powder were to be used as a starting point. It is known that in studies for slurry coatings binders are generally used, for example in alumina based slurries. The type of binder and the amount used are the most important parameters affecting the stability and film smoothness. A study on whether the use of a binder would be required was done.

The binder used as well as its content was taken from experiments done with alumina based slurries. These experiments had proved that the best binder and the content that provided optimum film viscosity and stability was PEG (polyethylene glycol) with a 3 wt. %. (75)

Activators are a usual component of slurries but as Titanium is a highly reactive material the use of a halide activator will be avoided.

Additionally, it is known that the pH affects the stability and behaviour of the film, affecting the ordering of the particles. For this reason the pH evolution will be controlled for each of the slurries. An incorrect pH can result in particle attraction instead of repulsion, causing undesired agglomerations; therefore obtaining a balance between the pH and the dispersant concentration is of utmost importance. An example of its importance is the case of the PAA dispersant where a low pH promotes the adsorption onto the powder particles. (111)

5.3.2 Slurry composition and preliminary computations

In both slurries the same %wt. solid content was attempted to be achieved. The dispersants used for each one were different due to the acidic or basic character of the solution. The pH of the water was adjusted for Ti_3SiC_2 to basic, whereas for Ti_2AlC no modification of the neutral character of water was done in case the acidic solution would react with the substrate. The

different powders have their character defined by the metal which dominates the behavior, Si and Al respectively.

The acid and base used to increase or decrease the pH of water are TMAH (Tetramethylammonium) and HNO_3 (Nitric acid) respectively. A thorough control of the pH was decided not to be maintained during the whole process because it would require adding more acid or base at each step, leading to an increase in the liquid content of the solution and a subsequent increase in the amount of powder needed to obtain a reasonable viscosity. Alternatively, what was checked is that we are in a reasonable range during the whole process (0.5 to 1 below and above the preset value).

The final composition of the slurries was obtained from the experiments done (To see the development of the tests see Annex I); from them the following conclusions were reached which were used to guide the composition of the two final slurries:

- Using PEG as a binder was necessary for both slurries in order to obtain a good adherence to the surface of the substrate and a more viscous slurry.

- As the slurries used in both cases dry off quite quickly there was no need to use a furnace to accelerate the drying, as it was thought of doing in a first approach. Using a furnace would ensure the evaporation of the liquid media and help drying. Leaving it for two hours or so would provide total drying off of the slurry, but in order to ensure total drying once the slurry was deposited a day would be left before putting the pieces in the vacuum furnace to allow the diffusion of the coatings to the titanium samples.

- The pH of the initial solution for the case of the Ti_3SiC_2 slurry would be done without any further volume addition to improve the viscosity of the final slurry. The volume of water needed for the slurry would already be pH∼9.

- Particle size is quite relevant, as the powder particle size is for both cases in the order of 10^{-6} a good viscosity is achieved, bigger particle size would lead to problems related to the particle suspension and if increasing the solid content to try and achieve a less fluid slurry far too solid for proper managing and spreading on the surface. Despite the fact that Ti_2AlC grain size is slightly larger than the Ti_3SiC_2 grain-size, this small size difference doesn't lead to suspension problems.

With this the components that were to be used for the slurry could be listed:

❖ COMPONENTS OF THE SLURRY

1. MAX phase powder: Ti_3SiC_2 and Ti_2AlC→ 60% wt. solid content.

   Regarding the sizes of the powder particles used for the slurries are:

- For the 211 slurry: D(50)=9.801 µm
- For the 312 slurry: D(50)=5.58 µm

2. Binder: PEG (polyethylene glycol) in this case→ 3%wt. with respect to the total solid content. The PEG used for the calculations was PEG 20000.

3. Dispersant: PEI for Ti_3SiC_2 and PAA for Ti_2AlC (a brief overview of their properties was given in Chapter 4).

   - PEI (polyethyleneimine): PEI was provided in a solution 1:10, so using the required mass and the density value the volume needed for the slurry was calculated. The PEI wt.% with respect to the solid content will be 0.2.

   - PAA (poly acrylic acid): Provided in a solution with a 25% water content therefore the calculations done for the quantity needed had to be transformed from 100% purity to a 75% purity. The PAA wt.% with respect to the solid content will be 2.

4. Distilled water.

❖ PRELIMINARY COMPUTATIONS

To calculate the masses and volumes for the preliminary calculations the densities of each component were needed, the values for the different densities used can be seen in the next Table (112):

DATA	
COMPOUND	**Densities (g/ml)**
H_20	1
PEG	1.128
PEI	1.08
Ti_3SiC_2	4.53
Ti_2AlC	4.11
PAA	1.2

Table 9 Density values for starting materials

The final slurries where done for a volume of 10 ml to avoid using such large quantities of powder due to how expensive MAX- phase powder is.

Ti_2AlC

Using the weight percent values given for the components calculations for the mass composition will be developed according to the following formula:

$$m_{TOT} = \frac{V_{TOT}}{\frac{Ti_2AlC}{\rho_{Ti_2AlC}} + \frac{PAAwt\%}{\rho_{PAA}} + \frac{PEGwt\%}{\rho_{PEG}} + \frac{H_2Owt\%}{\rho_{H_2O}}}$$

Equation 6 Total mass composition for the Ti_2AlC slurry

m_{TOT} represents the total mass content to obtain a 10 ml volume and the wt% of each component is the represents the .wt% out of the total mass. Multiplying the total mass by the respective proportion of each component the final mass for each will be obtained.

The resulting masses and volumes used for the slurry can be seen in Tables 10 and 11, with the amount of PAA for the 75% volume purity solution provided already computed.

Volume of PAA needed for 100% purity (ml)	0.1845213
Volume of PAA needed for 75% purity (ml)	0.2460284

Table 10 Amount of PAA added in the final Ti_2AlC slurry

With PAA for Ti2AlC with PEG			
INPUT		OUTPUT	
Volume (ml)	10	mtotal (g)	18.4521302
		densitytotal (g/ml)	1.84521302

COMPOUND	% wt.	mass (g)
H20	0.37	6.827288176
Ti2AlC	0.6	11.07127812
PAA (2%wt. wrt. %solids)	0.012	0.221425562
PEG (3%wt. wrt. %solids)	0.018	0.332138344

Table 11 Final Ti_2AlC slurry composition

Ti_3SiC_2

Just as for the other MAX phase the same solid content, 60% wt. was used with a 0.02% wt. with respect to the solid content for the dispersant (PEI). The dispersant concentration was taken from previous studies for a similar MAX phase (Ti_3AlC_2).

The formula used to get the total mass content is similar to that used for Ti_2AlC (Equation 7) and the procedure to get the individual mass values for each component the same.

$$m_{TOT} = \frac{V_{TOT}}{\frac{Ti_3SiC_2\ wt\%}{\rho_{Ti_3SiC_2}} + \frac{PEG\ wt\%}{\rho_{PEG}} + \frac{PEI\ wt\%}{\rho_{PEI}} + \frac{H_2O\ wt\%}{\rho_{H_2O}}}$$

Equation 7 Total mass composition for the Ti_3SiC_2 slurry

The resulting PEI content for the 1:10 solution and masses of all the slurry components can be seen in Tables 12 and 13.

Volume of PEI needed for 100% purity (ml)	0.02095175
Volume of PEI needed for 1:10 purity (ml)	0.20951754

Table 12 Amount of PEI added in the final Ti_3SiC_2 slurry

With PEI for Ti3SiC2 with PEG			
INPUT		OUTPUT	
Volume (ml)	10	mtotal (g)	18.856579
		densitytotal (g/ml)	1.8856579

COMPOUND	% wt.	mass (g)
H20	0.3808	7.180585264
Ti3SiC2	0.6	11.31394737
PEI (0.2%wt. wrt. %solids)	0.0012	0.022627895
PEG (3%wt. wrt. %solids)	0.018	0.339418421

Table 13 Final composition of the Ti_3SiC_2 slurry

❖ PROCESS FOLLOWED

The starting point for both slurries is the same. First of all, you pour the amount of distilled water calculated into a beaker. The initial pH is measured, as its water it should be around 7. The beaker is placed on a magnetic mixer and a magnet is put inside the beaker. With the magnetic field created the magnet will start spinning mixing all the components.

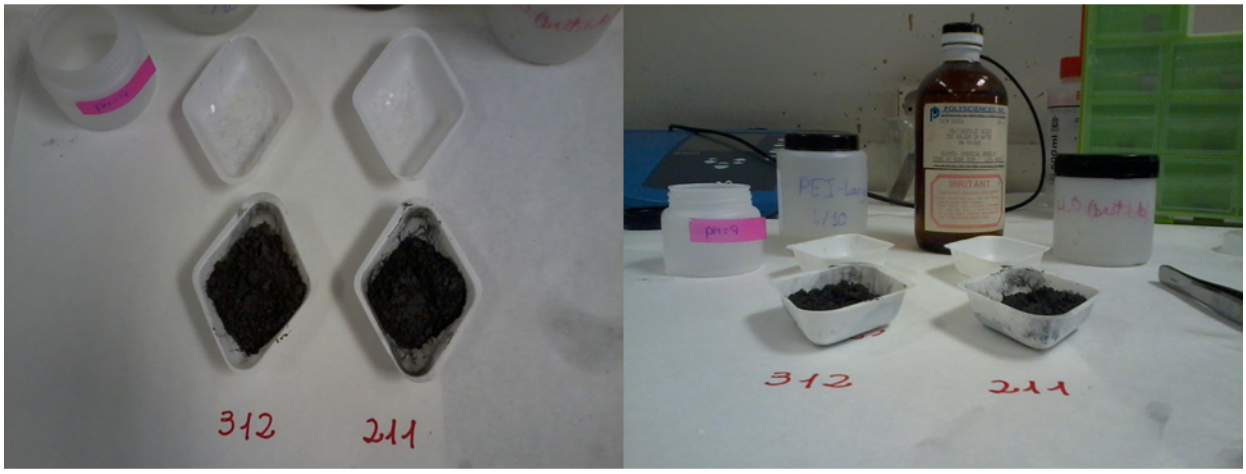

Powder and PEG **All Slurry Components**

Figure 26 Photographs of the components used to prepare the slurries

The first thing that is added is the dispersant, PAA or PEI in each case. After this the pH is measured once again, to determine the effect of PAA. Next, PEG is added. When it is seen that all the PEG has dissolved the pH is newly measured. Last of all the MAX phase powder is added and mixed. Once the slurry is finished and the solution completely mixed the pH is measured for the last time and it is passed through the ultrasounds machine to break apart possible agglomerations and leave a more uniform slurry; this is done for 30 seconds. The effects of subjecting the slurry to ultrasounds were visible; both slurries became less dense than before and seemed to be more liquefied.

Each slurry had to be made twice, one for each diffusion process because properties may be lost from the time the first diffusion process is carried out until the second one takes place. Although in our case the time between one and the other was just one day a new slurry was made nonetheless.

Ti_2AlC

The reason for using PAA dispersant instead of PEI for this slurry is that in experiments done for Ti_3AlC_2 is showed it had an excellent stability in a pH of around 5 when adding 2 wt.%. At first it was considered making the water solution acid (pH~5) but given the fact that Ti-6Al-4V is very reactive and that adding HNO_3 to the slurry might cause undesired reactions it was

decided that that the natural pH obtained from mixing the different components would be maintained without controlling it with an acid or base; though a thorough control of the pH was done in each test to see how it evolved through the process. (113)

The general process followed to obtain the slurry using a binder is indicated in the following figure:

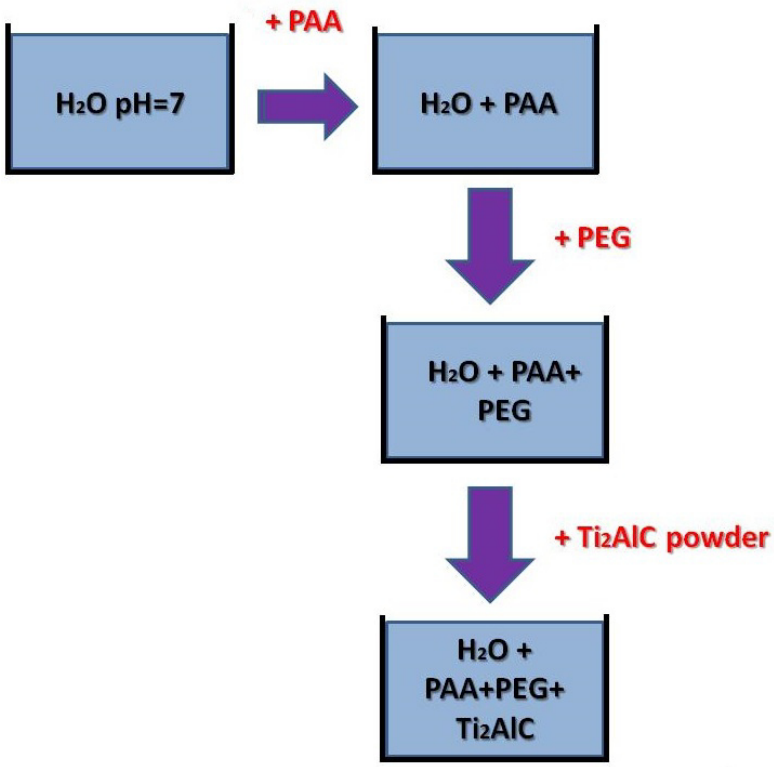

Figure 27 Schematic diagram of the steps followed to obtain the Ti_2AlC slurry

The measurements of the pH evolution obtained for the two Ti_2AlC slurries at each step were obtained using a pH-meter the results were the following:

pH Evolution Ti_2AlC Diffusion at 1100℃	
STEP	**pH**
Initial value of water	7.22
After PAA addition	3.6
After PEG Addition	3.96
Final-After powder addition	4.31

Table 14 Final pH Evolution for Ti_2AlC slurry for diffusion at 1100℃

pH Evolution Ti_2AlC Diffusion at 1200℃	
STEP	**pH**
Initial value of water	6.74
After PAA addition	4.15
After PEG Addition	4.23
Final-After powder addition	4.18

Table 15 Final pH Evolution for Ti_2AlC slurry for diffusionat 1200℃

Ti_3SiC_2

In this case the process is the same but with a slight variation; the initial pH is set to 9.The summary of the steps followed for this case is seen below:

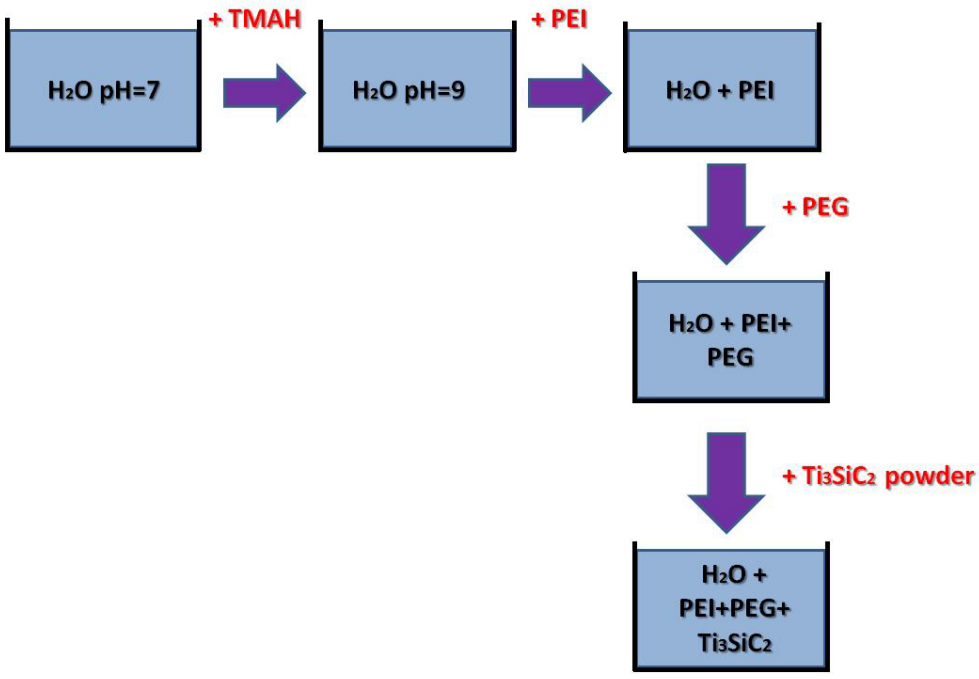

Figure 28 Schematic diagram of the steps followed making the Ti_3SiC_2 slurry

The pH evolutions obtained for the two diffusion temperatures for this slurry are:

pH Evolution Ti_3SiC_2 Diffusion at 1100℃	
STEP	**pH**
Initial value of water	10.19
After PEI addition	10.65
After PEG Addition	9.35
Final-After powder addition	8.41

Table 16 Final pH Evolution for Ti_3SiC_2 slurry for diffusion at 1100℃

pH Evolution Ti_3SiC_2 Diffusion at 1200℃	
STEP	**pH**
Initial value of water	9.55
After PEI addition	10.56
After PEG Addition	8.3
Final-After powder addition	7.5

Table 17 Final pH Evolution for Ti_3SiC_2 slurry for diffusion at 1200℃

Once the slurries were finished they were spread on the pieces with a brush and left to dry off at room temperature for 24 hours, this way the carrier liquid was eliminated before being put in the vacuum furnace to be subjected to a heat treatment so the slurries diffused in the substrate. In Figure 29 the evolution of the samples during the application of the slurry coating can be seen.

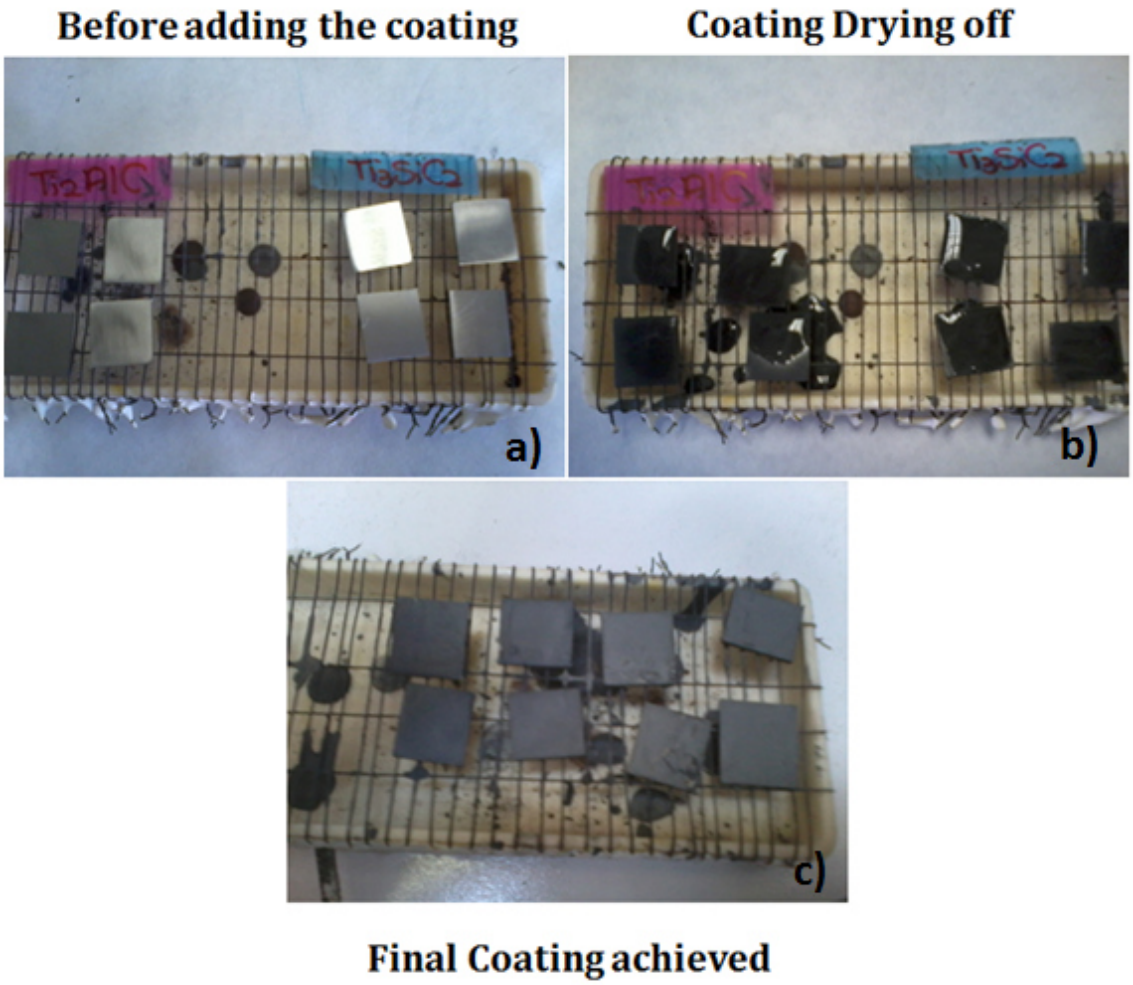

Figure 29 Photograph of the coating process: a) uncoated samples b) after deposition of the slurries on the samples c) final coated samples after 24 hours drying

The samples have to be coated homogeneously over the whole surface in order to achieve an even diffusion coating all over. If the bottom part of the samples, which was touching the wires was not completely covered with the coating when dry, the pieces were turned around and another layer of coating was spread on top.

5.4 Diffusion process

Once the slurry coatings had dried off the pieces were placed on a layer of zirconium oxide inside a crucible. Zirconium oxide is used to prevent the samples from touching the crucible.

The diffusion process of the samples was done using a high vacuum furnace (Figure 31). Vacuum is the best condition to guarantee contact formation. It facilitates the evaporation of the impurities and the removal of the adsorbed gas. Diffusion layers obtained under vacuum are of even depth and high surface-finish quality. (91)

The temperature at which annealing or diffusion takes place affects the surface finish, favorable results for slurry aluminide coatings have been within the 850-1100℃ range. For our case diffusion was carried out at 1100℃ and 1200℃ due to the ceramic character of the slurries.

Figure 30 Photograph of the samples before the diffusion treatment at 1100℃

During the diffusion process the coating elements diffuse into the substrate. The binder on the other hand evaporates. This fact will be corroborated when studying the final composition; it will be noticed how no traces of binder will be found.

Figure 31 Vacuum Furnace used for the diffusion process

The furnace was programmed to follow the cycle seen in Figure 32 (in this case for diffusion at 1100°C) to have an increase of 5°C per minute until reaching either 1100°C or 1200°C according to whichever of the two sintering conditions was being carried out.

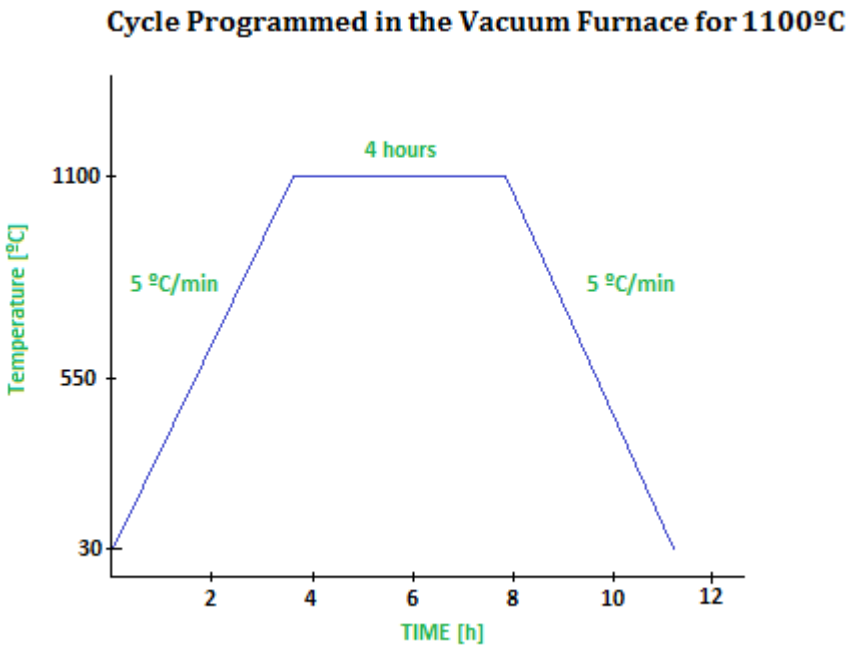

Figure 32 Cycle for Diffusion at 1100°C in the Vacuum Furnace

The samples were subjected to a diffusion treatment during 4 hours at 1100°C/1200°C so the coatings would diffuse into the substrate. During the diffusion process, the pressure was kept at conditions close to vacuum, around $2 \cdot 10^{-5}$ mbar. After the four hours the furnace decreased at a theoretical rate of 5°C/min until reaching 25°C, it is known that the actual rate of decent is longer than the expected.

The process was repeated all over again for the pieces that were to diffuse at 1200℃. The pictures of how the pieces were before the diffusion treatment can be seen in Figures 30 and 33.

Figure 33 Photograph of the samples before the diffusion treatment at 1200℃

After the diffusion treatment had taken place, before moving on to the next step the pieces were cleaned with the ultrasounds machine using acetone (for 5 minutes again), to remove all remains of the coating that had not diffused. The ultrasounds machine did not seem to be able to remove all the remaining slurry, despite cleaning them several times powder still fell off progressively.

5.5 Oxidation Treatment

After the diffusion of the coating the pieces were ready to start the oxidation process. Prior to the start of the oxidation treatment the pieces that were to be inserted in the oxidation furnace had to be carefully measured and weighted.

The pieces were weighted in order to determine the mass gain through oxidation, this was done using the microbalance seen in Figure 34, which allowed a precision of four decimals; and measured with a caliper to get the initial surface of the samples. No surface variation will be considered through the oxidation process; therefore the initial surface was used as reference at each step.

When carrying out oxidation experiments there are two processes which are generally used. They are isothermal processes, in which oxidation is studied under several different temperatures; or cyclic oxidation consisting of a series of repetitive processes in which the samples are oxidized in the furnace then brought out and measured. The process we have used is the cyclic oxidation one.

Figure 34 Microbalance used for the mass measurements during the Oxidation cycles

The mass measurements were done three times to reach more accurate results and the dimension measurements were done on both sides of the sample and in the middle. The initial reference area will be computed using the mean of the three values for each measurement (length, width and thickness).

Fifteen pieces were placed inside the furnace, three for each coating and sintering condition (4 conditions) and 3 Ti-6Al-4V that had not been treated, as reference to compare the evolution of the oxidation. The furnace used for the oxidation treatment can be seen in Figure 35.

Figure 35 Furnace used for the Oxidation treatment

For the oxidation treatment the samples have to have the most surface possible exposed to the oxidizing atmosphere (air atmosphere). In order to do this a crucible with high temperature resistant wires was made. This item allowed the pieces having the highest area possible exposed to air and samples from not touching one another. The placing of the samples on the crucible is shown in Figure 36.

The oxidation process was to be done for 300 hours. Along the process the pieces were to be brought out of the furnace and measured at several steps of the treatment, these measurements done were at: 12 hours since the beginning, 24 hours, 48 hours, 100 hours, 150 hours and 300 hours (end of oxidation).

The temperature at which oxidation was to take place was 600℃. The cycle programmed for the furnace was a rate of climb of 10℃/min until 600℃, dwell at this temperature for as long as established in the treatment (therefore it would be 12 hours, 12 hours, 24 hours, 52 hours, 50 hours and finally 150 hours) and last of all return to 30℃ at a rate of 10℃/min.

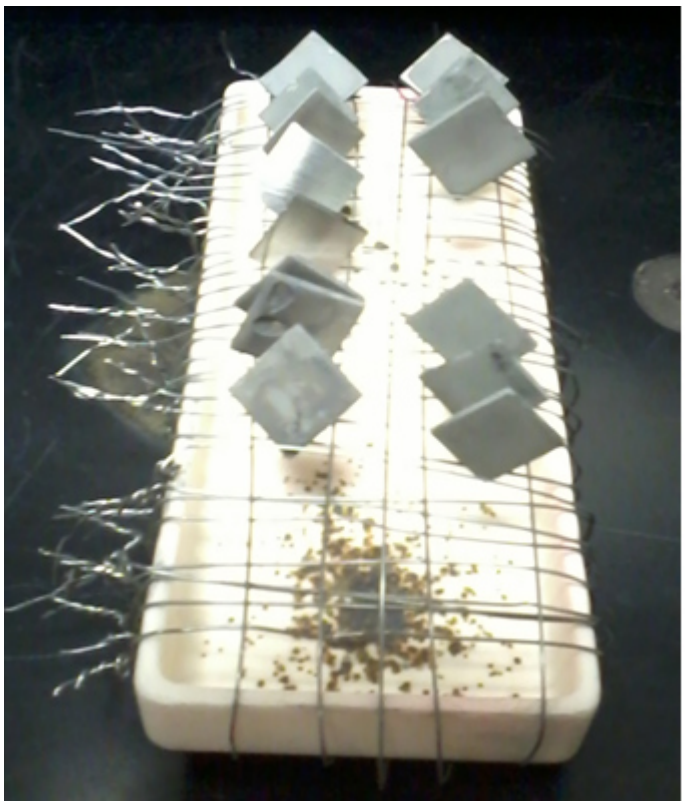

Figure 36 Photograph of the sample setup before starting the oxidation treatment

A fact of importance noticed even before starting oxidation and that will affect the results obtained is that although the sintered pieces were carefully cleaned using the ultrasounds machine the coating progressively fell off, therefore the measurements obtained after the first oxidation cycle the weight decreases, and also the oxide created on some of the samples is very light that despite developing on the piece it cannot be considered when measuring the

samples because if blows off. The reason for this behavior will be analyzed when studying the results.

5.6 Metallographic preparation of the samples

The two methods of analysis that were used to study our results were: SEM (Scanning Electron Microscopy) and XRD (X-Ray Diffraction).

When all the samples are ready to be analyzed they were specially prepared before being able to be observed by SEM. The reason for doing this is that to be able to do SEM the pieces cross-section has to be perfectly prepared for observation. The samples to be characterized by XRD do not require this step. The working principles of both SEM and XRD will be discussed in the next section.

To prepare the samples several steps were followed. The most important ones are the first two in order to ensure that when cutting the pieces to observe the cross-section the slurry coating doesn't fall off. They are as follows:

1) GOLD COATING. The samples were coated with gold. This was done by ion bombardment. The whole purpose of this preliminary step is to make the pieces conductive and to ease the deposition of the later copper layer.

2) COPPER COATING. This new coating will allow the slurry to remain unaltered and prevent it from falling off when cutting the pieces in half, in other words the copper layer has a protective purpose. The coating will be formed by electrodeposition. The electrolyte used was a solution with the following composition:

$$CuSO_4(22\ g) + H_2SO_4(3.3\ ml) + H_2O \rightarrow Final\ 100\ ml\ solution$$

The amount of water added will be that needed in order to obtain 100 ml of solution.

In order to deposit the coating a copper plate was used as anode and the substrate acted as cathode. Each sample which was to be coated had to be done independently. The experimental setup can be seen in Figure 37.

To achieve electrodeposition of the copper coating a continuous current of around 100 mA (in our particular case 105 mA) was applied for around half an hour with a tension of 10 V. The look the pieces get once they have been coated with copper is seen in Figure 38.

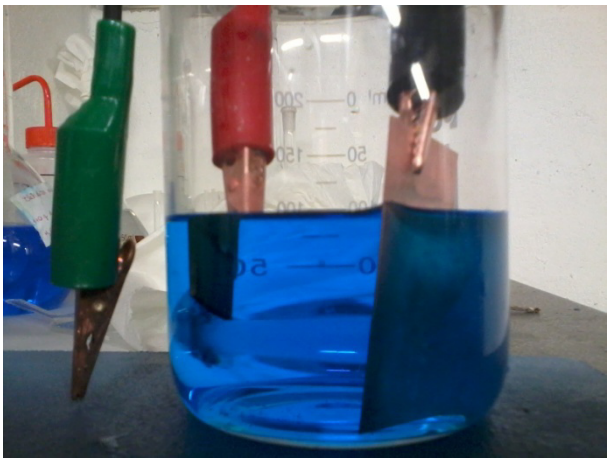

Figure 37 Photograph of the experimental Setup for coating with copper

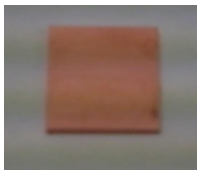

Figure 38 Snapshot of a sample coated with copper

3) CUTTING. Posterior to the application of the copper coating the pieces are cut using the micro-cutter (see Figure 39), the reason for this is that when doing SEM analysis to have a representative view of the cross-section the edge sections shouldn't be used.

Figure 39 Micro-Cutter used for cutting the samples after the oxidation treatment

4) MOUNTING. The pieces that had been cut were then paired up and mounted in an acrylic conductive resin to ease later operations. Additionally, on top of the conductive

resin we placed a layer of non-conductive resin for labeling the pieces. To mount the pieces the cycle programmed was one at a temperature of 170℃ for 15 minutes.

Figure 40 Machine used to mount to samples

5) GRINDING AND POLISHING. As the cross sections are going to be zoomed in a tiny scratch would seem huge therefore to remove any possible defect on its surface the mounted pieces have to be grinded and then carefully polished.

Grinding was done using the following sequence of grit paper: 120, 180, 320, 400, 600, 1000. The operating principle was the same as in the step in which the substrate was prepared to be coated, and so was the machine (see Figure 24). The grains of the sample were all oriented in the same direction and the surface of the sample was left at the same level. First the grit paper with larger grain and then the fine one to achieve a fine surface finish.

Polishing on the other hand was done using diamond suspensions. Just as in the grinding the polishing process was done by polishing through three different plates. Polishing is based on adding an abrasive fluid or paste to remove all the scratches from the sample. For the first plate used the abrasive used was a water based diamond suspension with a particle size of 1µm, with this one the deeper scratches were removed. For the next plate a diamond paste with particle size of 0.1 µm was used and eventually on the third plate used a water based colloidal silica suspension with a particle size of 0.06 µm was used as abrasive agent. The proportion used for this last suspension was 1:10 (1 ml of colloidal silica for 10ml solution). Additionally for the first two plates a water based diamond lubricant was used to ease the operation. The machine used for the polishing operation can be seen in Figure 41.

With this done the pieces were then ready to be characterized by SEM.

Figure 41 Polishing machine

5.7 Sample Characterization

5.7.1 Characterization by X-Ray Diffraction (XRD)

The first study done on the surface of the samples was done by the XRD technique. XRD allows determining the crystalline structure of the material. To do this especial equipment had to be used. The machine used was a PHILIPS X-PERT. It used a copper anode as emission source with a voltage of 40kV and a current of 40 mA. Two different cycles were programmed to obtain the diffraction pattern of the samples. The only parameters varied from one cycle to the other were the diffraction angle range and the step size. The first sample analyzed (Ti-6Al-4V without treatment) was done using CYCLE 1 but in order to obtain more accurate results all subsequent samples analyzed used CYCLE 2 (see the conditions of each cycle in Table 18).

Cycle	Starting position (2θ°)	Ending position (2θ°)	Step Size (s)	Duration (h:min)
CYCLE 1	20.0100	99.9900	1.7	1:53
CYCLE 2	30.0100	89.9900	2.2	1:50

Table 18 *XRD Analysis conditions used to obtain the diffraction patterns of each sample*

The machine we used to analyze the samples can be seen in the following picture.

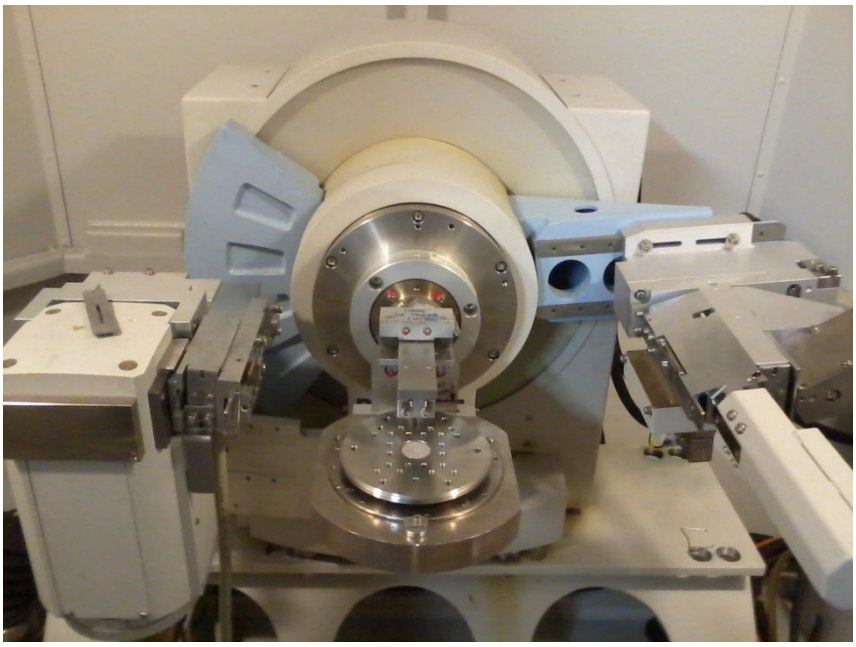

Figure 42 XRD Machine PHILIPS X-PERT

In the diffraction experiment an incident wave is directed into a material and a detector is typically moved to record directions and intensities of the diffracted waves. The type of atom and its position is closely related to the direction in which the waves are diffracted.

The result of X-ray diffraction is a diffraction pattern. Diffraction patterns are like the digital fingerprints of a material; they are a shadow of the distances in a material. Large spacings cause diffraction at small angles, whereas small spacings do at high diffraction angles. For diffraction to be effective the incident waves must have wavelengths comparable to the spacing between the atoms. The principle of operation XRD is based on is quite simple. A monochromatic X-ray beam with wavelength λ impinges on the lattice planes at an angle θ, diffraction will only occur when the distance travelled by the reflected rays from successive planes differs by a complete number of wavelengths n, satisfying Bragg's Law. (114)

$$n\lambda = 2dsin\theta$$

Equation 8 Bragg's Law

d: interplanar spacing.

In the case of cubic crystals the interplanar spacing results from the lattice (a_o) parameter and the Miller indices (hkl) following Equation 9.

$$d_{hkl} = \frac{a_0}{\sqrt{h^2 + k^2 + l^2}}$$

Equation 9 Interplanar Spacing

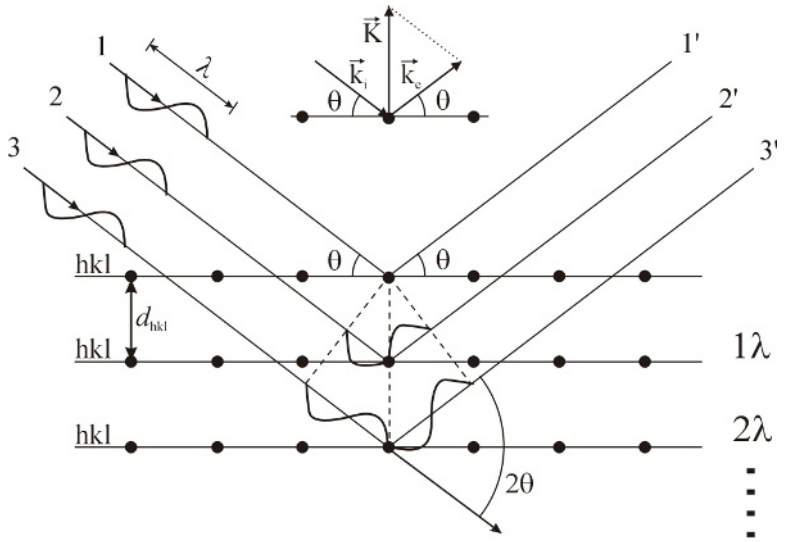

Figure 43 Diffraction: Geometry for the interference of a wave.

Varying the angle θ makes Bragg's Law be satisfied for different spacings (d) in crystalline materials. Plotting the intensities and diffraction peaks produced provides the resultant characteristic diffraction pattern of each sample. With the diffraction pattern we can obtain the phases present in the sample (peak positions), the phase concentrations (peak heights), the amorphous content (background bump) and crystalline size (peak widths).

The resulting diffraction patterns obtained from the scan will then be analyzed to determine the existing phases and composition of the samples. The analysis of the possible species was done using the program X-Pert High Score. What this program does is identify the possible peaks found in the diffraction pattern with the diffraction patterns of the phases it has stored in the database it uses, in our case the PDF2 database. The PDF2 database, however, does not include the diffraction pattern of the Ti_2AlC MAX phase, therefore to obtain the 211 peaks a comparison had to be made with reported diffraction patterns from different authors (109)**,** (115)**-** (116)**.**The results of the analyses can be seen in Chapter 6.

5.7.2 Characterization by Scanning Electron Microscopy (SEM)

The second characterization method used to study the samples is the Scanning Electron Microscopy (SEM). SEM provides information about the external morphology, chemical composition, crystalline structure and the orientation of the composition of the materials that make up the sample.

What SEM does is use electrons to form an image which allows seeing the features of the material with a much greater accuracy. To do so it uses a beam of high-energy electrons to generate many different signals on the surface of the material, this beam is produced at the top of the microscope by an electron gun. (114)**,** (117)

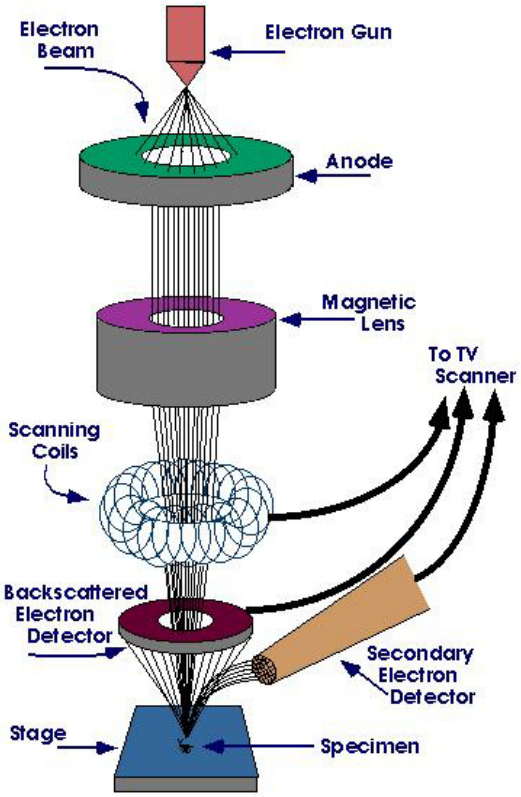

Figure 44 Scanning Electron Microscopy (SEM). **(118)**

The beam of electrons follows a vertical path through the microscope, which is held in vacuum. The impinging beam contains large amounts of kinetic energy, when bombarding on the sample, the incident electrons are decelerated by the sample receiving them.

Once the beam hits the sample, electrons and X-rays are ejected from the sample (Figure 45). The signal contains secondary electrons (SE), which are the ones responsible for creating the SEM images, backscattered electrons (BSE) and diffracted backscattered electrons (EBSD). These last ones are the ones that allow determining the crystal structures and orientations of metals. In general what can be said is that backscattered allow determining the chemical composition whereas the secondary electrons provide an idea of the topography of the sample.

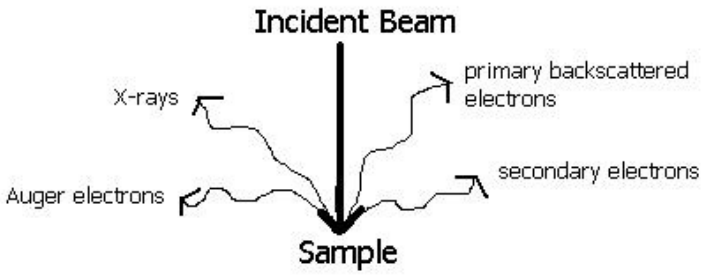

Figure 45 Signal emitted from electron bombardment (SEM). **(118)**

Some of the limitations of this method of analysis are that the samples that can be observed must be solid and an appropriate size to fit in the microscope chamber, and also that for pieces that are insulators a conductive coating must be applied to the sample. The most common conductive coatings applied are carbon (suitable when an elemental analysis is the main goal of the analysis) and gold (when what's wanted is to achieve a high resolution in the electron images).

Figure 46 SEM machine used

The samples were placed inside the SEM machine. To make them conductive a colloidal graphite isopropanol based solution was spread on each corner of the samples. Once the machine reached vacuum the analysis could start. For the characterization of our samples the tension used was 20kV.

The results obtained for the cross-section of the samples, both the images and the EDS analyses are presented in Chapter 6.

CHAPTER 6: RESULTS & DISCUSSION

6.1 Introduction

To analyze the results obtained in this project four analysis will be done. They are: visual inspection of the samples, graphs of oxidation evolution (mass gain per unit area vs. time of exposure), analysis of the results obtained by X-Ray diffraction (XRD) and analysis of the transversal cross-sections of the samples by Scanning Electron Microscopy (SEM).

6.2 Diffusion and Oxidation observations. Visual Inspection.

Prior to the analysis of the results obtained it is considered of interest to mention what was observed in the diffusion and during the oxidation treatment.

In the two pictures below (Figures 47 and 48) the look the samples had when brought out of the furnace from the diffusion treatment can be seen. Their relevance lies in the fact that they will be the starting point of the analysis. In both photographs the 4 samples located on the right are the ones that were coated with the 211 slurry, whereas the 4 samples on the left were coated with the 312 slurry.

A general glimpse of the look the samples had before and after the oxidation process can be seen in Figure 49. Additionally, any observation made throughout the process will be mentioned. This was done to keep track of any unexpected turnouts during the oxidation cycle.

When opening the furnace the most astounding fact noticed after the first 12 hours of oxidation in air at 600ºC was that the samples that had been coated with the 211 slurry seemed to have exploded (this phenomenon will be discussed in section 6.6). A white dust, probably titanium oxide, covered all the samples that had been coated with the 211 MAX phase.

Figure 47 Photograph of the samples coated with MAX phase slurry after a diffusion treatment at 1100℃ for 4 hours.

Figure 48 Photograph of the samples coated with MAX phase slurry after a diffusion treatment at 1200℃ for 4 hours.

Note: Taking a close look at the samples after diffusion at 1200℃ the pieces seem to have lost part of the coating, something that did not happen in samples treated at a temperature of 1100℃. This might have been due to evaporation or decomposition of the coating, or it might have completely diffused inside the sample.

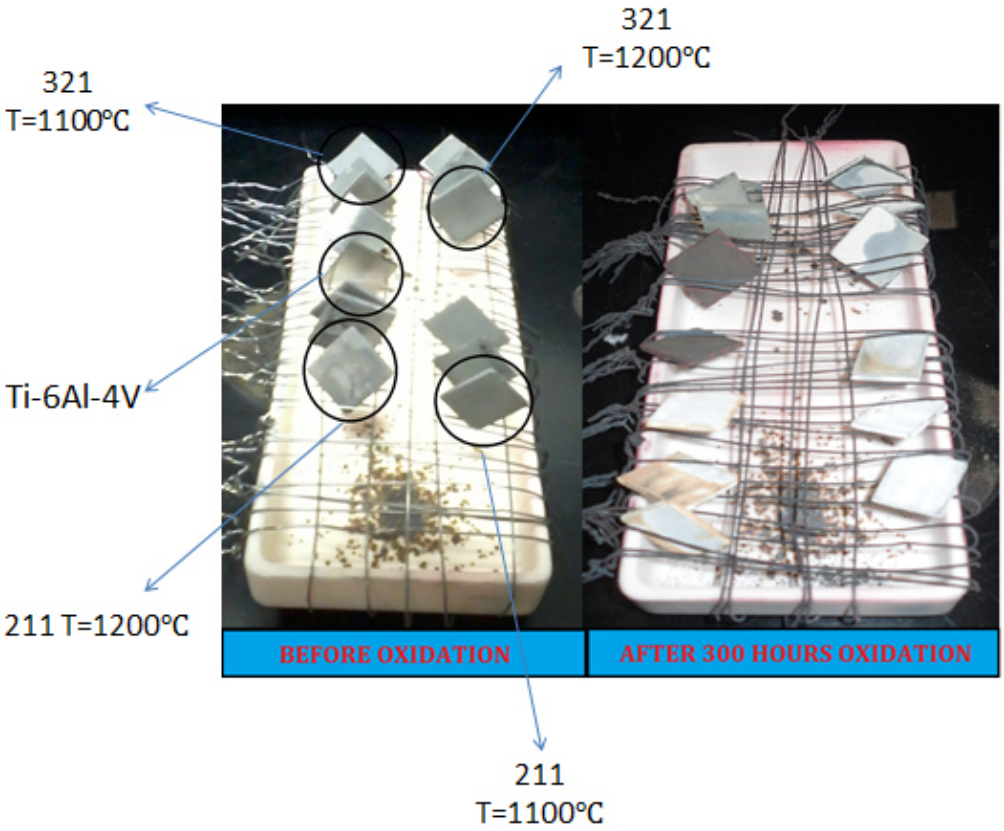

Figure 49 Comparative photographs of the samples in the crucible before and after 300 hours of oxidation in air at 600℃

Another important observation was the fact that the coatings that had diffused at 1100℃ seemed to have had a better oxidation resistance, in the case of 312 samples, they appeared to have no noticeable titanium oxide (white region) whereas for 1200℃ the pieces had started turning green and had small patches of white. The 211 samples that had diffused at 1200℃ also displayed a larger amount of oxide after the first cycle.

Figure 50 Snapshot of the look the 211 samples had after 12 hours oxidation.

The general observation after the 300 hours oxidation in air at 600℃ was that the samples had not oxidized homogeneously. A more detailed visualization of the transformation that the samples suffered after the 300 hours of oxidation in air at 600℃ is seen in Table 19, where the different regions the samples exhibit are clearly noticed. From the visualization it would seem that the samples that appear to have performed best are the samples coated with the 312 MAX phase slurry that diffused at 1100℃.

VISUAL INSPECTION OF THE SAMPLES: TRANSFORMATION			
Ti-6Al-4V with 211 coating			
Diffusion at 1100℃		**Diffusion at 1200℃**	
BEFORE	**AFTER**	**BEFORE**	**AFTER**
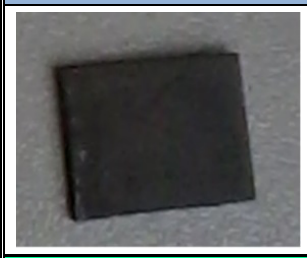	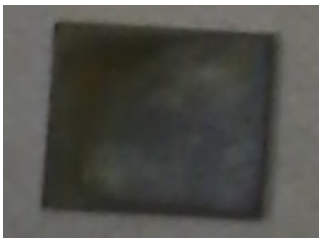	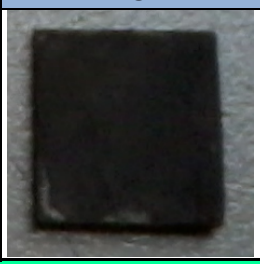	
Ti-6Al-4V with 312 coating			
Diffusion at 1100℃		**Diffusion at 1200℃**	
BEFORE	**AFTER**	**BEFORE**	**AFTER**
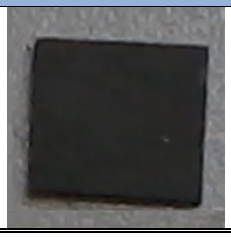		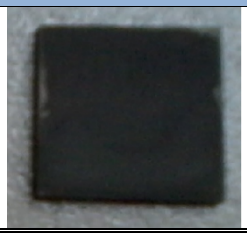	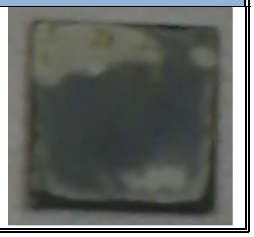

Ti-6Al-4V	
BEFORE	AFTER
	

Table 19 Summary of the visual transformation of the samples before and after the 300 hours oxidation treatment in air at 600℃

6.3 Characterization of Coatings

An analysis of both oxidized and non-oxidized samples will be made for each of the different conditions carried out.

6.3.1. Characterization of the Ti-6Al-4V uncoated substrate

The substrate is the reference condition used to determine the performance of the coated samples.

NON-OXIDIZED SAMPLE

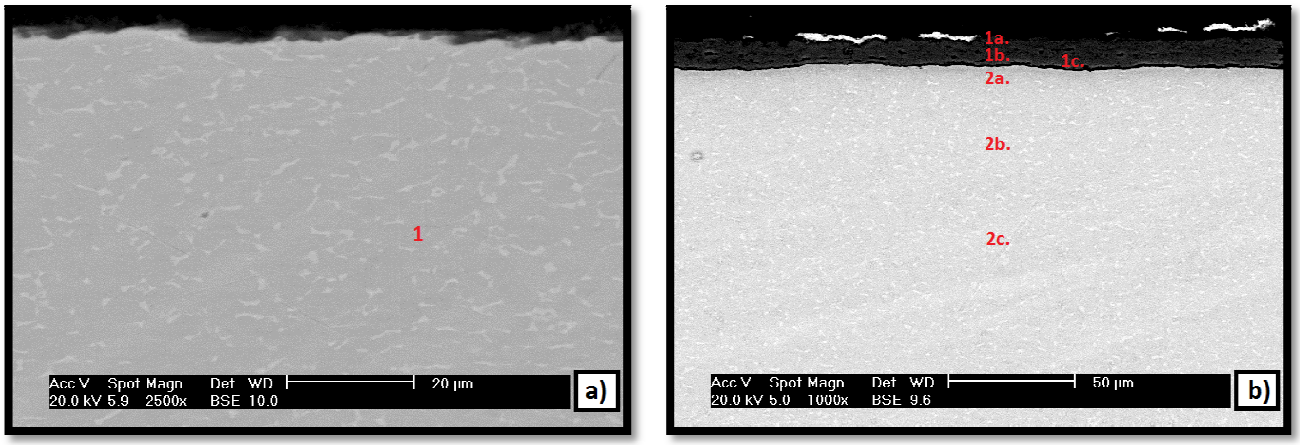

Figure 51 Backscattered Electron image of the cross-section of the Ti-6Al-4V uncoated substrate (a) before and (b) after oxidization in air for 300 hours at 600℃

The substrate by itself exhibits the typical microstructure of this kind of alloy (see Figure 51a). Vanadium is present in the lighter areas which correspond to the β phase that appears in the titanium alloy. The microstructure exhibited is a fine equiaxed α+β structure, in which the small amount of intergranular β can be noticed.

The composition obtained for point 1 can be seen in Table 20. From it, it can be noted that it is a typical composition of the Ti-6Al-4V alloy, similar to the stoichiometric which is 90 wt.% Ti, 6 wt.% Al and 4 wt.% V, which in terms of atomic percent would be around 86.65 at.% Ti, 10.27 at.% Al and 3.08 at.%.

COMPOSITION ANALYSIS						
Point	Elements (at.%)					Location
	O	Al	Ti	V	C	
1	-	11.28	85.67	3.05	-	30 µm from the surface

Table 20 EDS analysis of the Ti-6Al-4V uncoated sample before oxidation in air at 600℃ for 300 hours

Regarding the phases present in the Ti-6Al-4V uncoated substrate before oxidation, from the diffraction pattern obtained what can be made out is that the composition of the substrate contains, just as expected, a higher amount of titanium α phase than β one (Figure 52a).

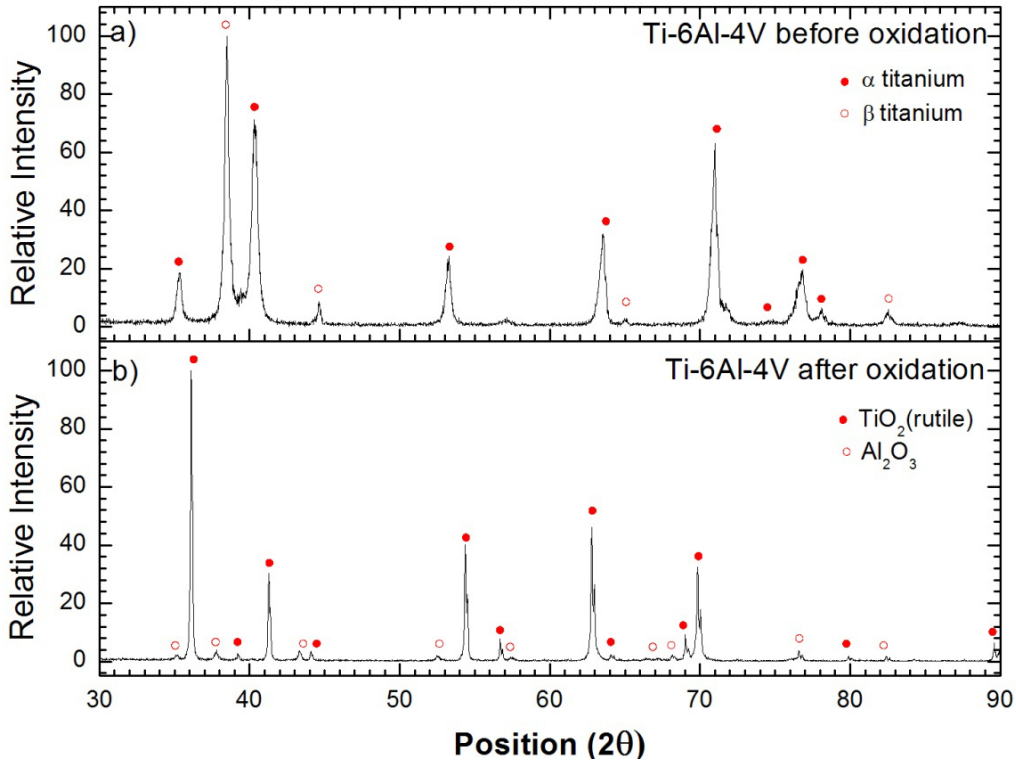

Figure 52 Diffraction patterns of the uncoated Ti-6Al-4V samples (a) before and (b) after oxidation in air at 600℃ for 300 hours

OXIDIZED SAMPLE

The cross-section of sample was visualized by the SEM backscattered electrons (BSE) obtaining the following results for the Ti-6Al-4V uncoated sample oxidized for 300 hours in air at 600°C (Figure 51b). From the image we can detect different regions, more precisely two different regions. The first region (marked with a 1) is the oxide that has formed, whereas the second region (2) is the substrate.

The characteristics that are easily noticed from the oxide layer when scanning the whole substrate are:

1) **Discontinuous**: It easily detaches from the surface of the substrate (see Figure 53). However, in those regions where it remains its thickness is about 12 µm.
2) **Porous:** The oxide is porous; pores can be seen all over.
3) The thickness of the interface between the oxide and the substrate changes over the sample surface.

In Figure 53 it is made clear how discontinuous the oxide layer formed is, in Figure 53a) picture shown the oxide is shown intact and even some copper from the protective coating applied can be seen (white layer on top of the oxide). In the Figure 53b) some oxide is found in the rightmost side of the sample, but besides that there's no oxide left. Figure 53c) shows a region with no oxide at all.

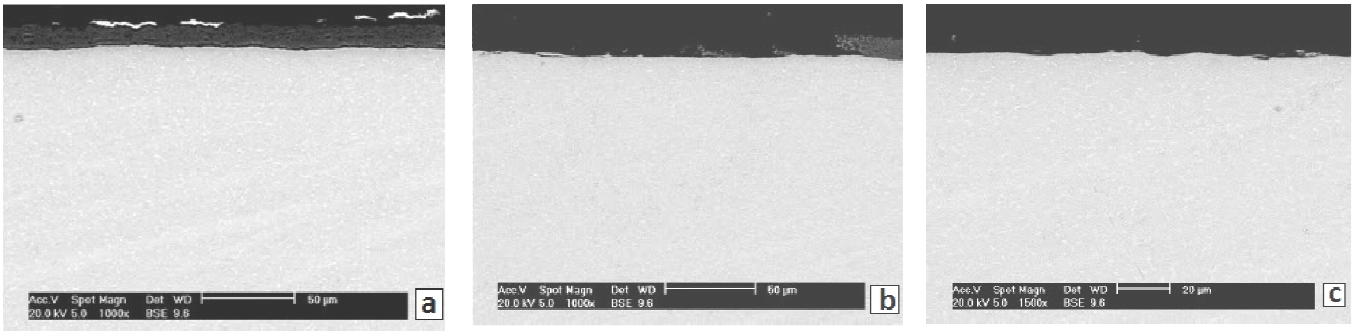

Figure 53 Backscattered Electron images showing the different oxide regions in the uncoated Ti-6Al-4V sample oxidized in air for 300 hours at 600°C

Analysis of the composition of the transversal cross-section of the sample was done using EDS (Energy Dispersive X-Ray Spectroscopy), obtaining the composition of the oxide and substrate in the different regions marked in Figure 51b. The results obtained are displayed in Table 21. From the analysis it can be noticed that the highest amount of aluminum is found on the upmost part of the oxide.

The composition shows the presence of oxygen, titanium, aluminum and vanadium (although in a much lower proportion) in the oxide, this leads to concluding that the oxide scale formed will probably have several types of oxides, titanium oxide preferentially, but also

aluminum oxide. The large carbon content found at the surface of the oxide is probably from the resin used to mount the samples.

COMPOSITION ANALYSIS						
Point	Elements (at.%)					Location & Observations
	O	Al	Ti	V	C	
1a.	48.49	12.01	15.86	-	23.64	Surface of the oxide layer, Al_2O_3 and TiO_2.
1b.	57.90	1.88	39.13	1.09	-	Middle of the oxide layer, TiO_2.
1c.	59.12	0.59	39.60	0.69	-	Almost at the interface of the oxide layer, TiO_2.
2a.	-	12.32	84.83	2.85	-	Surface of the substrate: point where Al content is the highest.
2b.	-	11.84	85.37	2.79	-	30 µm from the surface of the substrate. Typical Ti-6Al-4V composition.
2c.	-	11.04	85.98	2.98	-	60 µm from the surface of the substrate. Typical Ti-6Al-4V composition.

Table 21 EDS analysis of the Ti-6Al-4V uncoated sample after oxidation in air for 300 hours at 600℃

Going back to the XRD results obtained for the uncoated Ti-6Al-4V sample oxidized for 300 hours at 600℃ (Figure 52b) it can be seen that the phases present in the sample are TiO_2 and Al_2O_3. Comparing the intensity of the TiO_2 phases with that of the Al_2O_3 it is clearly noticed how the intensity of the peaks of the former phase is much lower than the intensity for those peaks corresponding to TiO_2. This indicates that TiO_2 is probably the major species.

6.3.2. Characterization of the 211 Slurry Coating

I. 211 Slurry Coating Diffused at 1100 ℃

NON OXIDIZED SAMPLE

When looking at the cross-section of the samples coated with 211 slurry the first thing that is noticed is the extended porosity that there is in the interface of the coating and the substrate. Looking carefully, the lighter phase noticed in the substrate in Figure 54a is the β phase rich in vanadium from the substrate (α+β phase). Three different layers can be pointed out (see Figure 54a). The first layer is the copper coating (1), the second one with a slightly different grey shade (2), is the 211 slurry coating, and below this one the substrate (3).

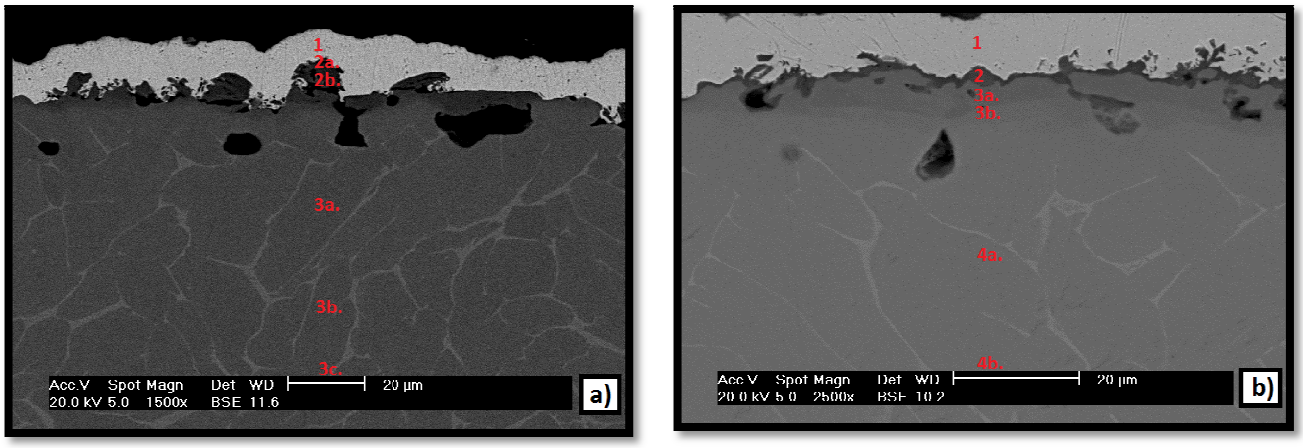

Figure 54 Backscattered Electron Image of the Ti-6Al-4V sample coated with the 211 slurry and diffused at 1100℃ (a) before and (b) after oxidation 300 hours oxidation in air at 600 ℃

Despite the uniform appearance the sample has in Figure 54a there are many areas where the coating has completely disappeared from the surface of the substrate. Additionally in the regions where there is coating its thickness does not exceed 5 µm.

Regarding the substrate microstructure, the diffusion treatment seems to have caused a change in the microstructure of the Ti-6Al-4V substrate. The microstructure of the uncoated Ti-6Al-4V samples before oxidation was fine equiaxed, whereas the microstructure observed in Figure 54a resembles more a fine lamellar one.

The study of the composition for this coating analyzed using the EDS is seen in Table 22.

COMPOSITION ANALYSIS						
Point	Elements (at.%)					Location & Observations
	O	Al	Ti	V	C	
2a.	-	20.66	60.56	0.07	18.70	Surface of the coating. Probably Ti_2AlC or Ti_3AlC.
2b.	-	22.52	67.12	0.03	10.32	Middle of the coating. Probably Ti_2AlC or Ti_3AlC.
3a.	-	12.96	71.80	2.94	12.30	30 µm from the surface of the substrate. Considerable C and Al has diffused into the substrate.
3b.	-	14.77	81.96	3.27	-	60 µm from the surface of the substrate. Al diffusion into the substrate.
3c.	-	10.54	86.32	3.14	-	Middle of the substrate. Typical Ti-6Al-4V composition.

Table 22 EDS analysis of the Ti-6Al-4V sample with 211 slurry coating and diffusion at 1100℃ before oxidation

From the previous results it is observed that the coating is composed of, as expected, Ti, Al and C. Another fact that can be noted is that C has diffused about 30 µm into the substrate by the diffusion treatment., whereas Al has diffused even further, finding it in a considerable amount even at the middle of the substrate.

Examining the phases present in the sample coated with the 211 slurry and diffusion at 1100°C before oxidation (Figure 55a) the first thing that is noticed is that the 211 phase is not as dominant as might have been expected. It is made clear that the original MAX phase decomposed during the diffusion treatment into several phases of similar nature. The phases found are: TiC, Ti_3AlC_2, Ti_2AlC and Ti_3AlC. All of them include carbon, being this a possible explanation for the high carbon content encountered in the coating and even in the substrate when carrying out the EDS analysis.

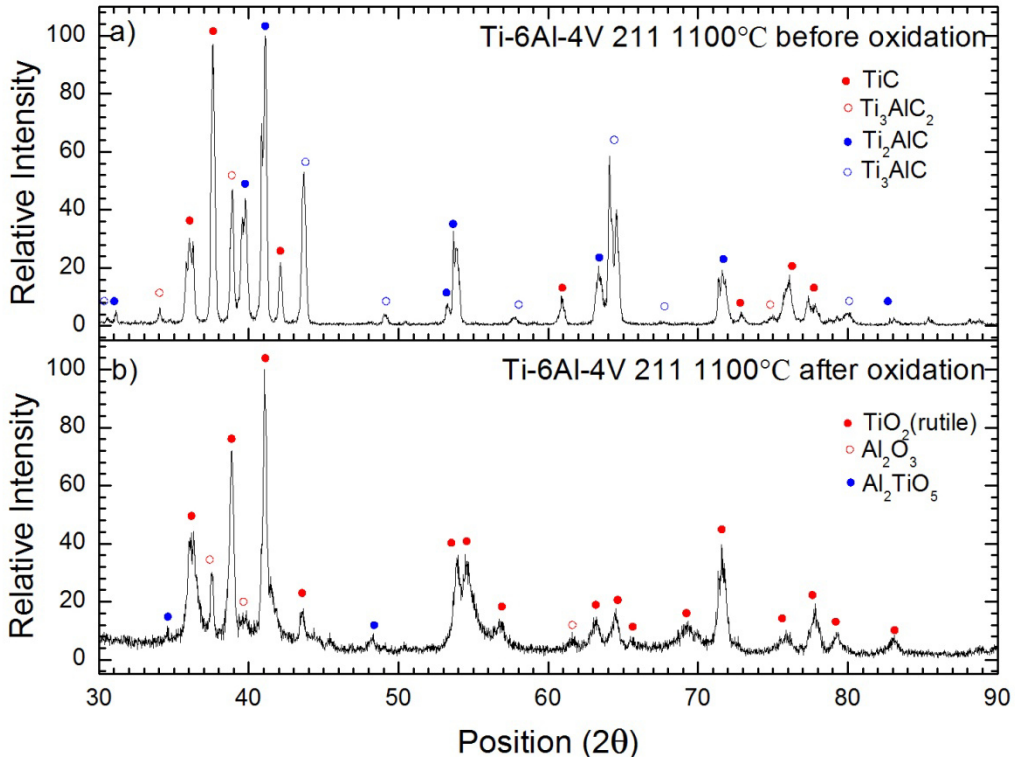

Figure 55 Diffraction patterns of the Ti-6Al-4V samples with 211 slurry coating and diffusion at 1100 °C (a) before and (b) after oxidation in air at 600°C for 300 hours

OXIDIZED SAMPLE

The look of the cross-section of the oxidized samples after 300 hours oxidation in air at 600°C can be seen in Figure 54b. In it four different regions can be pointed out. As already noted in other samples the first one is the copper coating (1), the second one is the layer of oxide formed (2), underneath this one lies the third layer (3), which is slightly darker than the substrate and finally the substrate with its different phases (4). The coating seems to have completely oxidized.

It is of interest to determine the composition of the oxide along with the one of the darker region in the substrate (represented by points 2 and 3a and 3b in the composition analysis). In Table 23 the results from the composition analysis at the different points indicated in Figure 54b are displayed.

COMPOSITION ANALYSIS						
Point	Elements (at.%)					Location & Observations
	O	Al	Ti	V	C	
2	55.04	1.14	43.82	-	-	Oxide. TiO_2.
3a.	-	24.48	75.45	0.07	-	Region 3 (I). Titanium rich aluminide.
3b.	-	23.22	75.68	1.10	-	Region 3 (II). Titanium rich aluminide.
4a.	-	15.84	81.28	2.88	-	30 µm from the surface of the substrate. Al has diffused into the substrate.
4b.	-	14.00	81.58	4.43	-	60 µm from the surface of the substrate. Al has diffused into the substrate.

Table 23 EDS analysis of the Ti-6Al-4V sample with 211 slurry coating and diffusion at 1100℃ after 300 hours oxidation in air at 600℃

From Point 2 we can conclude that the composition of the oxide is probably mainly titanium oxide given the large amount of oxygen and titanium. Additionally, there's a small amount of aluminum, although not much, so a small amount of aluminum oxide will most certainly have also formed. This is also confirmed by XRD diffraction (Figure 55b) where TiO_2 and Al_2O_3 both appear present. If other regions of the oxide were analyzed we might find areas with a higher amount of aluminum.

The first thing that can be noticed when looking at the results is that the carbon from the coating seems to have disappeared, there's no C content in neither of the points. Regarding the third region (characterized by points 3a. and 3b. in Figure 54b) the change in color is justified by a large amount of aluminum in the sample, most probably originated from the slurry coating. In this region the aluminum content was found to be 24.48%.at, which is more than that found in the substrate; it is possible that this corresponds to a titanium rich aluminide (Ti_3Al).

Examining the results obtained from the diffraction pattern of the Ti-6Al-4V sample coated with the 211 slurry and oxidized for 300 hours at 600°C (Figure 55b) it is seen that three oxides are found: aluminum oxide (Al_2O_3), rutile (TiO_2) and a mixed oxide (Al_2TiO_5). Out of the three the one that represents the highest number of peaks and the ones with the highest intensity is rutile. The fact that no phase with carbon is present corroborates the results obtained from EDS in which no carbon was detected.

II. 211 Slurry Coating Diffused at 1200 ℃

NON-OXIDIZED SAMPLE

A characteristic region of the sample's lateral cross section can be seen in Figure 56a. The coating seems to have disappeared leaving a porous layer behind. This would make sense as when the samples where brought out of the vacuum furnace they seemed to have lost part of the coating. Just as for all the samples in which the coating diffused, a large amount of porosity is observed in the substrate; it can even be noted that it seems to be greater than for the 211 samples treated at 1100 ℃ diffusion temperature.

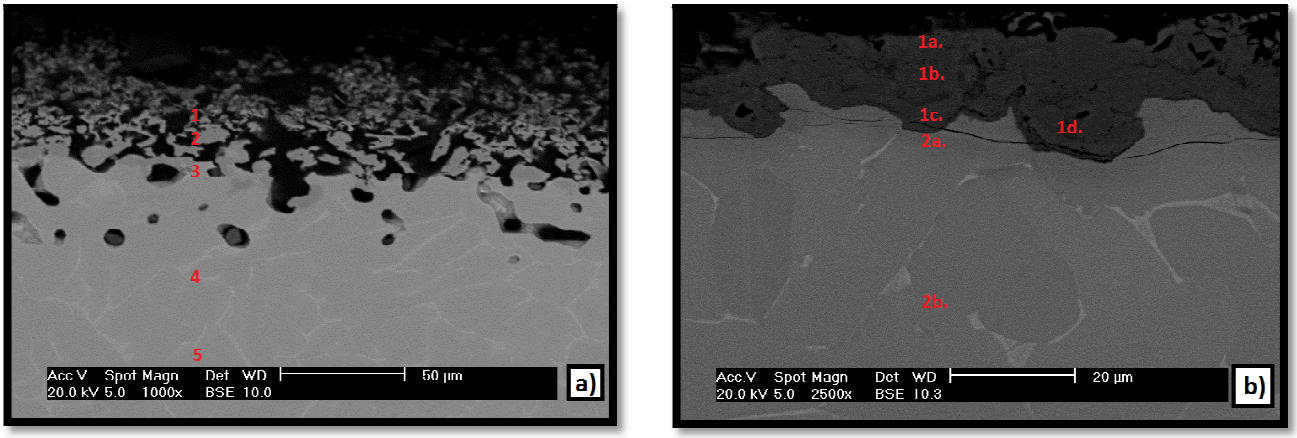

Figure 56 Backscattered Electron image of the cross-section of the Ti-6Al-4V sample coated with the 211 slurry and diffusion at 1200℃ (a) before and (b) after oxidation in air for 300 hours at 600℃

From the previous picture it can be seen that unlike in the other samples slurry coated with the 211 MAX phase that diffused at 1100℃ no clear distinction of regions can be made. The composition analysis carried out the points indicated in Figure 56a can be seen in Table 24.

Looking at the composition obtained in the coating there seems to have been a change in phase MAX composition. The aluminum from the MAX phase is gone and part of it has probably diffused into de substrate causing only C and Ti to remain, forming what will most probably be TiC.

COMPOSITION ANALYSIS						
Point	Elements (at.%)					Location & Observations
	O	Al	Ti	V	C	
1	-	-	75.51	-	24.49	Upmost part of the sample. TiC.
2	-	-	58.52	-	41.48	Coating-Interface. TiC.
3	-	15.80	83.18	1.02	-	Upper part of the substrate. Al has diffused into the substrate.
4	-	14.98	82.61	2.41	-	60 µm in the substrate. Al has diffused into the substrate.
5	-	11.94	85.48	2.57	-	Centre of the substrate. Typical substrate composition.

Table 24 EDS analysis of the Ti-6Al-4V sample with 211 slurry coating and diffusion at 1200℃ before oxidation

Looking at the diffraction pattern for the Ti-6Al-4V sample coated with the 211 slurry and diffused at 1200℃ before oxidation (Figure 57a) it can be seen how the phases present are the same as for the 211 slurry coated sample treated at 1100℃, indicating that at this temperature decomposition of the 211 slurry also took place. It is noticed though, that the intensity of the Ti_2AlC peaks is much lower than for the previous case, gaining a higher importance the TiC phase. From these results it is noticed that although no aluminum seems to appear in the EDS results the phases which contain aluminum still appear in the diffraction pattern.

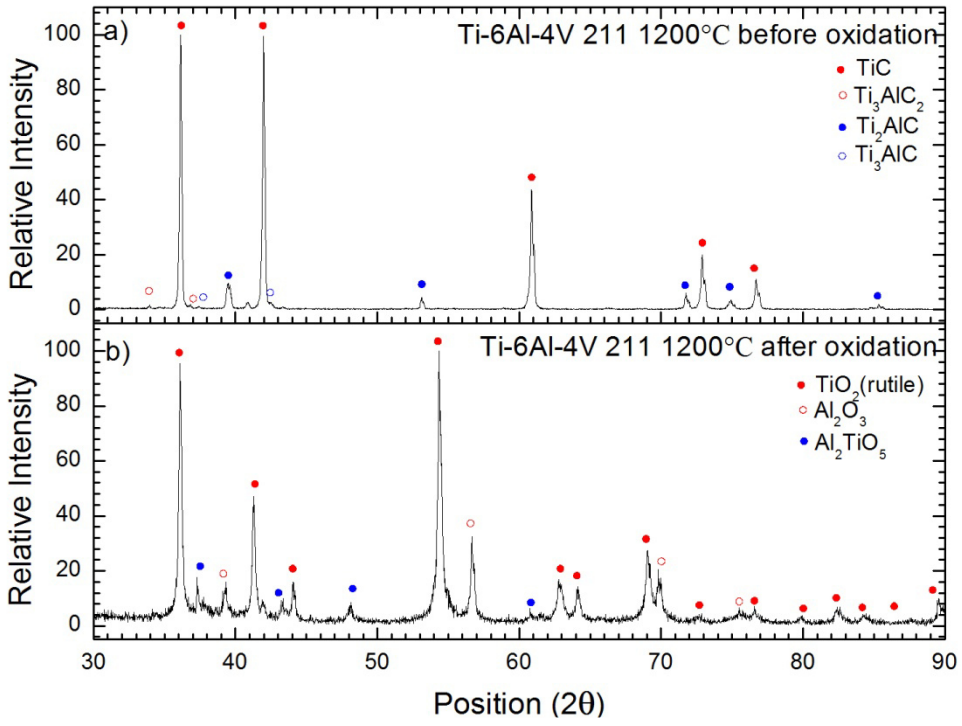

Figure 57 Diffraction patterns of the Ti-6Al-4V samples with 211 slurry coating and diffusion at 1200 ℃ (a) before and (b) after oxidation in air at 600℃ for 300 hours

OXIDIZED SAMPLE

The cross-section of the oxidized sample shows that the previously porous sample surface has been covered by a uniform film of oxide which in some regions has a certain porosity as well. Among the observations made, it has been noticed that cracks have developed between the coating and the substrate (see Figure 56b). The cracks do not seem to be related with the pores, what seems to have cracked is the oxide.

There are two regions, the oxide and the substrate. In the oxide two different shades can be observed, this will probably mean that the oxide formed has more than one composition.

The cracks developed have caused the oxide layer to fall off in some areas of the substrate.

The EDS analysis was carried out for the series of points indicated in Figure 56b (point 2c is out of the range of the image of the cross section); the results obtained are indicated below:

COMPOSITION ANALYSIS						
Point	Elements (at.%)					Location & Observations
	O	Al	Ti	V	C	
1a.	52.62	0.73	46.65	-	-	Upper region of the oxide. TiO_2.
1b.	54.84	1.21	43.94	-	-	Centre part of the oxide.TiO_2.
1c.	56.77	0.53	42.70	-	-	Oxide region closest to the substrate. TiO_2.
1d.	52.89	12.50	34.61	-	-	Dark region in the oxide. Al-rich oxide.
2a.	-	15.43	81.95	2.61	-	Upper region in the substrate. Al diffusion into the substrate.
2b.	-	15.85	81.69	2.46	-	30 µm in the substrate. Al diffusion into the substrate.
2c.	-	15.87	81.90	2.24	-	60 µm in the substrate. Al diffusion into the substrate.

Table 25 EDS analysis of the Ti-6Al-4V sample with 211 slurry coating and diffusion at 1200℃ after oxidation in air for 300 hours at 600℃

The oxide is characterized by being formed by different concentrations of Ti and Al. The lighter regions have almost no Al and the darker ones are the ones in which all the aluminum content is higher.

Comparing the results obtained from the EDS analysis with the species found present in the diffraction pattern of this sample (Figure 57b) the presence of the three elements found in the oxide (Al, Ti and O) is corroborated by the phases identified: TiO_2, Al_2O_3 and Al_2TiO_5. The peaks with the highest intensity correspond to TiO_2 meaning that this phase is probably the most abundant.

6.3.3. Characterization of the 312 Slurry Coating

I. 312 Slurry Coating Diffused at 1100 ℃

NON-OXIDIZED SAMPLE

Analysis of the cross-section of the 312 slurry coating diffused at 1100℃ before oxidation was similar to the one of the 211 slurry coating that had diffused at the same temperature. The 312 coating is continuous, porous and homogenous all over. There is porosity between the substrate and the coating (see Figure 58a). The thickness of the coating seems to be greater than the one for the 211 coating, for the 312 case it is around 10 µm.

Three different regions are noticed. The first one (1) is the copper coating, the second (2) the 312 coating and last of all the substrate (3).

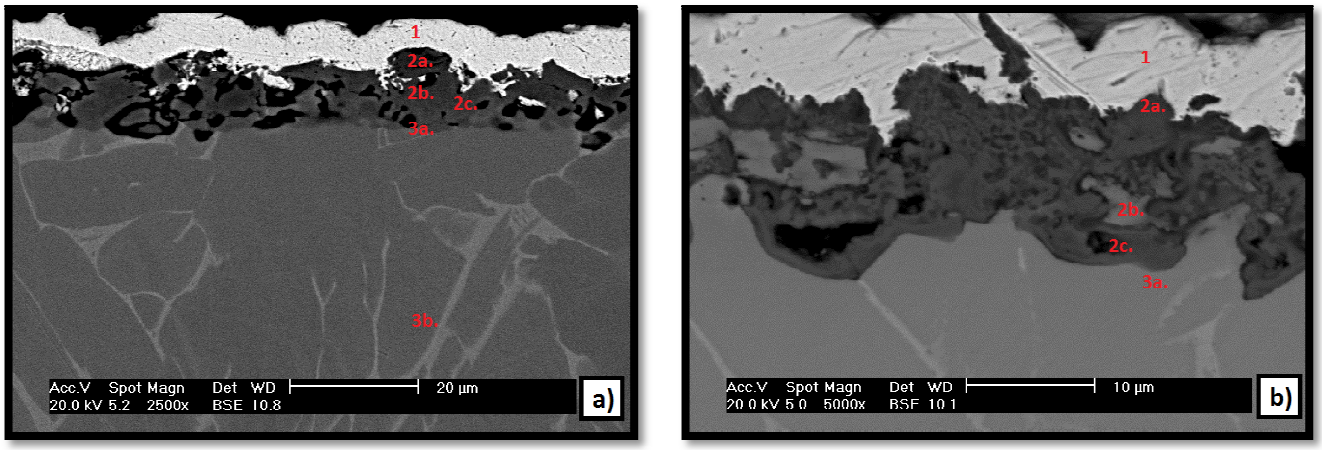

Figure 58 Backscattered Electron image of the cross-section of the Ti-6Al-4V sample coated with the 312 slurry and diffusion at 1100℃ (a) before and (b) after oxidation in air for 300 hours at 600℃

The substrate just as in the 211 slurry coated samples for both before and after oxidation for 300 hours treated at either temperature shows a different microstructure (lamellar) than the uncoated Ti-6Al-4V substrate (equiaxed).

The analysis of the composition for the different points indicated in Figure 58a and point 3c, which is out if the range of the cross section image shown, is seen in Table 26.

COMPOSITION ANALYSIS							
Point	Elements (at.%)						Location & Observations
	O	Al	Ti	V	Si	C	
2a.	-	-	56.82	-	17.79	25.39	Upmost part of the coating: Homogenous porous coating
2b.	-	-	63.12	-	10.74	26.15	Middle of the coating: High carbon content.
2c.	-	-	68.99	-	16.05	14.97	Coating point III.
3a.	-	2.20	57.87	0.64	34.10	5.19	Interface coating-substrate. Si diffusion into the substrate.
3b.	-	8.97	83.98	4.58	2.47	-	30 µm from the surface of the substrate. Si diffusion into the substrate.
3c.	-	10.23	84.12	4.02	1.63	-	60 µm from the surface of the substrate. Si diffusion into the substrate.

Table 26 EDS analysis of the Ti-6Al-4V sample coated with the 312 slurry and diffusion at 1100℃ before oxidation

From the composition analysis we can point out the large Si content found in the coating and the interface. As expected the main elements found in the coating are Si, Ti and C. However, Si has diffused into de substrate, reaching its maximum value at the interface. Carbon from the coating does not diffuse into the substrate as silicon, already when at 30 µm from the surface of the substrate no carbon is found.

Regarding the phases found present in the diffraction pattern of the 312 slurry coating diffused at 1100℃ before oxidation (Figure 59a) it can be seen that just as the 211 slurry coating treated at the same temperature before oxidation the peaks corresponding to the MAX phase are few, indicating that this slurry has also decomposed. The decomposition of the 312 MAX phase slurry is also corroborated by the other species found present, Ti_8C_5 and Ti_5Si_3.

The fact that no other species besides Ti_3SiC_2 that combines C and Si leads to believing that the decomposition has caused Si and C to react independently with titanium, giving way to two different individual compounds.

The phase which corresponds to the peaks with the highest intensity is the Ti_8C_5, meaning that this is probably the phase found in the highest concentration corroborating the high carbon content encountered in the coating by the EDS analysis.

It is also of interest to mention that the carbide that has formed from decomposition of the 312 MAX phase, Ti_8C_5, is not the same as the one formed for the 211 coating, TiC.

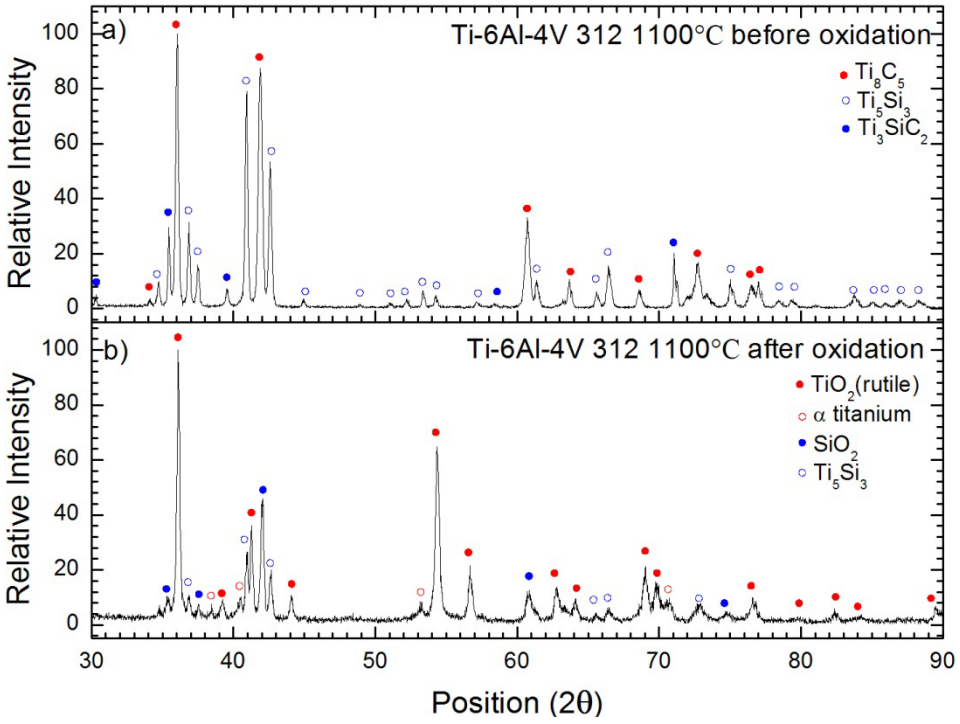

Figure 59 Diffraction patterns of the Ti-6Al-4V samples with 312 slurry coating and diffusion at 1100 ℃ (a) before and (b) after oxidation in air at 600℃ for 300 hours

OXIDIZED SAMPLE

The cross-section of the 312 slurry coated sample diffused at 1100℃ after oxidation in air for 300 hours at 600℃ is similar to that of the same sample before oxidation. The oxide formed has two different colors, indicating different composition. Just as the sample before oxidation, pores can be found. The four regions clearly differentiated are (see Figure 58b): the copper coating (1), a lighter region also in the oxide layer (2b) a darker region in the oxide layer (2c), and finally the substrate (3a).

The composition analysis done for the points indicated in Figure 58b and two more which are out of the range of the image shown can be seen in Table 27.

COMPOSITION ANALYSIS							
Point	Elements (at.%)						Location & Observations
	O	Al	Ti	V	Si	C	
2a.	57.53	-	30.88	-	11.59	-	Surface of the oxide. Si-rich oxide.
2b.	60.02	-	39.28	-	0.69	-	Light region in the oxide. TiO_2.
2c.	58.35	1.48	25.53	-	14.64	-	Dark region in the oxide. Si-rich region.
3a.	-	12.49	83.90	1.35	2.26	-	Surface of the substrate.
3b.	-	11.03	83.13	3.52	2.31	-	30 µm from the surface of the substrate. Si diffusion into the substrate.
3c.	-	10.94	83.84	3.47	1.75	-	60 µm from the surface.

Table 27 EDS analysis of the Ti-6Al-4V sample with the 312 slurry coating and diffusion at 1100℃ after 300 hours oxidation at 600℃

From the analysis of the composition it can be easily noticed that the oxide composition is not uniform in the sense that three different regions can be identified inside it. The first point we analyzed in the uppermost part of the substrate has a high Si content which is beneficial given the good protective properties of silicon. The second one which was located in the light region of the coating proved on the other hand to have a very low Si content, therefore being mostly titanium oxide. Lastly, the third point on the dark region of the oxide has a high Si content, even higher than the one quantified on the surface of the substrate. Traces of silicon can be found even at 60 µm indicating the extent of the diffusion treatment.

Looking at the diffraction pattern of this sample (Figure 59b) the oxides formed are TiO_2 (rutile) and SiO_2 (silicon oxide). The oxide that has the highest intensity peaks is TiO_2. Apart from the formation of the oxides two other species are found present, titanium and Ti_5Si_3. The appearance of other species beside oxides is something did not happen in the oxidized 211 slurry coated samples, all the species found contained oxygen.

Regarding the presence of titanium in the oxidized 312 slurry coated sample diffused at 1100℃, it can be said that it is probably from the substrate. This finding corroborates what was indicated during the SEM observations in which regions where the oxide had fallen off were found.

Overall, the EDS results corroborate the presence of the species found in the XRD analysis, being the elements found the same that compose the species identified.

II. 312 Slurry Coating Diffused at 1200 ℃

NON-OXIDIZED SAMPLE

The transversal cross-section of the sample can be seen in Figure 60a. Just as for the other diffusion temperature for the same coating it can be seen that it is very porous, although homogeneous all over the sample.

The coating (1) and the substrate (2) can be differentiated by the different colours which indicate different composition.

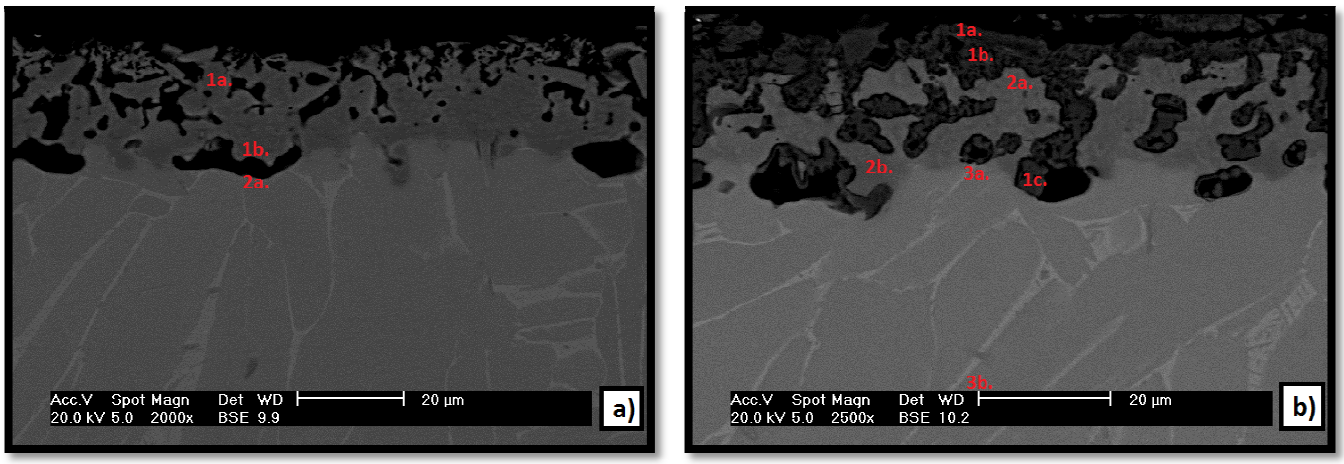

Figure 60 Backscattered Electron image of the cross-section of the Ti-6Al-4V sample coated with the 312 slurry and diffusion at 1200℃ (a) before and (b) after oxidation in air at 600℃ for 300 hours

In Table 28 the results of the analysis of the composition for the points indicated and several more out of the range of the image was done:

COMPOSITION ANALYSIS							
Point	Elements (at.%)						Location & Observations
	O	Al	Ti	V	Si	C	
1a.	-	-	64.37	-	9.97	25.66	Upmost part of the coating. Ti_8C_5.
1b.	-	11.31	85.99	-	2.71	-	Coating-Interface. Si diffusion into the substrate.
2a.	-	11.10	84.08	2.17	2.65	-	Substrate-Interface. Si diffusion into the substrate.
2b.	-	11.77	83.89	1.95	2.39	-	60 µm in the substrate. Si diffusion into the substrate.
2c.	-	11.55	84.15	2.14	2.17	-	140 µm in the substrate. Si diffusion into the substrate.
2d.	-	10.77	85.88	3.35	-	-	Centre of the substrate.

Table 28 EDS analysis of the Ti-6Al-4V sample coated with the 312 slurry and diffusion at 1200℃ before oxidation

From the analysis it can be noted how the composition of the coating is the expected one, Si, C and Ti. Additionally, it is worth pointing that out the diffusion of Si into the substrate has been very effective, finding Si up to 140 µm from the surface of the substrate.

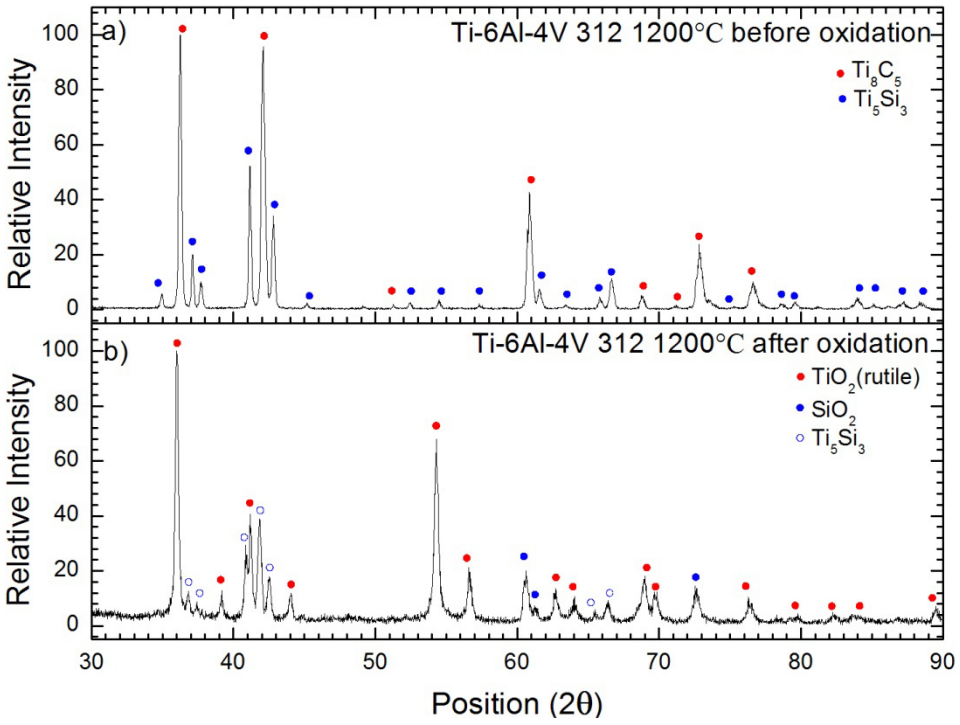

Figure 61 Diffraction patterns of the Ti-6Al-4V samples with 312 slurry coating and diffusion at 1200 ℃ (a) before and (b) after oxidation in air at 600℃ for 300 hours

The information obtained for the diffraction pattern of the 312 slurry coated sample diffused at 1200℃ before oxidation (Figure 61a) indicates that the species present are Ti_8C_5 and Ti_5Si_3, there is no Ti_3SiC_2 phase; indicating that complete decomposition of the Ti_3SiC_2 has taken place during the diffusion treatment at this temperature. The phases identified contain the same elements that have been found in the EDS analysis for this sample.

OXIDIZED SAMPLE

The cross section of the 312 slurry coated oxidized sample diffused at 1200℃ resembles a great deal the one of the non-oxidized one with the only difference that the coating has oxidized and the existing pores have been covered by oxide (Figure 60b). The main regions are the oxide (1), the interdiffusion region (2) and last of all the substrate (3).

Each of the regions mentioned above can be subdivided at the same time because when looking in detail areas of different composition (different colour) can be noticed. This will be seen more clearly when studying the composition. The composition results obtained for the points indicated in Figure 60b and an additional one located 60µm from the surface of the substrate can be seen in Table 29.

COMPOSITION ANALYSIS							
Point	Elements (at.%)						Location & Observations
	O	Al	Ti	V	Si	C	
1a.	55.76	-	43.91	-	0.33	-	Oxide region I: Top part. TiO_2.
1b.	53.32	-	36.37	-	10.31	-	Oxide region I: In the center of the oxide (dark region). Si-rich oxide.
1c.	57.94	-	41.09	-	0.97	-	Oxide region III: Inside a pore. TiO_2.
2a.	6.85	-	83.04	-	10.12	-	Interdiffusion region: clear zone. Si-rich oxide.
2b.	-	-	92.07	-	7.93	-	Interdiffusion region: dark zone. Possibly Ti_5Si_3.
3a.	-	10.17	83.24	3.66	2.93	-	Interface of the substrate.
3b.	-	11.49	83.72	1.88	2.90	-	30 µm from the surface of the substrate. Si diffusion into the substrate.
3c.	-	10.89	83.03	3.29	2.79	-	60 µm from the surface of the substrate. Si diffusion into the substrate.

Table 29 EDS analysis of the Ti-6Al-4V sample coated with the 312 slurry and diffusion at 1200℃ after 300 hours oxidation in air at 600℃

From the analysis the main conclusion reached is that the oxide has areas of different composition in which the silicon and titanium content vary. The oxides found none the less, will probably be silicon oxide and titanium oxide, the former most surely in a higher concentration. Also, the interdiffusion region has different composition depending on the region under study. There is a region with a small amount of oxygen and another where only silicon and titanium remain.

Regarding the substrate, when looking at the composition of the points in the substrate, it can be seen that the silicon content seems to have a standard value when going from the surface of the substrate up to 30 µm. At higher distances from the substrate a decrease in content is noticed, the reduction is not abrupt but rather gradual, therefore diffusion was quite homogeneous.

Additionally it is seen, as in all the pieces that went through the oxidation treatment that the carbon that was found in the coating is gone.

Studying the species the identified species obtained in the diffraction pattern (Figure 61b) it can be seen how the most dominant peaks are the rutile ones. The other phases present are SiO_2 and Ti_5Si_3, just like in the oxidized 312 slurry coated sample diffused at 1100℃, however, no α titanium phase is found in this case.

6.3.4. Summary of Results

In this section a visual summary of the results from both SEM and XRD analyses will be made, along with the layout of the key points observed during the observations. This way comparison between the samples will be easier.

<table>
<tr><th colspan="2">BEFORE</th><th>AFTER</th></tr>
<tr><td colspan="3">SUBSTRATE</td></tr>
<tr><td colspan="2"> 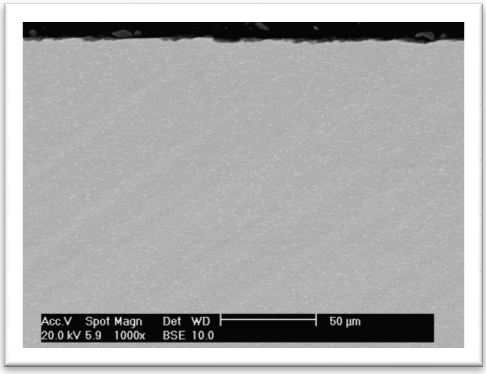

a) Uncoated Ti-6Al-4V sample before oxidation</td><td> 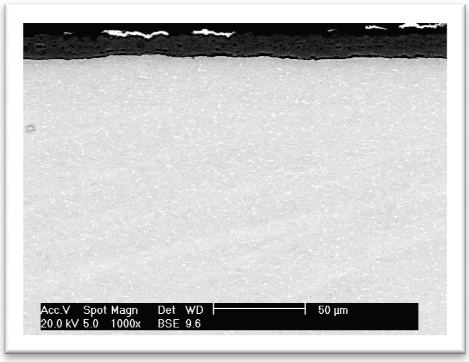

b) Uncoated Ti-6Al-4V sample after 300h oxidation in air at 600℃</td></tr>
<tr><td colspan="3">211 COATING</td></tr>
<tr><td>T=1100℃</td><td> 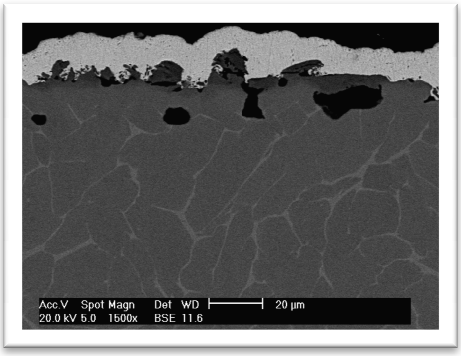

c) 211 slurry coated Ti-6Al-4V diffused at 1100℃ before oxidation</td><td> 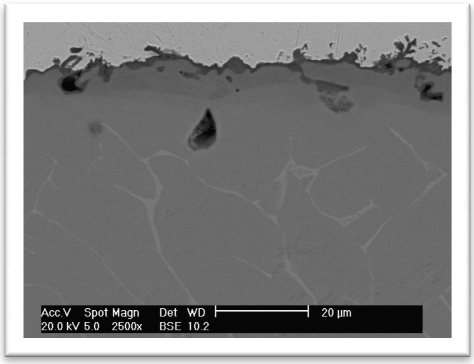

d) 211 slurry coated Ti-6Al-4V diffused at 1100℃ after 300h oxidation in air at 600℃</td></tr>
<tr><td>T=1200℃</td><td> 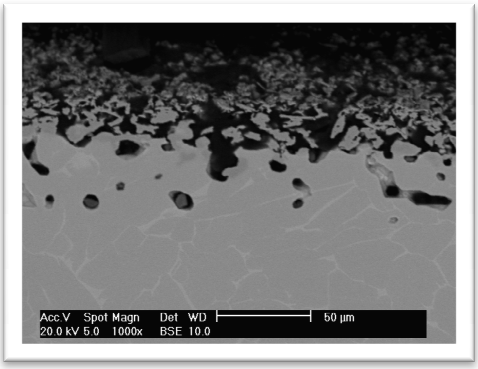

e) 211 slurry coated Ti-6Al-4V diffused at 1200℃ before oxidation</td><td> 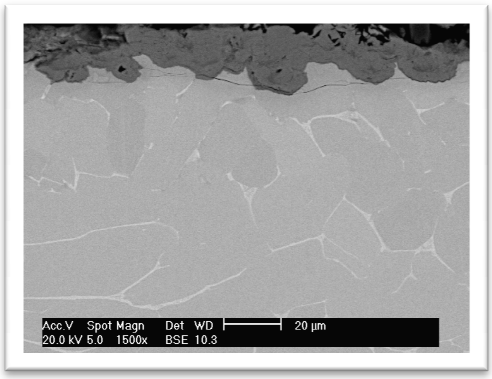

f) 211 slurry coated Ti-6Al-4V diffused at 1200℃ after 300h oxidation in air at 600℃</td></tr>
</table>

BEFORE		AFTER
312 COATING		
T=1100℃	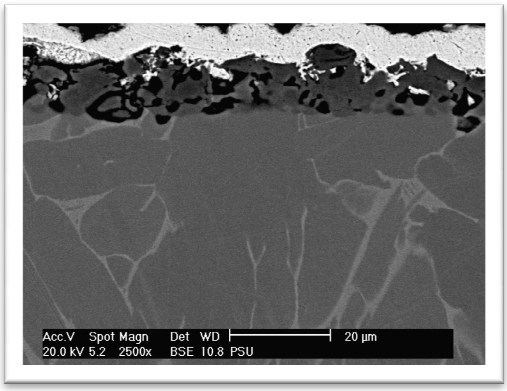 *g)312 slurry coated Ti-6Al-4V diffused at 1100℃ before oxidation*	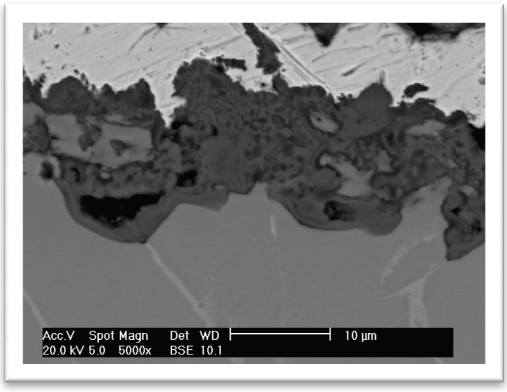 *h) 312 slurry coated Ti-6Al-4V diffused at 1100℃ after 300h oxidation in air at 600℃*
T=1200℃	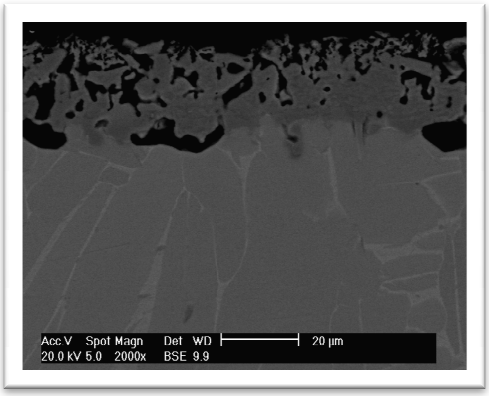 *i)312 slurry coated Ti-6Al-4V diffused at 1200℃ before oxidation*	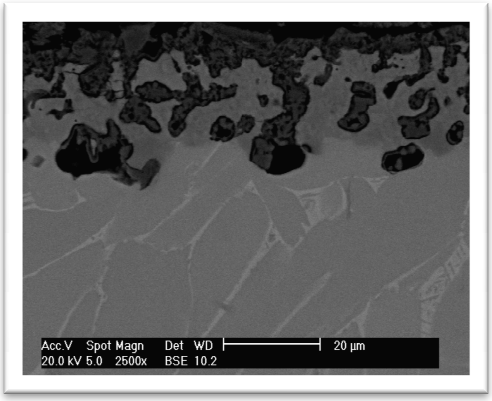 *i) 312 slurry coated Ti-6Al-4V diffused at 1100℃ after 300h oxidation in air at 600℃*

Table 30 Summary of the characteristic Backscattered Electron images for each of the slurry coatings at the different diffusion temperatures and their corresponding transformation after oxidation in air for 300 hours at 600℃

RESULTS FROM DIFFRACTION PATTERNS					
Sample	**Species**	**Reference Code**	**Sample**	**Species**	**Reference Code**
Ti-6Al-4V	**α-Ti**	00-044-1294	-	-	-
	β-Ti	01-088-231			
Oxidized Ti-6Al-4V	**TiO_2**	01-083-2242			
	Al_2O_3	01-071-1683			
211 T1	**Ti_3AlC**	01-089-2282	**211 T2**	**Ti_3AlC**	01-089-2282
	TiC	00-001-1222		**TiC**	00-001-1222
	Ti_3AlC_2	00-052-0875		**Ti_3AlC_2**	00-052-0875
	Ti_2AlC	-		**Ti_2AlC**	-
Oxidized 211 T1	**TiO_2**	03-065-0192	**Oxidized 211 T2**	**TiO_2**	01-075-1757
		01-088-1174			
		01-076-1941			
	Al_2O_3	00-034-0493		**Al_2O_3**	00-047-1292
	Al_2TiO_5	00-018-0068		**Al_2TiO_5**	01-074-1759
312 T1	**Ti_3SiC_2**	01-074-0310	**Oxidized 312 T1**	**Ti_5Si_3**	01-078-1429
	Ti_5Si_3	01-078-1429		**TiO_2**	01-089-4202
	Ti_8C_5	01-072-2496		**SiO_2**	01-085-0621
				α-Ti	00-001-1198
312 T2	**Ti_5Si_3**	00-008-0041	**Oxidized 312 T2**	**Ti_5Si_3**	01-078-1429
	Ti_8C_5	01-072-2496		**TiO_2**	01-076-0318
				SiO_2	01-082-1553

Table 31 Summary of the Species and Reference codes identified in the Diffraction Patterns of the samples before and after oxidation in air at 600℃ for 300 hours

*Note: **T1**-Diffusion at 1100℃*
__T2__- Diffusion at 1200 ℃

The species obtained for each of the samples along with the reference code for their characteristic diffraction patterns are presented in Table 31.

From the combination of both the results obtained by SEM and those obtained by XRD the following points can be highlighted:

- A large amount of carbon is found in all the samples analyzed before oxidation, regardless of the slurry coating. This carbon content seems to be mainly concentrated in the TiC or Ti_8C_5 phases present for each of the MAX phase slurry coatings; TiC for the 211 slurry coating and Ti_8C_5 for the 312 one. This reveals that a phase transformation has taken place in the samples during the diffusion treatment.

- The minor presence of the MAX phases in the diffused samples before oxidation reveals that the decomposition of the MAX phase slurry coatings during diffusion has taken place.

- In the 312 samples the diffusion region is clearly defined and has an important silicon content both in the samples before and after oxidation. The presence of Si in the oxide is noticed in the 312 slurry coated samples after oxidation slurry coated ones, although the titanium oxide (rutile) peaks are still present.

- In the 211 samples Al diffusion into the substrate has occurred. A mixture of Al_2O_3 and TiO_2 is found in the samples after oxidation.

- None of the slurry coated samples, regardless of the slurry, contain any carbon content after 300 hours oxidation in air at 600℃.

- The oxides formed on the 312 samples are of inhomogeneous composition, there's a region with mixed silicon and titanium oxides (rutile), followed by a region of mainly titanium oxide and below that one a newly mixed layer.

- At 1200℃ cracks develop causing in both the substrate and the oxide, making this last one break off and leave the substrate unprotected.

6.4 Oxidation Curves

The curves displayed in this section show the behaviour of each of the coated samples in comparison with the average curve exhibited by the three uncoated Ti-6Al-4V samples. The calculations done to obtain the resulting values that provide the graphs can be seen in Annex II.

The reference oxidation curve for the uncoated Ti-6Al-4V sample can be seen in Figure 62. For obtaining this curve the average value of the three uncoated Ti-6Al-4V samples was used due to the similar behaviour of each of the samples, this is proved by looking at Figure 62 and seeing the small error the average curve has. The kinetics of oxidation exhibited by the sample is close to parabolic during the first 12 hours, but after that it becomes almost completely linear. The mass gained achieved after the 300 hours of oxidation in air is 2.215 mg/cm^2.

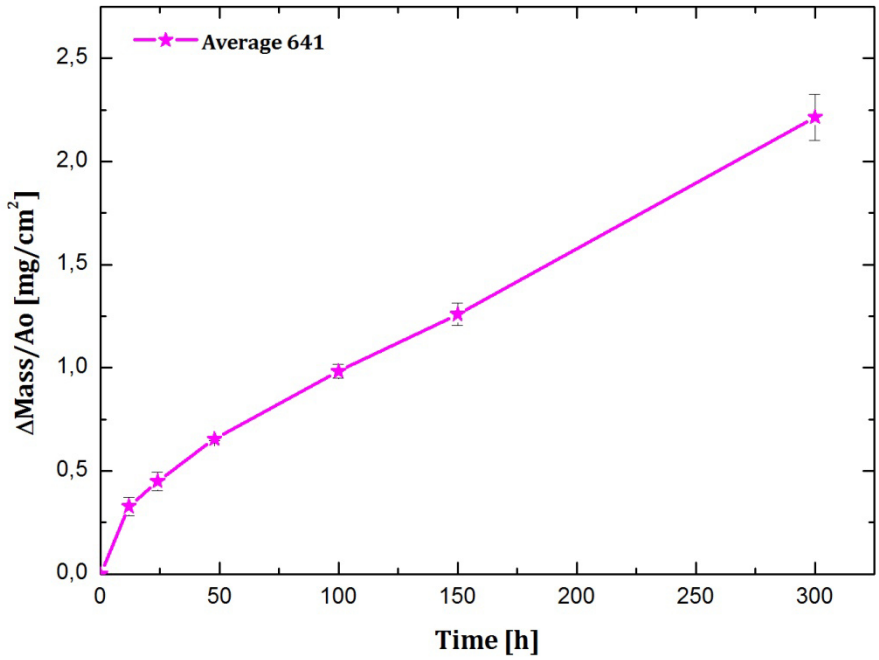

Figure 62 Mass gain of the uncoated Ti-6Al-4V sample after oxidation in air for 300 hours at 600℃

6.4.1. Comparison 211 Coating at 1100℃ and 1200℃

The performance of the 211 coating is largely affected by what happened during the first 12 hours of oxidation. In the oxidation curves (Figure 63) shown for these samples it can be noticed that on the contrary to the untreated Ti-6Al-4V samples that were oxidized, the samples with the 211 coating do not experience a noticeable mass gain. During the first 12 hours cycle they experience a drastic weight decrease, after that they remain at a value close to the one obtained from that initial loss.

It can be seen that for the 211 samples the kinetics of the oxidation process does not seem influenced by the diffusion temperature. Both temperatures are characterized by the abrupt loss in the first 12 hours followed by a more or less constant behaviour. The only difference that could be mentioned is that it seems that for the 1100 ℃ diffusion treatment the initial loss seems to be in general greater than for the 1200 ℃ samples.

Due to the initial loss, it is difficult to ascertain whether the behaviour after the 12 hours is actually as the one obtained or oxide has formed and then fallen off. If the behaviour is really as we have obtained once the initial loss could be prevented the coating would satisfy its protective purpose, remaining almost constant and below the original mass gain of Ti-6Al-4V. The stable behaviour of the coating after the initial 12 hours is probably due to the formation of Al_2O_3 in addition to TiO_2, as confirmed by microstructural and XRD analysis of the coating.

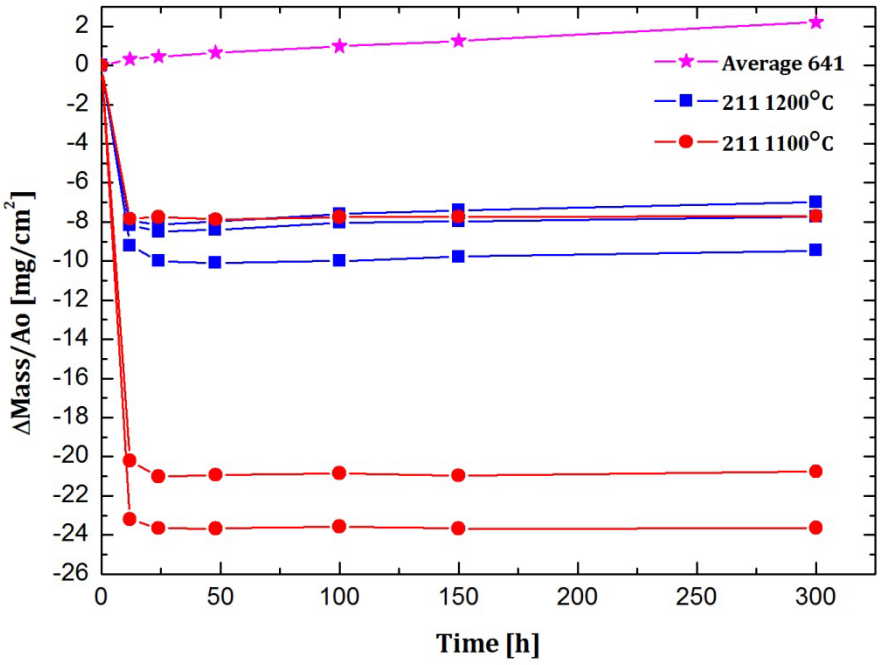

Figure 63 Mass gain of Ti-6Al-4V samples coated with 211 slurry coating diffused at 1100℃ (blue lines) and at 1200℃ (red lines) after oxidation in air for 300 hours at 600℃ compared with the mass gain of the uncoated Ti-6Al-4V sample

6.4.2. Comparison 312 Coating at 1100℃ and 1200℃

Comparing the oxidation curves of the 312 coated samples and the Ti-6Al-4V uncoated substrate (see Figure 64) it can be seen that unlike for the 211 samples the behaviour of all the samples was not the same.

The general behaviour exhibited by 312 samples were diffusion took place at 1200℃ is to experience a weight increase. Looking at the graph it can be seen that from the 3 samples two have experienced the initial mass loss during the first cycle as the 211 samples, but while one has continued losing mass through the cycles, the other one recovers from this initial loss and remains at this value for all subsequent cycles. The third sample, however, experienced an initial increase but had several mass losses towards the end.

For the ones that diffused at 1100℃ something similar happens, just as for the case of diffusion at 1200℃, two lose weight initially, but in this case no posterior recovery takes place. The one that experiences an atypical behaviour with respect to the other two is the third one, instead of the characteristic drastic loss or moderate gain during the first 12 hours, it has a very large increase (much higher than the Ti-6Al-4V) and after that remains at this value.

The lack of uniformity makes it hard to determine whether one temperature or the other was better as the pieces do not exhibit a uniform behaviour. It would seem that although

reaching lower mass gains than the uncoated substrate for the most representative samples the coating has not satisfied its oxidation resistant purpose.

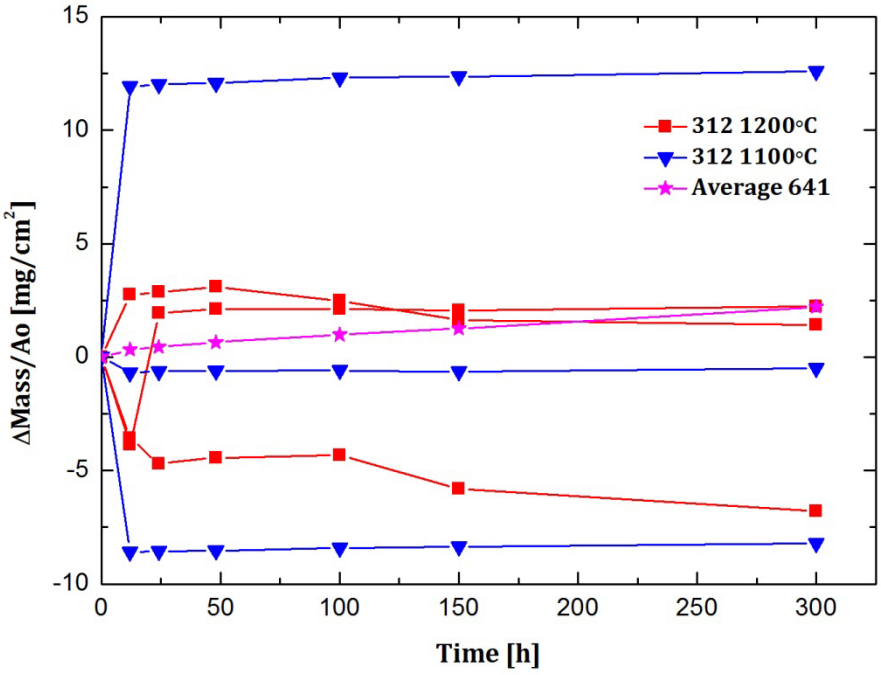

Figure 64 Mass gain of Ti-6Al-4V samples coated with 312 slurry coating diffused at 1100℃ (blue lines) and at 1200℃ (red lines) after oxidation in air for 300 hours at 600℃ compared with the mass gain of the uncoated Ti-6Al-4V sample

6.5 Discussion of Results

In this section we will explain anything that might have been considered of relevance during the development of the experiment along with a comparison of the operating conditions, diffusion temperature used and coating. It will be the basis of the conclusions.

6.5.1 Phenomenon on 211 pieces during oxidation. What happened?

It is of importance to be able to explain what happened during oxidation and why. As we already mentioned the 211 pieces suffered something that resembled a dust explosion, which led to a drastic mass loss, after some research it was concluded that what had probably happened was the phenomenon known as “Metal Dusting”.

Metal Dusting is a catastrophic form of corrosion in which metals exposed to carbon-supersaturated gas disintegrate forming metal-rich particles dispersed in a voluminous carbon deposit. It is common of iron, nickel, cobalt and Cr forming ferritic and austenitic alloys in environments with a high carbon content. (119)

What is known of Metal Dusting from its occurrence in iron and nickel is that for it to take place two requirements need to be satisfied. (120)

- Be in a temperature range within 400-800℃.
- Carbon activity must be greater than one ($a_c > 1$), being in a carbon-supersaturated environment.

When it takes place, dissolution of carbon (from hydrocarbons or CO) happens and is followed by diffusion of the same into the substrate forming carbon. Carbon is then transferred to the solid phase attacking the substrate material and causing decomposition of the same.

The mechanism followed in a supersaturated carbon environment can be summarized in a series of steps (120):

1) C from the gaseous phase in the environment transforms from gas to solid.
2) The metal in the substrate reacts with the solid phase C forming carbides.
3) Graphite starts to grow on top of the carbides with an activity of 1 becoming unstable.
4) The unstable carbon decomposes releasing metal particles that will act as catalysts for further the repetition of the process

Going back to the conditions needed for Metal Dusting to take place and seeing the steps that would be followed we can notice that although the first of the two conditions needed for it to take place were indeed satisfied, the oxidation treatment temperature was 600 ℃, the second wasn't. The operating environment at which oxidation took place was a carbon free one.

As the requirement for Metal Dusting of being in a supersaturated carbon environment is needed, this condition must have somehow been achieved for it to take place. From the results obtained by XRD and SEM it has been made very clear that before oxidation the carbon content in the samples was very high due to decomposition of the original MAX phases. A hypothesis of what might have happened is that the carbides formed during the diffusion treatment reacted with the oxygen in the oxidation furnace creating the supersaturated carbon environment needed.

If the case our hypothesis were satisfied the carbon activity would be greater than one and would follow the mechanism mentioned above starting from point 3) (the carbides are already present in the sample therefore that step has already been achieved during the diffusion treatment) and Metal Dusting would indeed occur.

To prove our hypothesis we will assume that the reaction that took place for the 211 samples was:

$$TiC(s) + 2O_2(g) \rightarrow TiO_2(s) + CO_2(g) \quad T = 600℃$$

Equation 10 Reaction of TiC with O_2 in the 211 slurry coated samples at 600℃

And that for the 312 samples it was:

$$Ti_8C_5(s) + 13O_2(g) \rightarrow 8TiO_2(s) + 5CO_2(g) \quad T = 600℃$$

Equation 11 Reaction of Ti_8C_5 with O_2 in the 312slurry coated samples at 600℃

If the reactions we have assumed are spontaneous it would prove that the reactions may have easily have taken place. It is worth mentioning however, that the actual reaction that took place will most probably be more complex than the assumed ones, but this way an idea of the scope of the mechanism can be attained.

Gibbs Free energy was calculated for Equation 10 to determine whether we can assume the reactions are spontaneous or not. Developing the calculation (development and values used can be seen in Annex III), using the values of entropy and enthalpy provided in the Nist Janaf Thermochemical tables (121)the resulting free energies obtained for the reactions is:

Reaction	Free energy ΔG^o(kJ) at 600℃
Equation 10 at T=600℃	-1006.601

Table 32 Gibbs Energy for the Reaction of TiC with O_2 at 600℃

As they have proved to be negative, the reaction is therefore spontaneous. With this information it is reasonable to assume that Metal Dusting may have occurred.

There are techniques which could protect the substrate material from metal dusting, some of the most common techniques used are: alloying, coatings (the two types of coating methods mentioned in Chapter 4), surface poisoning (adding elements that adsorb on the surface more than carbon so they are adsorbed instead), protective oxide formers, etc. (120)

From all the methods mentioned above the one of most importance to our experiment is the protective oxide one because it means that if Metal Dusting took place it was because the oxide formed wasn't protective. If a protective oxide scale is formed, metal dusting can be slowed down and even prevented, avoiding the carbon attack and preserving the surface from damage. Protective scales could be aluminum oxide and silicon oxide scales.

Alumina scales are known to be protective when the aluminum content is around 4 wt%. Higher aluminum contents increase the brittleness of the oxide scale formed (122). Alloy additions can also improve the alumina scale formation; some which are known to do this are Cr, Nb, Ta, V and Ti at relatively high temperatures (above 650℃). At temperatures below the previous the oxide scale does not satisfy its protective function and once the scale is damaged the attack takes place. Silicon scales on the other hand slow down the rate of metal dusting even when the Si scale formed is not Si rich. (119)

The occurrence of Metal Dusting in the 211 slurry coated samples shows that its oxide scale formed was not too protective. However, the aluminum present in the 211 slurry coating did

form aluminum oxide (Al_2O_3) which is more usually more protective than titanium oxide (rutile) and therefore the formation of this oxide is beneficial to achieve oxidation protection.

The fact that the 312 slurry coated samples were not characterized by the same visual explosion as the 211 slurry coated samples does not mean they did not suffer what has been considered to be Metal Dusting, as they are also characterized by the same initial weight loss found in the 211 slurry coated samples during the first 12 hours of oxidation. What might have happened is that the Si present in the 312 slurry coated sample slowed down the rate of decomposition and in some cases prevented the occurrence of the Metal Dusting phenomenon. It is for this reason that some oxidation curves of the 312 coating show a mass increase instead of a loss.

6.5.2 Influence of the kind of coating selected

From the analysis of the results from both SEM and XRD it is made clear that for the oxidation of the 211 samples two oxides are formed: Al_2O_3 (aluminum oxide) and TiO_2 (rutile). From SEM it is clearly seen that de Al content is very low and by XRD it is clearly noticed that the dominant phase is TiO_2. For the 312 on the other hand, regions where the silicon content was quite high were noticed. They were however, located points and the dominant composition of the overall oxide was still rutile.

Additionally comparing visually the look the samples had it could be mentioned that out of the two coatings although none showed an homogeneous oxidation (look at Table 19) although the 312 exhibited a more homogeneous look. This is clearly seen when analyzing the composition of the oxide formed and seeing that analyzing different points in the oxide the composition changes.

Both coatings seemed to have the ability, neglecting a first step in which they lost (in most cases) a large amount of mass, to keep a constant oxidation rate for most of the samples. This led to what seems to be a better performance than the one of bare Ti-6Al-4V. However, due to the common mass losses found whether this is the actual behaviour exhibited cannot be confirmed.

After the 300 hours of oxidation in air at 600°C both kind of samples exhibited an oxide with a large content of rutile, however additionally the MAX phase coating provided an additional kind of oxide according to the composition of each coating. In the Ti_2AlC coated samples the protective coating that formed was Al_2O_3, whereas for the other it was SiO_2.

Al_2O_3 is an extremely brittle oxide which leads to cracking if the aluminum content is not high enough to provide a continuous scale. This is why cracks probably developed in the 211 oxide. When this happens the protective oxide scale does not regenerate, making the substrate protection disappear and causing its oxidation. (74), (120)

The presence of silicon in the 312 coating is supposed to reduce the oxidation rate of titanium by creating a protective scale which reduces the diffusion rate of atoms through the

scales (2). Its effect regarding oxidation has not been noticed, however, it is true that Si is what has protected the 312 samples from Metal Dusting.

As none of the protective oxides were neither present in a high concentration nor formed an homogeneous stable scale, as we have seen in the XRD and SEM results, oxidation was not slowed down as a whole in the coated samples.

6.5.3 Influence of the diffusion temperature

The influence of the temperature at which diffusion takes place in MAX phases is a topic which is rarely discussed in the available literature. In this project it is one of the parameters which is studied, for this reason pointing out the relevance and the differences between using one temperature and the other is of importance.

Regarding the diffusion temperature it can be said that it has largely influenced the whole experiment. The temperatures selected for the diffusion treatment (1100 and 1200℃) caused the decomposition of the MAX phase slurry coatings leading to the creation of new phases. For the 1100℃ small concentration of the MAX phase could still be found, but at 1200℃ almost complete decomposition of the MAX phase took place, especially for the 312 case. Carrying out a comparison of the original MAX phase powders with the diffraction pattern obtained in this experiment after diffusion, the complete decomposition of the 312 MAX phase is made clear as no peaks from the original pattern match the new ones (see Figure 65).

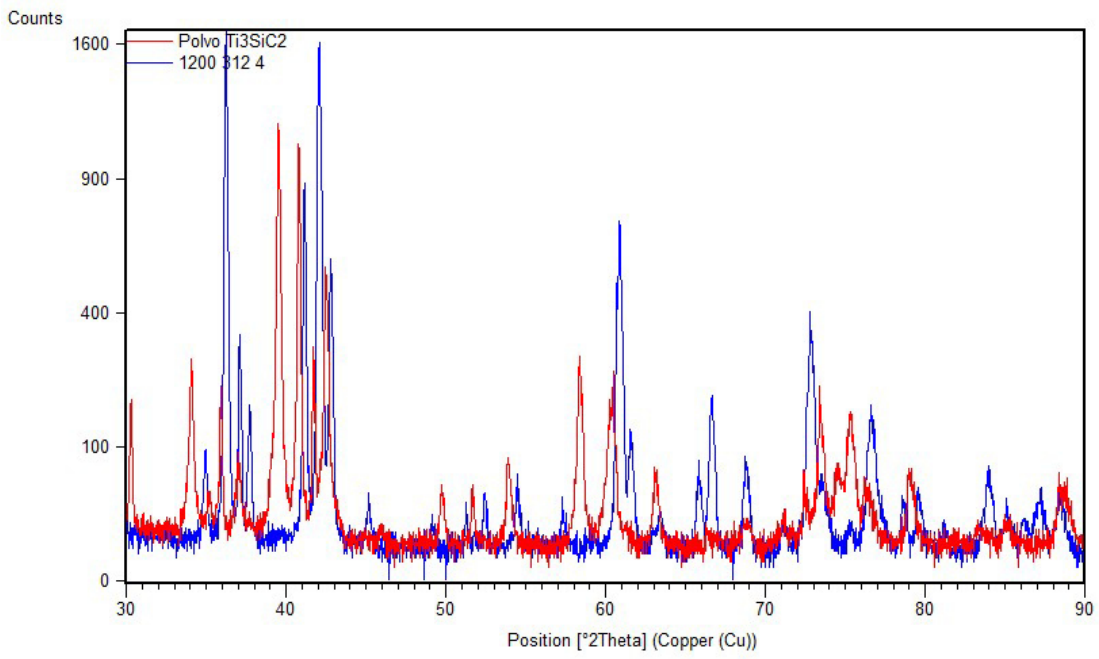

Figure 65 Comparison of the Ti_3SiC_2 MAX phase Powder with Ti_3SiC_2 slurry coating after diffusion at 1200℃

The fact that Ti_3SiC_2 decomposed at this temperature is not strange, there is information indicating that films of this MAX phase when heated in vacuum at temperatures of 1000-1200℃ decompose. Additionally, it is mentioned that the higher the amount of impurities the lower the decomposition temperature. (70)

In order to determine how the diffusion temperature really affected the slurry coating applied on the substrate, an analysis of the phases present under the two different temperatures will be made.

As it can be seen from the XRD results (Figures 55a and 57a for the 211 slurry coating and Figures 59a and 61a for the 312 one) the 211 slurry coating decomposed into the following phases: TiC (titanium carbide), Ti_3AlC and Ti_3AlC_2. In the 312 coating on the other hand, the decomposition led to the formation of two different phases in which C and Si reacted independently with Ti. It decomposed into: Ti_5Si_3 and Ti_8C_5.

Research done on Ti_8C_5 showed that this phase is found when sintering Ti_3SiC_2 at high temperatures (123). Additionally it has also been reported that as temperature increases Ti_8C_5 is believed to convert to TiC (124)**.** The other phase in which it decomposed, Ti_5Si_3, is found quite often in oxidized Ti_3SiC_2 and also in bulk Ti_3SiC_2, being in this last case considered an impurity.

Comparing the phases present for the same slurry coating and different diffusion temperatures it is made clear that at 1200℃ the original MAX phase coating decomposes even further into a higher amount of TiC given the fact that the peaks for the MAX phase slurry coatings are found in a lower amount and also have a higher intensity than the ones for diffusion at 1100℃ so the TiC content is probably higher.

In general, the comparison of the diffraction patterns at both temperatures for both the oxidized and non-oxidized 211 slurry coated samples show that they do not present a high resemblance (Figures 55a vs. 57a and Figures 55b vs. 57b). However, when comparing the 312 slurry coated samples (Figures 59a vs. 61a and Figures 59b vs. 61b) carefully it can be noticed how they exhibit similar diffraction patterns and the same phases are present.

From the diffraction patterns of the 312 samples before oxidation (Figures 59a and 61a) it can easily be made out how the temperature has affected the samples. In the case of the 312 slurry coating diffused at 1100℃ (Figure 59a) the MAX phase decomposed mostly into titanium carbide and titanium silicon; however despite the decomposition traces of Ti_3SiC_2 still remain. However, for the 1200℃ diffusion temperature (Figure 61a) Ti_3SiC_2 has been found to have completely decomposed. The additional peaks found in the plot (Figure 59a) for the 312 slurry coated sample diffused at 1100℃ before oxidation correspond to the remaining 312 MAX phase slurry. This indicates clearly that a higher decomposition has taken place for the 1200℃ diffusion temperature.

As already mentioned in Chapter 3, TiC is not resistant to oxidation, therefore it makes sense that the samples were affected by TiC obtaining a worse performance. TiC presence in the coating also has additional effects; it has the ability of producing CO and CO_2 which may result in pores during oxidation and it increases the oxidation rate (78)**.** For our experiment

what must have happened in that when exposed to the oxidizing environment TiC reacted with oxygen producing CO and CO_2, providing the carbon-supersaturated environment. If this is what has happened, the combustion experienced by C would probably explain the lack of C in the substrate after the oxidation treatment.

Barsoum (28) mentioned back in 2000 that the presence of TiC in Ti_3SiC_2 had a detrimental effect on oxidation kinetics; he also pointed out how it was not considered as important as it should.

Apart from the decomposition noticed, from the results obtained from the composition when characterizing by SEM it can be easily noticed how the higher the diffusion temperature the further the diffused species travel in the substrate. Also, it can be seen that the diffusion treatment is the cause of the formation of pores in the substrate, as for the case of the untreated sample almost no pores were present.

6.5.4 Influence of the oxidation temperature

Information on the oxidation behavior of these two MAX phases at 600 ℃ is rarely reported as the purpose these studies generally have is to be able to implement these materials for high temperature operations, therefore the typical range of values for which results are generally found is 900-1400℃.

Studies carried out on Ti_2AlC and Ti_3SiC_2 have proved they have excellent oxidation resistance at temperatures above 900℃. However when carried out under lower temperatures in the 500-900℃ range anomalous behaviors have been detected. This corroborates our results as the usual oxidation behavior of 211 is to follow parabolic or cubic oxidation kinetics and in our case this does not happen. (125)

Barsoum (28) mentioned in his study on Ti_3SiC_2 that binary carbides and nitrides are not very resistant in air above 500 to 800℃ proving a confirmation of what has been noticed in this study.

The oxidation resistance of Ti_2AlC is based on the formation of the protective α-Al_2O_3 scale. It is known that when oxidation takes place at temperatures in the 500-600℃ range the anatase-rutile transformation that takes place causes the development of induced cracks which affect the protective characteristics of the scale, preventing the fulfillment of its purpose. This fact could explain the formation of the cracks found during the SEM observation for the samples where diffusion took place at 1200℃. It has also been reported that the minimum temperature needed for the formation of a continuous α-Al_2O_3 layer on Ti_2AlC is 700℃. (126)

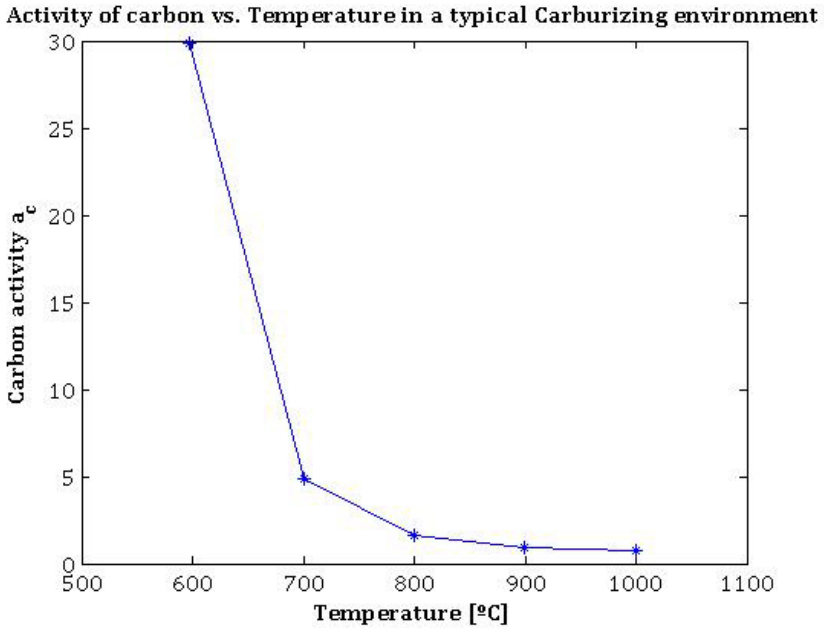

Figure 66 Carbon activity as a function of temperature for a typical carburizing environment. **(127)**

Temperature in Metal Dusting is also known to play an important role. Increases in temperature lead to a decrease in the dusting rates. As it can be seen in Figure 66 the reaction of carbon has a very high activity at 600°C, at temperatures above this value the metal consumption by carbon decreases; for this reason our selected oxidation temperature is not probably the best.

CHAPTER 7: CONCLUSIONS

7.1. Conclusions

The main conclusion reached is the fact that the deposition of a MAX phase slurry coating on a Ti-6Al-4V substrate has been successfully achieved, starting with this project the development of the use of MAX phases in the slurry coating method.

The outstanding discovery of this project is the decomposition of the original MAX that has taken place during the diffusion treatment. The diffusion temperature chosen is what has determined the extent of decomposition. In the 312 samples it was complete when carried out at 1200°C. This decomposition has given way to the formation of carbides that along with the oxidizing environment could have possibly created a supersaturated carbon environment, and led probably to the phenomenon known as Metal Dusting. The possible occurrence of Metal Dusting has conditioned the whole experiment leading to considerable losses in weight of the samples. Additionally these losses can also be used as evidence to demonstrate that the oxide formed is not adherent enough to the substrate.

Regarding the morphology and composition of the coatings after the diffusion treatment it can be said that they are characterized by being homogenous porous films, which after the oxidation cause the formation of an oxide with similar characteristics. Additionally, the diffusion treatment has caused the formation of pores in the substrate which during oxidation are also filled up with oxide.

By the Metal Dusting reaction the carbon reacted with the substrate and coating, disintegrating them. For this reason regions where no oxide was found and a clear fractures and cracks appeared were so common in all oxidized samples, except for the uncoated Ti-6Al-4V substrate.

The behaviour in the 211 samples led to a small amount of aluminum to remain there and create the oxide, reason why the oxide formed contains a mixture of Al_3O_2 and TiO_2 oxides; the aluminum content found in the sample is greater than the one exhibited by the uncoated samples. The oxide formed is uniform and porous, but inhomogeneous in composition.

Although the 312 samples were also affected by an initial loss in weight (as the oxidation curves have shown) probably also due to the possible Metal Dusting phenomena, the silicon present in the Ti_5Si_3 formed during diffusion protected the samples to an important extent. This made it possible to obtain several samples which resisted Metal Dusting in which a clear mass gain was noticed. However, they did not exhibit a good oxidation performance either.

As silicon protected the 312 samples a larger silicon content was found in the oxide. Although the characteristics of the oxide formed are the same as for the 211 samples, being uniform and porous in those regions where it still remained, if the silicon content in the coating had been higher it might have been able to create a more protective oxide. The oxide formed for the 312 coating seemed to be made up of several regions:

- The first region would be the top layer composed mainly of rutile, but with a significant amount of silicon oxide.

- The second region is the intermediate layer beneath the latter where a discontinuous oxide is created. Here there are differentiated lighter regions can be noticed in which the oxide is almost exclusively titanium oxide (rutile).

- A third region, almost unnoticeable, which is made up of located points with a darker visualization where the silicon composition is even greater than for the first region.

Regarding the oxidation protection of these slurry coatings on Ti-6Al-4V, the results we have obtained have not been as we would have liked. The MAX phase slurry coatings have indeed, contributed to the composition of the resulting oxide scale but the protective effect it has had in improving the oxidation resistance is slight due to the probable occurrence of Metal Dusting.

Overall, the experiment has shown a different environment in which if Metal Dusting has taken place it could occur. So far, Metal Dusting has been defined for environments with a supersaturated carbon content which lead to the formation of carbides that when become unstable react with the substrate disintegrating it. In our case the environment was carbon free; instead the carbides had already formed due to the diffusion treatment, and upon exposure to oxygen possibly reacted following the Metal Dusting mechanism. If the assumption that Metal Dusting occurred were correct it would indicate that a new mechanism that has not been reported for Metal Dusting exists. Additionally, Metal Dusting is not considered a characteristic phenomenon of MAX phases, meaning that if it were the case this could be one of the first times where is has happened.

7.2. Future Studies

This work has shown that there are several subjects that could be considered of interest in the future and which might help determine with greater accuracy what happened in this study. Very few studies on oxidation of MAX phases have been carried out in the temperature range of 500-900℃ because anomalous behaviours were detected. In studies made on 211 the behaviour has been suggested to be related with the anatase-rutile transformation that takes place in the TiO_2 layer, it has also been considered the source of cracks (125). It would be of interest to see if the high oxidation kinetics encountered at this temperature might also be related with the high activity of carbon encountered at this temperature.

Another interesting thing to study is the behaviour that the 211 and 312 MAX phases have in bulk form under the same oxidation conditions to see how subjecting them to a previous diffusion treatment really affects them. Additionally a study of the temperature at which the MAX phases start to decompose could also be made, as this has been determinant in this study.

From the results of the composition of the oxides formed it was clearly seen how there was a lack of homogeneity in the composition. Research on how to control the uniformity in

the composition could be helpful in order to achieve a uniform stable scale that is capable of fulfilling the oxidation protection purpose.

Just as we have seen during the SEM observations, both the coating and oxide were porous, this was not the first time this is noticed, it has been mentioned that porosity in Ti_2AlC and Ti_3AlC_2 is a common characteristic and so are cavities given the limited methods of preparation of these ceramics**.** (128)

As we have mentioned previously the selected parameters for this project might not have been the optimum. Just as we have seen the oxidation temperature selected is one for which carbon has a very high activity, therefore increasing the temperature would decrease the activity of the same and the probable Metal Dusting phenomenon could possibly be avoided. If it is avoided then a proper determination of the oxidation resistance of these coatings to oxidation could be made.

Additionally, it has been considered that several improvements could be made along the development of the experimental part. This could be taken into consideration when carrying out experiments of similar characteristics.

Regarding the slurry process it has been considered that an improvement in the application method might be useful. Instead of applying the coating with a brush using a spraying gun or something similar might provide a more uniform coating.

For the pieces measurement it would be useful to have a more accurate method to obtain the measurements of the dimensions rather than using a caliper, also because in the case of some samples the geometry shows regions with variable lengths and thickness decreasing the accuracy we are trying to achieve.

References

1. **Williams, G. Lütjering and J.C.** *Titanium.* s.l. : Springer, 2007.

2. **D.Vojtěch, T. Kubatík, K.Jurek and J. Maixner.** Cyclic-oxidation resistance of protective silicide layers on titanium. *Oxidation of metals.* 2005, Vol. 63, 5/6.

3. **C. Leyens, in: C.Leyens, M.Peters (Eds).** *Titanium and Titanium Alloys.* Weinheim : Wiley-VCH, 2003.

4. **Chang, Raymond.** *Chemistry.* s.l. : McGraw-Hill, 2010.

5. **Zhengwei Li, Wei Gao.** *High Temperature Corrosion of Intermetallics.* s.l. : Nova Science Publishers, 2009.

6. **S.Barter., R. Wanhill and.** *Fatigue of Beta Processed and Beta Heat Treated Titanium Alloys.* s.l. : SpringerBriefs in Applied Sciences and Technology , 2012.

7. **Donachie., Matthew J.** *Titanium: A Technical Guide.* s.l. : ASM International, 2000.

8. **Iglesias, Beatriz Martín de Hijas.** *Molibdenizado-Alumnizado de sustratos de titanio y Ti6Al4V pulvimetalúrgico y laminado mediante pack cementation.* Proyecto Fin de Carrera. Universidad Carlos III de Madrid. 2011.

9. **E.O. Ezugwu, Z.M. Wang.** Titanium alloys and their machinability-a review. *Journal of Materials Processing Technology.* 1997, Vol. 68, 262-274.

10. **P.-J. Arrazola, A. Garay, L.-M. Iriarte, M. Armendia, S. Marya, F. Le Maître.** Machinability of titanium alloys (Ti6Al4V and Ti555.3). *Journal of Materials Processing Technology .* 2009, Vol. 209, 2223–2230.

11. **Kuznesof, Paul M.** Titanium dioxide. *Titanium dioxide (CTA).* 2006, 1-8.

12. **J. Guarrapa, D. Venugopala Reddy.** Characterization of Ti Alloy, IMI-834, for corrosion resistance under different environmental conditions. *Journal of Alloys and Compounds.* 2005, Vol. 390, 270-274.

13. ASM Aerospace Specification Metals: Titanium. [On line] 20 de February de 2014. http://www.aerospacemetals.com/titanium-ti-6al-4v-ams-4911.html. .

14. **Gerard Welsch, Rodney Boyer, E.W. Collings.** *Materials Properties Handbook: Titanium Alloys.* s.l. : ASM International, 2007.

15. **Pederson, Robert.** *Microstructure and phase transformation of Ti6Al4V.* Licentiate Thesis. Lulea University of Technology. 2002.

16. **Udomphol., Tapany.** *Titanium and its alloys. Lecture 5. Suranaree University of Technology.* 2007.

17. **P.G. Esteban, L.Bolzoni, E.M. Ruiz Navas y E. Gordo.** *Introduction to powder metallurgy processes for titanium manufacturing.* s.l. : Revista de Metalurgia, 2011. Vol. 47.

18. **R.O. Suzuki, T.N. Deura, R.Ishii, T. Matsunaga, T.N. Harada, M. Wakino and K. Ono.** Titanium Powder preparation from TiCl4 in the molten salt. *Proc. of 2000 Powder Metallurgy World Congress (PM2000).* November 2000.

19. **Zhi-Yuan, Kuo-Chih Chou and Fu-Shen Li.** *An Investigation of Electro-deoxidation Process for producing Titanium from Dense Titanium Dioxide Cathode.* s.l. : Journal for Manufacturing Science & Production. Vol. 13. 2191-037.

20. **Manfred Peters, Jörg Kumpfert, Charles H. Ward and Christoph Leyens.** Titanium Alloys for Aerospace Applications. *Advanced Engineering Materials.* 2003, Vol. 5, 3.

21. **C.N. Elias, J.H.C. Lima, R.Valiev, and M.A. Meyers.** Biomedical applications for Titanium and its Alloys. *Journal of the Minerals, Metals and Materials society.* 2008.

22. **F.H. Froes, H. Friedrich, J. Kiese, and D. Bergoint.** Titanium in the Family Automobile: The cost challenge. *Journal of the Minerals, Metals and Materials Society.* 2004.

23. **Rodrigo., Ignacio Pérez.** *Estudio del comportamiento frente a la corrosión de aleaciones de titanio pulvimetalúrgicas.* Madrid. España.Máster Oficial en materiales estructurales para las nuevas tecnologías. Universidad Carlos III de Madrid y Universidad Rey Juan Carlos de Madrid : s.n., 2010.

24. **Company, Iluka.** Titanium Metal. *Mineral Sands Briefing Paper.* October 2010.

25. **Reid., Rebecca.** *Lightweight aircraft design driving growth for titanium fasteners.* s.l. : Canadian Manufacturing., August 15, 2012.

26. **Moxon V.S., Froes F.H.** *Fabricating sports equipment components via powder metallurgy.* s.l. : Journal of the Minerals Metals & Materials Society, 2001. Vol. 53. 39-41.

27. **Nowotny, H.** Struktuchemie Einiger Verbindungen der Ubergangsmetalle mit den elementen C, Si, Ge, Sn. *Progress in Solid State Chemistry.* 1970, Vol. 227.

28. **Barsoum., Michel W.** The MN+1AXN Phases: A New Class of Solids. Thermodynamically Stable Nanolaminates. *Progress in Solid State Chemistry.* 2000, Vol. 28, 201-281.

29. **W. Jeitschko, H. Holleck, H. Nowotny.** Die Kristallstructur von Ti3SiC2- Ein Neuer Komplexcarbid. *Typ. Monatshefte Für Chemie.* 1967, Vol. 98, 329-337.

30. **H. Wolfsgruber, H. Nowotny and F. Benesovsky.** . Die Kristallstruktur von Ti3GeC2. *Monatshefte Für Chemie.* 1967, Vol. 98, 2401.

31. **Sun., Z. M.** Progress in the research and development on MAX phases: a family of layered ternary compounds. *International Materials Review.* 2011, Vol. 56, 3.

32. **Schuster., M.A. Pietzka and J.C.** Summary of Constitution Data of the system Al-C-Ti. *Journal of Phase Equilibria.* 1994, Vol. 15, 392.

33. **J.C.Schuster., M.A. Pietzka.** The Ternary Boundary Phases of the Quaternary System Ti-Al-C-N. 1992, in Concerted Action on Materials Science, Leuven Proceedings, Part A, Comission of the European Communities. Brussels, Belgium.

34. **Per Eklund, Manfred Beckers, Ulf Jansson, Han Högberg, Lars Hultman.** *The Mn+1AXn phases: Materials science and thin-film processing.* s.l. : Thin Solid films, 2010. Vol. 518.

35. **Barsoum, Professor Michel W.** *MAX phases-An Introduction to MAX phases.* [On line] [Cited on: 3 May 2014.] http://www.azom.com/article.aspx?ArticleID=5133..

36. **Chunfeng Hu, Haibin Zhang, Fangzhi Li, Qing Huang, Yiwang Bao.** New phases' discovery in MAX family. *International Journal of Refractory Metals and Hard Materials.* 2013, Vol. 36, 300-312.

37. **Michel W. Barsoum, Tamer El-Raghy.** The MAX Phases: Unique New Carbide and Nitride Materials. *American Scientist.* 2001, Vol. 89.

38. **Barsoum., Miladin Radovic and Michel W.** MAX phases: Bridging the gap between metals and ceramics. . *American Ceramic Society Bulletin.* 2013, Vol. 92, 3.

39. **Low., I. M.** *Advances in Science and Technology of Mn+1AXn Phases.* s.l. : Woodhead Publishing., 2012.

40. **J.J. Nickl, K.K. Schweitzer, P. Luzenberg.** Chemical Vapour Deposition in the System Ti-Si-C. *Jounal of the Less Common Metals.* 1972, Vol. 26, 335-353.

41. **T. Goto, T. Hirai.** Chemical Vapor Deposited Ti3SiC2. *Materials Research Bulletin.* 1987, Vol. 22, 1195-1201.

42. **Z.F. Zhang, Z.M. Sun and H. Hashimoto.** Rapid synthesis of ternary carbide Ti3SiC2 through pulse-discharge sintering technique from Ti/Si/TiC powders. *Metallurgical and Materials Transactions A.* 2002, Vol. 33, 3321-3328.

43. **J. Q. Zhu, B. C. Mei.** Synthesis of high-purity TiSiC and TiAlC by hot-pressing (HP) . *Journal of Materials Science Letters.* 2003, Vol. 22, 15,1111-1112 .

44. **J. Zhang, L. Wang, W. Jiang and L.Chen.** Fabrication of high purity Ti3SiC2 from Ti/Si/C with the aids of Al by spark plasma sintering. *Journal of Alloys and Compounds.* 2007, Vol. 437, 203-207.

45. **Z.F. Zhang, Z.M. Sun, H. Hashimoto and T. Abe.** Application of pulse discharge sintering (PDS) technique to rapid synthesis of Ti3SiC2 from Ti/Si/C powders. *Journal of the European Ceramic Society.* 2002, Vol. 22, 2957-2961.

46. **Z.F. Zhang, Z.M. Sun and H. Hashimoto.** Low temperature synthesis of Ti3 SiC2 from Ti/SiC/C powders . *Materials Science and Technology.* 2004, Vol. 20, 1252-1256.

47. **F. Zhang, Z.M. Sun, H. Hashimoto and T. Abe.** A new synthesis reaction of Ti3SiC2 through pulse discharge sintering Ti/SiC/TiC powder. *Scripta Materiala.* 2001, Vol. 45, 1461-1467.

48. **F. Zhang, Z.M. Sun, H. Hashimoto, T. Abe.** A new synthesis Reaction from Ti/TiSi2/TiC powder mixtures through Pulse Discharge Sintering (PDS) technique. *Material Research Innovations.* 2002, Vol. 5, 185-189.

49. **Z.M. Sun, Y. Zhou, S. Tada and H. Hashimoto.** Effect of Al addition on pressureless reactive sintering of Ti3SiC2. *Scripta Materiala.* 2006, Vol. 55, 1011-1014.

50. **J. P. Palmquist, S. Li, P.O. A. Persson, J. Emmerlich, O. Wilhelmsson, H. Högberg, M. I. Katnelson, B. Johansson, R. Ahuja, O. Eriksson, L. Hultman and U. Jansson.** Deposition of Ti2AlC and Ti3AlC2 epitaxial films by magnetron sputtering. *Physical Review B.* 2004, Vol. 75 Applied Physics Letters, 6,1066-1068.

51. **J. Emmerlich, H. Högberg, S. Sasvari, P.O. A. Persson, L. Hultman, J. P. Palmquist, U. Jansson, J. M. Molina-Aldareguia and Z. Czigany.** Growth of Ti3SiC2 thin films by elemental target magnetron sputtering. *Journal of Applied Physics.* 2004, Vol. 96, 4817-4826.

52. **Z. J. Lin, M. J. Zhuo, Y. C. Zhou, M. S. Li and J. Y. Wang.** Structural characterization of a new layered-ternary Ta4AlC3 ceramic. *Jounal of Materials Research.* 2006, Vol. 21, 2587-2592.

53. **C. F. Hu, Z. J. Lin, L. F. He, Y. W. Bao, J. Y. Wang, M.S. Li and Y.C. Zhou. J.** Physical and Mechanical Properties of Bulk Ta4AlC3 Ceramic Prepared by an In Situ Reaction Synthesis/Hot-Pressing Method. *Journal of the American Ceramic Society.* 2007, Vol. 90, 2542-2548.

54. **P. Eklund, J.P. Palmquist, J. Howing, D. H. Trinh, T. El-Raghly, H. Högberg and L. Hultman.** Ta4AlC3: Phase determination, polymorphism and deformation. *Acta Materiala.* 2007, Vol. 55, 4723-4729.

55. **P. Eklund, J. Emmerlich, H. Högberg, O. Wilhemsson, P. Isberg, J. Birch, R. O. A. Persson, U. Jansson and L. Hultman.** Structural, Electrical, and mechanical properties of nc-TiC/a-SiC nanocomposite thin films. *Jounal of Vacuum Scienece & Technology B.* 2005, Vol. 23B, 2486-2495.

56. **Tamer El-Raghly, Michel W. Barsoum, Mats Sundberg, Hans Petterson.** *Process for forming 312 Phase Materials and process for sintering the same. US Patent No: 6461989 B1* 2002.

57. **J.J. Nickl, K.K. Schweitzer and P. Luzenberg.** Gasphasenabscheidung im Systeme Ti-C-Si. *Less Common Metals.* 1972, Vol. 26, 283.

58. **Córdoba, Jóse M., Sayagués, María J., Alcalá, María D., Gotor, Francisco.** Synthesis of Ti3SiC2: Reaction Mechanism. *Journal of the American Ceramic Society.* 2007, Vol. 90, 3, 825-830.

59. **Wu, E., Kisi, W. H., Riley, D.P., R.J.** Intermediate phases in Ti3SiC2 synthesis from Ti/SiC/C mixtures studied by Time-resolved neutron diffraction. *J. Am. Ceram. Soc.* 2002, Vol. 85, 3084-3086.

60. **Edo., Éric Hernández.** *Estudio Estructural y mecánico de la fase MAX Ti3SiC2. Proyecto Fin de Carrera.* Escuela Técnica Superior de Ingenieros Industriales de Barcelona.

61. **Y.C.Zhou., X.H. Wang and.** Layered Machinable and Electrically Conductive Ti2AlC and Ti3AlC2 Ceramics: A Review. *Chinese Academy of Sciences, Shenyang 110016, China.*

62. **H. I. Yoo, M. W. Barsoum and T. El-Raghly.** Materials science: Ti3SiC2 has negligible thermopower. *Nature.* 2000, Vol. 407, 581-582.

63. **Radovic., Michel W. Barsoum and Miladin.** Elastic and Mechanical Properties of the MAX Phases. *Annual Review of Materials Research.* 2011, Vol. 41, 195-227.

64. **G. H. Meier, D. Appalonia, R.A. Perkins and K.T. Chiang.** Oxidation of Ti-base alloys, in oxidation of High Temperature intermetallics . *Oxidation of high temperature intermetallics.* 1989, 185-193.

65. **P.J.Spencer., A. Rahmel and.** Thermodynamic Aspects of TiAl and TiSi2 oxidation: The Al-Ti-O and Si-Ti-O phase diagrams. *Oxidation of Metals.* 1990, Vol. 35, 53-68.

66. **Z.M.Sun, Y.C. Zhou and.** Electronic structure and bonding properties of layered machinable Ti2AlC and Ti2AlN ceramics. *Physical Review B.* 2000, Vol. 61, 12570.

67. **P.F.Tortorelli., M. P. Brady and.** Alloy design of intermetallics for protective scale formation and for use as precursors for complex ceramic phase surfaces. *Intermetallics.* 2004, Vol. 12, Issues 7-9,779-789.

68. **M. P. Brady and P.F. Tortorelli, K.L. More, E.A. Payzant, B.L. Armstrong, H.T. Lin, M.J. Lance, F. Huang and M.L. Weaver.** Coating and near-surface modification design strategies for protective and functional surfaces. *Materials and Corrosion.* 2005, Vol. 56, 748-755.

69. **X. H. Wang, Y.C.Zhou.** Oxidation Behaviour of TiC-containing Ti3AlC2 based material at 500-900ºC in air. *Materials Research Innovations.* 2003, Vol. 7, 381-390.

70. **Barsoum, Michel W.** *Properties of Machinable Ternary Carbides and Nitrides.* s.l. : Wiley-VCH, 2013.

71. **M. Sundberg, G. Malmqvist, A. Magnusson, T. El-Raghly.** Alumina forming high temperature silicides and carbides. *Ceramics International.* 2004, Vols. 30, Issue7, 1899-1904, págs. 1899-1904.

72. **Ahmad., Zaki.** *Principles of Corrosion Engineering and Corrosion Control.* s.l. : Elsevier, 2006.

73. **Leszek Niewolak, Vladimir Shemet, Alekdander Gil, Lorenz Singheiser and Joe Willem Quadakkers.** Alumina-forming coatings for titanium and titanium aluminides. *Advanced Engineering Materials.* 2001, Vol. 3, 7.

74. **Bose., S.** *High Temperature Coatings.* s.l. : Elsevier Science and Technology Books., 2007.

75. **Mostafa Armirjan, Hamid Khorsand, Manouchehr Khorasani.** Processing and properties of Al-base Powder Suspension/Slurry: A comparison study of aqueous binder systems, stability and film uniformity. *Elsevier Powder Technology.* 2013.

76. **Schoeller, Harry E.** *Thermodynamics and and Kinetics of Oxidation and Temperature Dependent Mechanical Characterization of Pure Indium Solder.* Thesis. State University of New York. : s.n., 2005.

77. **Khanna, A.S.** *Introduction to High Temperature Oxidation and Corrosion.* s.l. : ASM International, 2002.

78. **Shibo Li, Laifei Cheng, Litong Zhang.** Oxidation Behaviour of Ti3SiC2 at high temperature in air. *Materials Science and Engineering:A.* 2003, Vols. 341, Issues 1-2, 112-120, págs. 112-120.

79. **Council., National Research.** Coatings for High-Temperature Structural Materials: Trends and opportunities. *Washington, DC: The National Academies Press.* 1996.

80. **Wasa, Kiyotaka.** *Handbook of Sputter Deposition Technology. Fundamentals and Applications for Functional Thin Films, Nano-materials and MEMS.* s.l. : Elsevier., 2012.

81. **Dennis William Cavanaugh, Canan Uslu Hardwicke, Matthew James O'Connel, Todd Steven Moran.** *Slurry diffusion aluminide coating composition and process. European Patent Specification No. EP 2060653 B1. 2008/ US Patent No. 0126833 A1* 2009.

82. **Chungen Zhou, Huibin Xu, Shengkai Gong, Kyoo Young Kim.** A study of aluminide coatings on TiAl alloys by the pack cementation method. *Materials Science and Engineering A341. Elsevier Science 2002.* 2003, 169-173. .

83. **Council, (U.S.) Committee on Coatings. National Research.** *High Temperature Oxidation-Resistant Coatings. Coatings for protection from oxidation of superalloys, refractory metals, and graphite.* s.l. : National Academy of Sciences/National Academy ef Engineering, 1970.

84. **Anders Juul Rasmussen, Alina Agüero, Marcos Gutierrez, María José Landeira Østergård.** Microstructures of thin and thick slurry aluminide coatings on Inconel 690. *Surface & Coatings Technology.* 2008, Vol. 202, 479-1485.

85. Plasma spray. [On line] [Cited on: 3 May 2014 .] http://www.tstcoating.com/plasma_spray.html..

86. An Introduction to Thermal Spray. [On line] [Cited on: 3 May 2014.] http://www.sulzer.com/en//media/Documents/ProductsAndServices/Coating_Equipment/Thermal_Spray/Brochures/Thermal_Spray_V4.pdf..

87. **Mattox, D.M.** *Handbook of Physical Vapor Deposition (PVD) processing.* s.l. : William Andrew Publishing, 1998.

88. **A., Camacho García.** *Recubrimientos de boro depositados por 'Pack Cementation' sobre sustratos de aleación Ti pulvimetalúrgicos y laminados.* s.l. : Proyecto Fin de Carrera. Universidad Carlos III de Madrid., 2009.

89. **Carreras L, Montalá F.** Actualidad industrial de las técnicas de recubrimientos de capas duras finas. Grupo TTC. Recubrimientos Avanzados. 2004.

90. **Goral, Marek.** The Microstructure and Oxidation Resistance of Aluminide MeCrAlY-Modifued Coatings Obtained by Slurry Method on Rene 80 Superalloy. Journal of Minerals and Materials Characterization and Engineering. 2012, Vol. 11, 719-723.

91. **Tamarin., Y.** *Protective coatings for Turbine Blades.* s.l. : ASM International, 2002.

92. **Dybkov, V.P.** *Growth kinetics of a chemical compound layers.* s.l. : Cambridge International Science publishing. , 1995.

93. **A. Agüero, J.C. del Hoyo, J. García de Blas, M. García, M. Gutiérrez, L. Madueño, S. Ulargui.** Aluminum slurry coatings to replace cadmium for aeronautic applications. *Surface & Coatings Technology.* 2012, Vol. 213, 229-238.

94. **Werner Freitag, Deiter Stoye.** *Paints, Coatings and Solvents. .* s.l. : Wiley-VCH, 1998.

95. **M.P Albano, L.B Garrido.** Aqueous tape casting of yttria stabilized Zirconia. Materials Science and Engineering A, 2006, Vol. 420, 171-178.

96. **Cedillo, Ismael Segura.** *Fused Metallic Slurry coatings for improving the oxidation resistance of wrought alloys. Thesis submitted to the University of Manchester.* 2011.

97. **S.K.Saxena.** Polyvynil Alcohol (PVA). Chemical and Technical Assesment (CTA). *Chemical and Technical Assesment (CTA) © FAO .* 2004.

98. **J.M. LeBeau, Yuttanant Boonyongmaneerat.** Comparison of aqueous binder systems for slurry-based processing. *Materials Science and Engineering A.* 2007, Vol. 458, 17-24.

99. **A. Kristofferson, E. Roncari and C. Galassi.** Comparison of Different Binders for Water-based Tape Casting Alumina. *Journal of the European Ceramic Society.* 1998, Vol. 18, 2123-2131.

100. **Busch, T., Schweizer, D. and Sorg, C.** Spray granulation of alumina with organic binders. *Ceramic Forum International.* 1991, Vol. 68(10/11), 527-530.

101. **Athena Tsetsekou, Christos Agrafiotis, Ioanna Leon, Aggelos Milias.** Optimization of the rheological properties of alumina based slurries for ceramic processing applications. Part II: Spray-Drying. *Journal of European Ceramic Society .* 2001, Vol. 21, 493-506.

102. **Wagner., Jean Irwin.** *Effect of structure of dispersing agent on efficiency of wet grinding.* 1936.Thesis (B.S.)--Massachusetts Institute of Technology, Dept. of Chemical Engineering.

103. **Tracton., Arthur A.** *Coatings Technology Handbook.* s.l. : Taylor & Francis, 2005.

104. **Magdy Y. Abdelaal, Mohammad S.I. Makki, Tariq R.A. Sobahi.** Modification and Characterization of Polyacrylic Acid for Metal Ion Recovery. *American Journal of Polymer Science.* 2012,, Vol. 2(4), 73-78.

105. **Robert Bianco, Mark A. Harper and Robert A. Rapp.** Codeposition of elements in diffusion coatings by the halide-activated pack cementation method. *Department of the Navy.* 1991.

106. **Boyce, Meherwan P.** *Gas Turbine Engineering Handbook. .* s.l. : Buttersworth-Heinemann, 2002.

107. **O. Wilhemsson, J.P. Palmquist, E.Lewin, J. Emmerlich, P.Eklund, P.O. Persson, H.H. Berg, S.Li, R. Ahuja, O. Eriksson, L. Hultman and U. Jansson.** Deposition and characterization of ternary thin films within the Ti–Al–C system by DC magnetron sputtering. *Journal of Crystal Growth.* 2006, 291, 290-300.

108. **C. Walter, C. Martinez, T. El-Raghly and J.M. Schneider.** Towards Large Area MAX Phase Coatings on Steel. *Steel Research International.* 2005, Vol. 76, 225-228.

109. **Jenny Frodelius, Marie Sonestedt, Stefan Björklund, Jens-Petter Palmquist, Krystyna Stiller, Hans Högberg, Lars Hultman.** Ti2AlC coatings deposited by High Velocity Oxy-Fuel spraying. . *Surface & Coatings Technology .* 2008, Vol. 202 , 5976-5981.

110. **Martin, Peter M.** Handbook of Deposition Technologies for Films and Coatings. *Elsevier.* 3rd, 2010.

111. **Kathy Lu, Chris S.Kessler.** Nanoparticle Colloidal Suspension Optimization and Freeze-Cast Forming. Synthesis and Processing of Nanostructures Materials. . *American Ceramic s Society.* William M. Mullins., 2007.

112. Chemical Book. [On line] www.chemicalbook.com.

113. **Ziqi Sun, Meishuan Li, Longfei Hu, Xinpo Lu, and Yanchun Zhou.** Surface Chemistry, Dispersion Behavior, and Slip Casting of Ti3AlC2 Suspensions. *The American Ceramic Society.* 2009, Vol. 92, 1695–1702.

114. **B. Fultz, J. Howe.** Transmission Electron Microscopy and Diffractometry of Materials.Graduate Texts in Physics. . *© Springer-Verlag Berlin Heidelberg.* 2013.

115. **Liangfa Hu, Rogelio Benitez, Sandip Basu, Ibrahim Karaman, Miladin Radovic.** Processing and characterization of porous Ti2AlC with controlled porosity and pore size. *Acta Materialia.* 2012, Vol. 60, 6266-6277.

116. **Z.J. Lin, M.J. Zhuo, Y.C. Zhou, M.S. Li, J. Y. Wang.** Microstructural characterization of layered ternary Ti2AlC. *Acta Materialia .* 2006, Vol. 54, 1009-1015.

117. SEM techniques. . [On line] March 2014. http://serc.carleton.edu/research_education/geochemsheets/techniques/SEM.html..

118. Scanning Electron Microscope. . [On line] [Cited on: 11 April 2014.] http://www.purdue.edu/rem/rs/sem.htm..

119. **Young., David John.** *High Temperature Oxidation and Corrosion of Metals.* s.l. : Elsevier, 2008.

120. **A. Agüero, M. Gutiérrez, L. Korcakova, T. T. M. Nguyen, B. Hinnemann, S. Saadi.** Metal Dusting Protective Coatings. A Literature Review. *Oxididation of Metals.* 2011, Vol. 76, 23-42.

121. Nist Janaf Thermochemical Tables. . [On line] http://kinetics.nist.gov/janaf/. .

122. **Roberge, Pierre R.** *Handbook of Corrosion Engineering.* s.l. : McGraw-Hill, 2000.

123. **Yong Zou, Zheng Ming Sun, Shuji Tada and Hitoshi Hashimoto.** Liquid Reaction during synthesis of Ti3SiC2 through Pulse Discharge Sintering Ti/Si/TiC Mixed Powders. *Materials Transactions. .* 2006, Vol. 47, 12 2987-2990.

124. **Wang Jianxin, Ni Yaru Gao Dongshan, Lu Chunhua, Fand Zhanggang, Xu Zhongzi.** A new method of fabrication of TiC by employing pyrolytic carbon clack and titanium. *Int. Journal of Refractory Metals and Hard Materials .* 2014, Vol. 45, 137-140.

125. **S.Basu, N. Obando, A. Gowdy and M. Radovic.** Long-term oxidation of Ti2AlC in air and water vapor at 1000-1300℃ Temperature Range. *Journal of The Electrochemical Society.* 2012, Vol. 159, 2.

126. **Sonestedt M., Frodelius J., Sundberg M.,Hultman L., Stiller K.** Oxidation of Ti2AlC bulk and spray deposited coatings. *Corrosion Science.* 2010, Vol. 52, 3955-3961.

127. **Nº910627, Ingeniería de Superficies y Materiales Nanoestructurados UCM.** Publicaciones Oxidación en mezclas de gases: Metal Dusting. Corrosión a elevada temperatura. [On line] http://pendientedemigracion.ucm.es/info/tuma/quimicas_superficie/dusting.html. .

128. **H.J. Yang, Y.T. Pei, J.C. Rao, J. Th. M. De Hosson, S.B. Li and G.M. Song.** High temperature healing of Ti2AlC: On the origin of inhomogeneous oxide scale. . *Scripta Materialia .* 2011, Vol. 65, 135-138.

DEFINITIONS OF INTEREST

- **Allotropic Transformation:** Complete transformation from one crystal structure into another.

- **Amphiphilic:** Compounds that contain hydrophobic groups and hydrophilic groups, in other words, they have a non-soluble and soluble component.

- **Anisotropic crystalline solid:** A crystalline solid is anisotropic when it has a lattice structure whose atoms are arranged or spaced differently when viewed in any of the three planes; in other words, when the spacing and arrangement of the atoms is different in at least 2 of the 3 planes.

- **Compensated conductor:** Material in which the concentration of electrons and holes is almost the same, but also its mobilities.

- **Defloccuant:** Substance that when added to scattered particles in suspension cause a decrease in the apparent viscosity of the coating. Defloccuants increase the repulsive forces between particles.

- **Electrodeposition:** It is a process in which an electrical current is used to reduce the cations of a material from a solution and coat that material as a thin film over a conductive substrate. If the substrate is not conductive then it cannot take place (reason for coating with gold non-conductive samples).

- **H phases:** Phases with a M_2AX structure. C and N atoms in this kind of structure do not occupy an interstitial octahedral site.

- **Hägg Phases:** Carbides, nitrides, borides and hydrides with close-packed or hexagonal arrays of metal atoms in which C, N, B or H occupy interstitial octahedral or trigonal sites.

- **Hall Effect**: Creation of a high voltage across an electrical conductor, transverse to an electric current in the conductor and a magnetic field perpendicular to it. The charge carriers have different polarizations if they are electrons (-) or holes (+).

- **Laquers:** Coatings converted to a solid film by evaporation of the liquid material.

- **Mill annealing:** Heat treatment done to Ti-6Al-4V by which a microstructure with globular crystals is created. It consists of heating up to 730 ℃ in the lower range of the α+β region and leaving it for 4 hours before furnace cooling up to 25℃.

- **Nanolaminates:** Layered materials that show unique physical properties when the nanolayer thickness is less than the characteristic length scale that defines the physical property.

- **Phase:** Chemically and structurally homogeneous are that forms part of the microstructure.

- **Polymorphism**: Ability of a solid material to exist in more than one form of crystal structure.

- **Seebeck-Peltier Effect**: Effect in which a temperature difference on both sides of a conductor creates a current. The charge carriers will determine the direction in which the current will move respect to the temperature gradient. It is measured by the Seebeck coefficient, which measures the induced voltage created by the temperature difference (V/K).

- **Spallation:** Fragmentation of the surface of a material due to adverse conditions (as corrosion) or mechanical causes.

- **Surfactant:** Substance used to lower the interfacial tension between the liquid and the solid. They attach themselves to the particles.

- $\boldsymbol{\beta}$ **Transus Temperature:** Temperature where the transformation from BCC to HCP takes place. It separates the β phase field from the α+β phase.

ABBREVIATIONS

- $\boldsymbol{a_c}$**:** Carbon activity
- **BCC:** Body Centered Cubic
- **BSE:** Backscattered Electrons
- **CMC:** Carboxy methyl cellulose
- **CVD:** Chemical Vapor Deposition
- **D(50):** Average particle diameter
- **EBSD:** Diffracted backscattered electrons.
- **EDS:** Energy Dispersive X-Ray Spectroscopy
- **%EI:** % Stiffness
- **HCP:** Hexagonal-Close Packed
- **HVOF:** High-Velocity Oxygen Fuel
- $\mathbf{K_{IC}}$**:** Fracture Toughness
- **PAA:** Poly Acrylic Acid
- **PEG:** Polyethylene Glycol
- **PEI:** Polyethyleneimine
- **PVD:** Physical Vapor Deposition
- $\mathbf{R_H}$**:** Hall coefficient
- **SEM:** Scanning Electron Microscopy
- **SE:** Secondary Electrons
- **TMAH :** Tetramethylammonium
- **XRD:** X-Ray Diffraction

Index of Figures

Figure 1 Comparison Specific strength of different materials with respect to temperature (3) . 11
Figure 2 Influence of alloying elements on the phase diagram of Titanium alloys. (3) 13
Figure 3 Crystal structure of the α phase in Titanium alloys. (3) 14
Figure 4 Crystal structure of the β phase in Titanium alloys. (3) 15
Figure 5 Summary of the properties of the different Titanium alloys. (3)..... 18
Figure 6 Pseudo-binary equilibrium phase diagram for Ti-6Al-4V. (7)..... 20
Figure 7 Schematic diagram of the Kroll process. (18)..... 21
Figure 8 Percentage of materials in large modern aircraft. (20) 23
Figure 9 Potential automotive applications of titanium. (22)..... 26
Figure 10 Elements in the periodic table that react to form MAX phases. (35)..... 30
Figure 11 Crystal Structures of MAX phases. (37) 31
Figure 12 Maxthal 211 and Maxthal 312 Powders fabricated by Sanvik heating technology, Sweden (38)..... 35
Figure 13 Thermal conductivity of some representative MAX phases (28)..... 40
Figure 14 Kink Bands analogy. Explanation of the behaviour of MAX phases by card-deck analogy. (37) 40
Figure 15 Schematic formation of an incipient Kink band, mobile dislocation Kink Bands and delaminations. (38) 41
Figure 16 Mass transport of the oxide scale during oxidation of a metal substrate (3) 49
Figure 17 Schematic representation of the rate laws for the oxide scale formation (3)..... 50
Figure 18 Schematic representation of oxide scales and oxygen diffusion zones of titanium-based alloys. (3)..... 50
Figure 19 Most common coating processes (74)..... 51
Figure 20 Range of operating thicknesses for the different Coating Methods (86)..... 54
Figure 21 Schematic diagram of distribution and treatments carried out to each of the samples 66
Figure 22 Approximate Substrate geometry of the samples treated..... 67
Figure 23 Cutting machine used to cut the wrought Ti-6Al-4V sheet into the different samples to be treated..... 67
Figure 24 Grinding machine to grind samples 68
Figure 25 Ultrasounds bath machine used for cleaning the samples 68
Figure 26 Photographs of the components used to prepare the slurries..... 74
Figure 27 Schematic diagram of the steps followed to obtain the Ti_2AlC slurry..... 75
Figure 28 Schematic diagram of the steps followed making the Ti_3SiC_2 slurry..... 76
Figure 29 Photograph of the coating process: a) uncoated samples b) after deposition of the slurries on the samples c) final coated samples after 24 hours drying..... 77
Figure 30 Photograph of the samples before the diffusion treatment at 1100℃..... 78
Figure 31 Vacuum Furnace used for the diffusion process..... 79
Figure 32 Cycle for Diffusion at 1100℃ *in the Vacuum Furnace*..... 79
Figure 33 Photograph of the samples before the diffusion treatment at 1200℃..... 80
Figure 34 Microbalance used for the mass measurements during the Oxidation cycles..... 81
Figure 35 Furnace used for the Oxidation treatment..... 81

Figure 36 Photograph of the sample setup before starting the oxidation treatment 82
Figure 37 Photograph of the experimental Setup for coating with copper 84
Figure 38 Snapshot of a sample coated with copper 84
Figure 39 Micro-Cutter used for cutting the samples after the oxidation treatment 84
Figure 40 Machine used to mount to samples 85
Figure 41 Polishing machine..... 86
Figure 42 XRD Machine PHILIPS X-PERT..... 87
Figure 43 Diffraction: Geometry for the interference of a wave...... 88
Figure 44 Scanning Electron Microscopy (SEM). (118)..... 89
Figure 45 Signal emitted from electron bombardment (SEM). (118)..... 89
Figure 46 SEM machine used 90
Figure 47 Photograph of the samples coated with MAX phase slurry after a diffusion treatment at 1100℃ *for 4 hours.* 92
Figure 48 Photograph of the samples coated with MAX phase slurry after a diffusion treatment at 1200℃ *for 4 hours.* 93
Figure 49 Comparative photographs of the samples in the crucible before and after 300 hours of oxidation in air at 600℃ 93
Figure 50 Snapshot of the look the 211 samples had after 12 hours oxidation...... 94
Figure 51 Backscattered Electron image of the cross-section of the Ti-6Al-4V uncoated substrate (a) before and (b) after oxidization in air for 300 hours at 600℃..... 95
Figure 52 Diffraction patterns of the uncoated Ti-6Al-4V samples (a) before and (b) after oxidation in air at 600℃ *for 300 hours* 96
Figure 53 Backscattered Electron images showing the different oxide regions in the uncoated Ti-6Al-4V sample oxidized in air for 300 hours at 600℃..... 97
Figure 54 Backscattered Electron Image of the Ti-6Al-4V sample coated with the 211 slurry and diffused at 1100℃ *(a) before and (b) after oxidation 300 hours oxidation in air at 600* ℃ 99
Figure 55 Diffraction patterns of the Ti-6Al-4V samples with 211 slurry coating and diffusion at 1100 ℃ *(a) before and (b) after oxidation in air at 600*℃ *for 300 hours*..... 100
Figure 56 Backscattered Electron image of the cross-section of the Ti-6Al-4V sample coated with the 211 slurry and diffusion at 1200℃ *(a) before and (b) after oxidation in air for 300 hours at 600*℃..... 102
Figure 57 Diffraction patterns of the Ti-6Al-4V samples with 211 slurry coating and diffusion at 1200 ℃ *(a) before and (b) after oxidation in air at 600*℃ *for 300 hours*..... 103
Figure 58 Backscattered Electron image of the cross-section of the Ti-6Al-4V sample coated with the 312 slurry and diffusion at 1100℃ *(a) before and (b) after oxidation in air for 300 hours at 600*℃..... 105
Figure 59 Diffraction patterns of the Ti-6Al-4V samples with 312 slurry coating and diffusion at 1100 ℃ *(a) before and (b) after oxidation in air at 600*℃ *for 300 hours*..... 107
Figure 60 Backscattered Electron image of the cross-section of the Ti-6Al-4V sample coated with the 312 slurry and diffusion at 1200℃ *(a) before and (b) after oxidation in air at 600*℃ *for 300 hours*..... 109
Figure 61 Diffraction patterns of the Ti-6Al-4V samples with 312 slurry coating and diffusion at 1200 ℃ *(a) before and (b) after oxidation in air at 600*℃ *for 300 hours*..... 110
Figure 62 Mass gain of the uncoated Ti-6Al-4V sample after oxidation in air for 300 hours at 600℃..... 116

Figure 63 Mass gain of Ti-6Al-4V samples coated with 211 slurry coating diffused at 1100℃ *(blue lines) and at 1200*℃ *(red lines) after oxidation in air for 300 hours at 600*℃ *compared with the mass gain of the uncoated Ti-6Al-4V sample*..... 117
Figure 64 Mass gain of Ti-6Al-4V samples coated with 312 slurry coating diffused at 1100℃ *(blue lines) and at 1200*℃ *(red lines) after oxidation in air for 300 hours at 600*℃ *compared with the mass gain of the uncoated Ti-6Al-4V sample*..... 118
Figure 65 Comparison of the Ti_3SiC_2 MAX phase Powder with Ti_3SiC_2 slurry coating after diffusion at 1200℃..... 122
Figure 66 Carbon activity as a function of temperature for a typical carburizing environment. (127) 125
Figure 67 Resulting coatings from the first Test 149

Index of Tables

Table 1 Summary of properties of Ti and Ti alloys 11
Table 2 Summary of some of the most important Titanium alloying elements and their effects (5) 12
Table 3 Elementary properties of Ti-6Al-4V (2), (13) 20
Table 4 Ceramic and metallic properties of MAX phases 30
Table 5 Properties of Maxthal 211 and 312 powders. Source: Swedish Ceramics Institute. Gothenburg, Sweden. 34
Table 6 Proposed synthesis mechanisms for Ti_3SiC_2 (60) 36
Table 7 Crystallographic information of Ti_2AlC *and* Ti_3SiC_2. (61) 38
Table 8 Property Requirements for high temperature coatings (73) 46
Table 9 Density values for starting materials 71
Table 10 Amount of PAA added in the final Ti_2AlC *slurry* 72
Table 11 Final Ti_2AlC *slurry composition* 72
Table 12 Amount of PEI added in the final Ti_3SiC_2 *slurry* 73
Table 13 Final composition of the Ti_3SiC_2 *slurry* 73
Table 14 Final pH Evolution for Ti_2AlC *slurry for diffusion at 1100*°C 75
Table 15 Final pH Evolution for Ti_2AlC *slurry for diffusionat 1200*°C 76
Table 16 Final pH Evolution for Ti_3SiC_2 *slurry for diffusion at 1100*°C 76
Table 17 Final pH Evolution for Ti_3SiC_2 *slurry for diffusion at 1200*°C 77
Table 18 *XRD Analysis conditions used to obtain the diffraction patterns of each sample* 86
Table 19 Summary of the visual transformation of the samples before and after the 300 hours oxidation treatment in air at 600°C 95
Table 20 EDS analysis of the Ti-6Al-4V uncoated sample before oxidation in air at 600°C *for 300 hours* 96
Table 21 EDS analysis of the Ti-6Al-4V uncoated sample after oxidation in air for 300 hours at 600°C 98
Table 22 EDS analysis of the Ti-6Al-4V sample with 211 slurry coating and diffusion at 1100°C *before oxidation* 99
Table 23 EDS analysis of the Ti-6Al-4V sample with 211 slurry coating and diffusion at 1100°C *after 300 hours oxidation in air at 600*°C 101
Table 24 EDS analysis of the Ti-6Al-4V sample with 211 slurry coating and diffusion at 1200°C *before oxidation* 103
Table 25 EDS analysis of the Ti-6Al-4V sample with 211 slurry coating and diffusion at 1200°C *after oxidation in air for 300 hours at 600*°C 104
Table 26 EDS analysis of the Ti-6Al-4V sample coated with the 312 slurry and diffusion at 1100°C *before oxidation* 106
Table 27 EDS analysis of the Ti-6Al-4V sample with the 312 slurry coating and diffusion at 1100°C *after 300 hours oxidation at 600*°C 108
Table 28 EDS analysis of the Ti-6Al-4V sample coated with the 312 slurry and diffusion at 1200°C *before oxidation* 109
Table 29 EDS analysis of the Ti-6Al-4V sample coated with the 312 slurry and diffusion at 1200°C *after 300 hours oxidation in air at 600*°C 111

Table 30 Summary of the characteristic Backscattered Electron images for each of the slurry coatings at the different diffusion temperatures and their corresponding transformation after oxidation in air for 300 hours at 600°C 113
Table 31 Summary of the Species and Reference codes identified in the Diffraction Patterns of the samples before and after oxidation in air at 600°C *for 300 hours*..... 114
Table 32 Gibbs Energy for the Reaction of TiC with O_2 at 600°C 120
Table 33 Calculations Composition Ti_2AlC Slurry without PEG..... 147
Table 34 PAA 75 % purity quantity added for composition without PEG..... 148
Table 35 Calculations Composition Ti_2AlC Slurry with PEG 148
Table 36 PAA quantity added for composition with PEG 148
Table 37 pH Evolution for Test I done on Ti_2AlC 149
Table 38 Calculations Composition Ti3SiC2 Slurry without PEG..... 150
Table 39 PEI quantity added for composition without PEG 150
Table 40 Calculations Composition Ti_3SiC_2 Slurry with PEG..... 151
Table 41 PEI purity 1:10 quantity added for composition with PEG 151
Table 42 pH Evolution for Test II with the Ti_3SiC_2 slurry coating 151
Table 43 pH Evolution for Test III 152
Table 44 Measurements of the samples done before oxidation used to calculate the resulting reference area 153
Table 45 Reference areas obtained for the samples and used to plot the oxidation curves..... 154
Table 46 Mass Evolution measurements recorded through the 300 hours of oxidation at 600°C 154
Table 47 Values used for calculating Gibbs Energy..... 155
Table 48 Enthalpy and entropy for the elements of the reaction 155

Index of Equations

Equation 1 Chlorination reaction: Kroll process 21
Equation 2 Reaction to obtain Titanium 21
Equation 3 Chemical composition of PEG 59
Equation 4 Chemical Composition of PAA-monomer of acrylic acid 61
Equation 5 Chemical Composition of PEI. Molecular formula 61
Equation 6 Total mass composition for the Ti_2AlC slurry 72
Equation 7 Total mass composition for the Ti_3SiC_2 slurry 73
Equation 8 Bragg's Law 87
Equation 9 Interplanar Spacing 87
Equation 10 Reaction of TiC with O_2 in the 211 slurry coated samples at 600℃ 119
Equation 11 Reaction of Ti_8C_5 with O_2 in the 312slurry coated samples at 600℃ 120
Equation 12 Computation of the masses without PEG 147
Equation 13 Computation of the exposed area of the samples 153
Equation 14 Enthalpy calculation at a certain temperature 155
Equation 15 Enthalpy of the reaction 155
Equation 16 Entropy of the reaction 156
Equation 17 Gibbs Energy Equation 156

ANNEX I: TESTS DONE ON SLURRIES

A. Tests for Ti_2AlC

In the first approach it was intended to achieve a slurry composition of 60%.wt in solids and 2%.wt with respect to the solids of dispersant. Initially no binder was used waiting to see the viscosity of the slurry obtained. For the tests 5ml of slurry where made, to limit the amount of powder used.

A.1 Test I

The first test done was with Ti_2AlC despite the fact there was no previous experience with this one due to the lack of PEI at the time. In the first test two slurries were made, one without using a binder and the other one using PEG with a 3 %.wt in solids. This way it would be able to determine whether the use of a binder would be needed to achieve an appropriate viscosity.

When not using the binder, the composition formula omits a term:

$$m_{TOT} = \frac{V_{TOT}}{\frac{solidswt\%}{\rho_{solids}} + \frac{PAAwt\%}{\rho_{PAA}} + \frac{H_2Owt\%}{\rho_{H_2O}}}$$

Equation 12 Computation of the masses without PEG

The composition of the slurries made is included below:

Composition for the slurry without PEG:

With PAA for Ti2AlC			
INPUT		**OUTPUT**	
Volume (ml)	5	**mtotal (g)**	9.19142313
		densitytotal (g/ml)	1.83828463

COMPOUND	% wt.	mass (g)
H20	0.388	3.566272173
Ti2AlC	0.6	5.514853876
PAA(2%wt. wrt. %solids)	0.012	0.110297078

Table 33 Calculations Composition Ti_2AlC Slurry without PEG

Amount of PAA added:

Volume of PAA needed for 100% purity (ml)	0.09191423
Volume of PAA needed for 75% purity (ml)	0.12255231

Table 34 PAA 75 % purity quantity added for composition without PEG

Composition for the slurry with PEG:

With PAA for Ti2AlC with PEG			
INPUT		**OUTPUT**	
Volume (ml)	5	**mtotal (g)**	9.2260651
		densitytotal (g/ml)	1.84521302

COMPOUND	% wt.	mass (g)
H20	0.37	3.413644088
Ti2AlC	0.6	5.535639062
PAA (2%wt. wrt. %solids)	0.012	0.110712781
PEG (3%wt. wrt. %solids)	0.018	0.166069172

Table 35 Calculations Composition Ti_2AlC Slurry with PEG

Amount of PAA added:

Volume of PAA needed for 100% purity (ml)	0.09226065
Volume of PAA needed for 75% purity (ml)	0.1230142

Table 36 PAA quantity added for composition with PEG

After adding the amount of water indicated and measuring the quantities of the components required the PAA was added. A sudden decrease in the pH was noticed, this decrease is quite reasonable due to the fact that PAA is an acid.

Throughout the process the difference of adding PEG was clearly noticed. When its addition took place the PAA seemed to dissolve it at a faster rate than when PAA is not used; not only this but the solution went from being transparent to being kind of white. Another thing that was noticed was the increase of viscosity induced by the PEG, besides this effect the pH remained almost constant (see Table 37). The addition of the powders into the stirring mixture also has a slight effect on the pH.

Test I- Ti_2AlC (pH)		
STEP	**Ti_2AlC without PEG**	**Ti_2AlC with PEG**
Initial Value of the water	7.9	7.4
After PAA addition	3.4	3.14
PEG addition	-	3.47
Final-After poder addition	3.6	3.64

Table 37 pH Evolution for Test I done on Ti_2AlC

Deposition of the slurry onto two samples was carried out to see how the final results would be. Regarding the PEG slurry, its adhesion to the substrate was much better than the other one and both when depositing it and drying of the film of slurry was seen to be more uniform than the other one and all the surface of the sample seemed to be fully covered. Another advantage was that the slurry didn't drip, whereas the other one did. The sample where the slurry without PEG was added once it dried of pores could be appreciated leaving parts of the substrate uncovered, not only this but the bottom part got stuck to the place where the surface where the slurries where placed so the sample once it had dried had to be turned around to try and achieve a film similar to the other one. After doing this the samples were left to dry off.

When returning several days later both samples where completely dry and it seemed that PEG didn't influence the actually affect the final result, but when taking both pieces in your hands it was the sample without PEG started losing the coating and the powder fell off leaving the surface unprotected. The one with PEG remained attached to the sample.

In Figure 67 it can be seen how the sample that was covered with the slurry containing PEG seem to have a greater thickness, giving us and idea of its higher viscosity respect to the other slurry used.

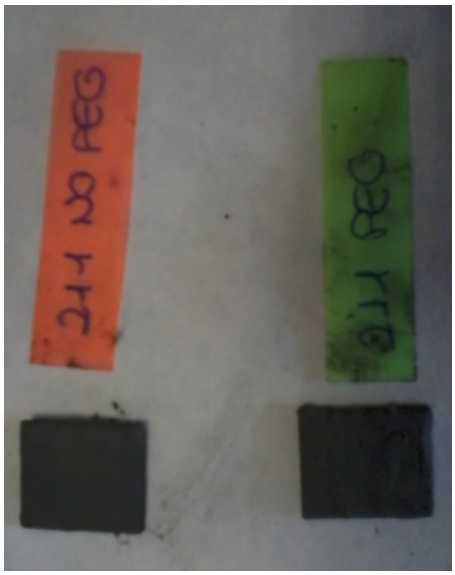

Figure 67 Resulting coatings from the first Test

As this test was quite satisfactory no need for further experiments with this powder were needed.

B. Tests for Ti_3SiC_2

B.1 Test I

In this test the pH was adjusted manually by adding TMAH to the initial water solution. The two slurries had the same concentration in solids, but in one of them PEG was added as a binder, just as in the previous test for Ti_2AlC.

The compositions used were also for a final volume of 5ml and the computations for the compositions were as follows:

Composition for the slurry without PEG:

Ti3SiC2 withoutusing PEG			
INPUT		OUTPUT	
Volume (ml)	5	mtotal (g)	9.39211521
		densitytotal (g/ml)	1.87842304

COMPOUND	% wt.	mass (g)
H20	0.3988	3.745575547
Ti3SiC2	0.6	5.635269127
PEI (0.2%wt. wrt. %solids)	0.0012	0.011270538

Table 38 Calculations Composition Ti3SiC2 Slurry without PEG

As the PEI used was not 100% pure but 1:10 in volume a correlation had to be done to get the actual volume that had to be added.

Amount of PEI added:

Volume of PEI needed for 100% purity (ml)	0.01043568
Volume of PEI needed for 1:10 purity (ml)	0.10435684

Table 39 PEI quantity added for composition without PEG

Composition for the slurry with PEG:

With PAA for Ti2AlC with PEG			
INPUT		OUTPUT	
Volume (ml)	5	mtotal (g)	9.42828948
		densitytotal (g/ml)	1.8856579

COMPOUND	% wt.	mass (g)
H20	0.3808	3.590292632
Ti3SiC2	0.6	5.656973685
PEI (0.2%wt. wrt. %solids)	0.0012	0.011313947
PEG (3%wt. wrt. %solids)	0.018	0.169709211

Table 40 Calculations Composition Ti_3SiC_2 Slurry with PEG

Amount of PEI added:

Volume of PEI needed for 100% purity (ml)	0.01047588
Volume of PEI needed for 1:10 purity (ml)	0.10475877

Table 41 PEI purity 1:10 quantity added for composition with PEG

The pH evolution control was also carried out at each step; the goal was to obtain a final pH within the 8.5-9.5 range. The results of how the pH varied can be seen in Table 42.

Test II- Ti_3SiC_2		
STEP	Ti_3SiC_2 without PEG	Ti_3SiC_2 with PEG
Initial Value of the water	9.13	9
After PEI addition	9.08	9.8
PEG addition	-	10.3
Final-After poder addition	8	8.66

Table 42 pH Evolution for Test II with the Ti_3SiC_2 slurry coating

From the pH evolution it can be observed how PEI dispersant has an opposite behaviour to PAA's; PEI increases the pH whereas PAA decreases it due to its acidic character. Another difference observed is that unlike in the previous case where the addition of PEG changed the colour of the solution here no change is noticed. Also it is worth pointing out the difference in the amount of dispersant added, which is one order of magnitude different. This last point may be the reason why when adding PAA a clear change in viscosity was seen and for the Ti_3SiC_2 no such thing is noticeable.

Regarding the outcome of the slurries, the slurry with PEG seemed to be even more liquid than the other one and it dripped much more than the other. Questioning what could be the

reason for this behaviour gave way to finding what the key to this problem was, when setting the pH to 9 different amounts of the acid and base were added to each slurry leading to a non-proportional increase in volume. Therefore, the results obtained with the slurries could not confirm the exact behaviour of the coatings.

Despite this fact, when observing the coated samples after drying off, it was clear the need of PEG just as for Ti_2AlC, the slurry without the binder after drying off proved to start falling off as if it were dust.

B.2 Test II

This test was the same in terms of quantities used and procedure, the only difference was the fact that in order to avoid the problem of different volume additions, a simpler approach was decided, the volume of water added would already be the desired pH. As from the previous test it was seen how the pH decreased along the process instead of setting the pH to 9 it was set to a higher value so its decrease was not as considerable.

Test III- Ti_3SiC_2		
STEP	**Ti_3SiC_2 without PEG**	**Ti_3SiC_2 with PEG**
Initial Value of the water	9.85	9.85
After PEI addition	10.15	9.84
PEG addition	-	10.17
Final-Afterpowderaddition	8.43	8.43

Table 43 pH Evolution for Test III

The evolution of the pH was similar to the one for Test II. With this test we were able to verify that PEG indeed increased the viscosity and that the final slurry with PEG was better than the other one.

CONCLUSIONS REACHED FROM SLURRY PREPARATION

- The 211 slurry seems to provide a more uniform and viscous coating when applied on the piece.
- PEG is required for binding the particles.

ANNEX II: MEASUREMENTS OF THE SAMPLES AND AVERAGES

For the calculation of the reference area of the samples three measurements were done and with them and average was calculated. The values measured and their respective average values are included in the Table below.

INITIAL MEASUREMENTS												
PIECE	MEASUREMENTS											
	Length (mm)			Av. Length	Width (mm)			Av. Width	Thickness (mm)			Av. Thick.
1200 312-1	16.73	16.66	16.66	16.6833007	17.09	17.08	17.01	17.0599628	1.65	1.66	1.76	1.68927971
1200 312-2	16.4	16.33	16.66	16.4627232	15.19	15.56	15.09	15.2786695	1.78	1.8	2.16	1.90567463
1200 312-3	18.23	18.21	18.32	18.2532707	16.72	17.04	17.09	16.9492041	1.57	1.56	1.52	1.54984862
1200 211-1	16.83	16.75	17.06	16.8794899	15.42	15.62	15.66	15.5663116	1.79	1.72	1.76	1.75643217
1200 211-2	17.75	17.83	17.76	17.7799644	16.53	16.62	16.44	16.5298367	1.56	1.6	1.69	1.6157609
1200 211-3	16.4	16.13	16.3	16.2762845	15.24	15.29	15.23	15.2533108	1.97	2.04	1.75	1.91592343
1100 312-1	14.82	14.91	14.91	14.8799394	14.81	13.99	13.99	14.2581604	1.43	1.50	1.50	1.47629399
1100 312-2	16.78	16.52	16.89	16.7292787	16.46	15.93	16.24	16.2085393	1.33	1.32	1.27	1.30640078
1100 312-3	14.72	14.64	14.9	14.7529335	14.56	14.91	14.88	14.7824806	1.60	1.50	1.52	1.53940045
1100 211-1	17.38	17.59	17.48	17.483123	14.15	14.36	14.56	14.3556904	1.53	1.63	1.99	1.70573163
1100 211-2	15.89	15.87	15.88	15.8799979	14.23	13.66	14.16	14.0143497	1.79	1.92	1.70	1.80108576
1100 211-3	15.69	15.44	15.62	15.5829768	14.03	13.92	13.8	13.9163496	1.90	1.86	2.11	1.95366307
641-1	16.62	16.54	16.71	16.6231883	13.6	13.45	13.53	13.5265278	1.55	1.54	1.54	1.54332614
641-2	16.74	16.71	16.58	16.6765218	16.24	16.07	16.16	16.1565174	1.5	1.53	1.51	1.51328204
641-3	17	17.27	17.24	17.1695735	14.79	14.71	17.74	15.6859739	1.44	1.44	1.45	1.44332565

Table 44 Measurements of the samples done before oxidation used to calculate the resulting reference area

These average values (in the yellow columns) were the values used to calculate the area of each piece according to Equation 13.

$$A_{exposed} = 2tw + 2lt + 2wl$$

Equation 13 Computation of the exposed area of the samples

Where t is the thickness, l the length and w the width of the samples. With this the values seen in Table 45 are obtained.

PIECE	MEASUREMENTS
	Area (mm2)
1200 312-1	683.2366023
1200 312-2	624.0345466
1200 312-3	727.8738339
1200 211-1	639.4804985
1200 211-2	698.6726854
1200 211-3	617.3510326
1100 312-1	510.3539295
1100 312-2	628.3743233
1100 312-3	527.1035651
1100 211-1	610.5815465
1100 211-2	552.7802562
1100 211-3	548.9797944
641-1	542.7697284
641-2	638.2403281
641-3	633.4854706

Table 45 Reference areas obtained for the samples and used to plot the oxidation curves

Using the previous values and the variation of mass at each step with respect to the initial mass the variation $\frac{\Delta mass}{A_{exposed}}$ is calculated and with this the oxidation curves can be plotted. The values of the mass recorded through the oxidation cycles can be seen in Table 46. The oxide formed on the pieces is very brittle and easily breaks and falls off, for this reason it is quite common to notice mass reductions instead of gains after an oxidation cycle.

PIECE	Mass (g)						
	Initial	12h	24h	48h	100h	150h	300h
1200 312-1	1.9534	1.9270	1.9666	1.9678	1.9679	1.9675	1.9687
1200 312-2	1.7383	1.7160	1.7090	1.7106	1.7113	1.7021	1.6959
1200 312-3	2.1208	2.1408	2.1417	2.1434	2.1389	2.1327	2.1312
1200 211-1	1.7644	1.7054	1.7005	1.6998	1.7005	1.7019	1.7039
1200 211-2	2.0280	1.9726	1.9711	1.9724	1.9750	1.9762	1.9792
1200 211-3	1.7720	1.7216	1.7195	1.7201	1.7223	1.7228	1.7243
1100 312-1	1.3380	1.3345	1.3348	1.3349	1.3350	1.3347	1.3355
1100 312-2	1.4760	1.4220	1.4222	1.4224	1.4232	1.4234	1.4244
1100 312-3	1.4179	1.4808	1.4813	1.4815	1.4828	1.4831	1.4843
1100 211-1	1.6805	1.6327	1.6332	1.6325	1.6332	1.6333	1.6335
1100 211-2	1.5439	1.4156	1.4131	1.4130	1.4136	1.4130	1.4132
1100 211-3	1.4912	1.3803	1.3758	1.3763	1.3768	1.3761	1.3772
641-1	1.5121	1.5141	1.5148	1.5156	1.5176	1.5192	1.5247
641-2	1.7895	1.7913	1.7921	1.7937	1.7958	1.7976	1.8037
641-3	1.5755	1.5776	1.5783	1.5797	1.5815	1.5831	1.5888

Table 46 Mass Evolution measurements recorded through the 300 hours of oxidation at 600℃

ANNEX III: CALCULATION OF THE FREE ENERGY FOR THE TiC REACTION

The data used for the calculation of the spontaneity of the reaction is summarized in the table below:

Element	$\Delta H_f°$ (kJ/mol)	H-H°(298.15K)(kJ/mol) @ T=800K	H-H°(298.15K)(kJ/mol) @ T=800K	$S°@800K$ (J/molK)	$S°@900K$ (J/molK)
CO_2	-393.522	22.806	28.030	257.494	263.645
TiO_2	-944.747	33.764	41.122	115.311	123.977
O_2	0	15.835	19.241	235.921	239.931
TiC	-184.096	22.558	27.583	67.31	73.227

Table 47 Values used for calculating Gibbs Energy

The enthalpy of each element was calculated by:

$$H = \Delta H_f° + (H - H(298.15\ K)°)$$

Equation 14 Enthalpy calculation at a certain temperature

The value for the temperature at which we are working, 873.16K (600°C) was then obtained by interpolation of the enthalpies of each element at 800K and 900K.

Element	$H@800K$ (kJ/mol)	$H@900K$ (kJ/mol)	$H@873.16K$ (kJ/mol)	$S@873.16K$ (J/molK)
CO_2	-370.716	-365.492	-366.894	261.9940716
TiO_2	-910.983	-903.625	-905.600	121.6510456
O_2	15.835	19.241	18.327	238.854716
TiC	-161.538	-157.862	-157.862	71.6388772

Table 48 Enthalpy and entropy for the elements of the reaction

Note: To calculate the entropy we have assumed we are working at 1 atm, for this reason no additional term has to be added to the equation.

With the values of enthalpy and entropy the overall enthalpy and entropy of the reaction $TiC(s) + 2O_2(g) \rightarrow TiO_2(s) + CO_2(g)$ can be calculated by doing:

$$\Delta H = H_{products} - H_{reactants} = \text{-1151.286 kJ}$$

Equation 15 Enthalpy of the reaction

$$\Delta S = S_{products} - S_{reactants} = \text{-165.703 J}$$

Equation 16 Entropy of the reaction

From the 2nd Law of Thermodynamics:

$$\Delta G = \Delta H - T\Delta S = -1006.601 \text{ KJ} < 0 \; SPONTANEOUS$$

Equation 17 Gibbs Energy Equation